National Library of Canada
Bibliothèque nationale du Canada

Canadian Theses Service
Service des thèses canadiennes

Ottawa, Canada
K1A 0N4

NOTICE

The quality of this microform is heavily dependent upon the quality of the original thesis submitted for microfilming. Every effort has been made to ensure the highest quality of reproduction possible.

If pages are missing, contact the university which granted the degree.

Some pages may have indistinct print especially if the original pages were typed with a poor typewriter ribbon or if the university sent us an inferior photocopy.

Reproduction in full or in part of this microform is governed by the Canadian Copyright Act, R.S.C. 1970, c. C-30, and subsequent amendments.

AVIS

La qualité de cette microforme dépend grandement de la qualité de la thèse soumise au microfilmage. Nous avons tout fait pour assurer une qualité supérieure de reproduction.

S'il manque des pages, veuillez communiquer avec l'université qui a conféré le grade.

La qualité d'impression de certaines pages peut laisser à désirer, surtout si les pages originales ont été dactylographiées à l'aide d'un ruban usé ou si l'université nous a fait parvenir une photocopie de qualité inférieure.

La reproduction, même partielle, de cette microforme est soumise à la Loi canadienne sur le droit d'auteur, SRC 1970, c. C-30, et ses amendements subséquents.

NL-339 (r. 88/04) c

Canada

National Library of Canada
Bibliothèque nationale du Canada

Canadian Theses Service
Service des thèses canadiennes

Ottawa, Canada
K1A 0N4

The author has granted an irrevocable non-exclusive licence allowing the National Library of Canada to reproduce, loan, distribute or sell copies of his/her thesis by any means and in any form or format, making this thesis available to interested persons.

The author retains ownership of the copyright in his/her thesis. Neither the thesis nor substantial extracts from it may be printed or otherwise reproduced without his/her permission.

L'auteur a accordé une licence irrévocable et non exclusive permettant à la Bibliothèque nationale du Canada de reproduire, prêter, distribuer ou vendre des copies de sa thèse de quelque manière et sous quelque forme que ce soit pour mettre des exemplaires de cette thèse à la disposition des personnes intéressées.

L'auteur conserve la propriété du droit d'auteur qui protège sa thèse. Ni la thèse ni des extraits substantiels de celle-ci ne doivent être imprimés ou autrement reproduits sans son autorisation.

ISBN 0-315-56310-9

Canada

In vivo quantitation of the phosphorus-containing metabolites in rat hind limb by Nuclear Magnetic Resonance Spectroscopy during four weeks of creatine depletion induced by feeding ß-guanidinopropionic acid.

by

Marcus Evan Brady

A Thesis Submitted in Partial Fulfillment of the Requirements for the Degree of

Master of Science

to

Department of Physiology
University of Ottawa

Graham Mainwood, Ph.D
Professor, Department of Physiology

Roxanne Deslauriers, Ph.D.
Biological Sciences, N.R.C.C.

© Marcus Evan Brady, Ottawa, Canada, 1989

UNIVERSITÉ D'OTTAWA
UNIVERSITY OF OTTAWA

Acknowledgement

Four years ago I started into this program. After a period of time we started, what was the first Department of Physiology/Medical Biophysics collaborative study. We were going to design an NMR probe, develop tension monitoring apparatus, design a method of sciatic nerve stimulation, develop a technique of quantitating phosphorus NMRS signals in vivo, monitor these changes during a brief muscle contraction, and then go on to determine where the energies for muscle contraction originated in the creatine-depleted rat. We accomplished only a small portion of this.

Since that time the focus of my project changed a number of times for an equal if not greater number of reasons. Throughout that period, however, the support of Dr. Graham Mainwood, Dr. Roxanne Deslauriers and the rest of the team at the National Research Council of Canada was undying.

Yes the work itself was stimulating, and I learned a great deal about science, its precepts and its methodologies. However, I learned even more about human nature and myself. This learning would not have been possible without the integrity and caring of these and many other individuals.

Subsequent to the completion of my experiments, I attempted to combine my interest in health promotion and some of my abilities in science by becoming involved in a new business start up in the health care industry. Here, I learned that everything must be cost effective, and that image is thought by many to be more important than content. I believe that this is a sharp contrast to the reality of the scientific community that I have come to know at the University of Ottawa and the NRCC. In the scientific community, I believe that most are motivated by fairly altruistic ideals. I believe that most scientists would like to see the world improved and advanced, in some way, by their work. In addition I believe that scientists hold content paramount.

I attribute my appreciation for these beliefs largely, if not entirely to my scientific mentors and to my family.

In this regard I would like to thank and dedicate this work, however significant it may turn out to be, to the following people.

To my parents, who only wanted me to be happy. They forever encouraged me to "understand the things I cannot change". They gave me the strength to " complete the things that I could" while "helping me to distinguish between the two".

To Dr. Graham Mainwood, who is without any doubt the kindest, most intelligent, caring individual I have ever met. It was a privilege to study with such a scholar. In retrospect, I wish I had more fully taken advantage of this opportunity. Thank you very much for your assistance and your guidance. I would also like to thank you for introducing me to my fiancée.

To Dr. Roxanne Deslauriers, one of the most determined and well organized individuals I have ever encountered. I appreciate all of your guidance and your patient insight into my personality.

To Monique St-Jean, who has seen more graduate students than anyone ever should. I am glad that God gave you that strength. Your help and expertise made my life much easier.

To Dr. Yves Geoffrion, a great father, a funny man and a great scientist. It was your love for your work which regularly spurred me on, and helped me to laugh at myself.

To Dr. Ian Smith, who taught me that everyone has a special area of expertise and that this expertise should be cultivated. In this regard, I have Ian to thank for assisting me in the selection of my future career.

To Dr. D. Parry, who gave me better appreciation of the field of muscle physiology and helped me to understand how my my work fits into the bigger picture of medical research.

To Paul Morris, who arrived about 6 months too late. Better late than never. His passion for electronics and mastery of NMR equipment helped us to develop a probe that would more than "do the job".

To the rest of my peers at the National Research Council including John Irene, Keith, Leo, Richard (who also has a passion for scientific investigation), Laura, Myrna, Eva, Tony, and Therese.

To Apple Canada, for their Macintosh product which made my life easier and more than paid for itself over the last year.

To Impagination, Laural Carr and Julie McNeil who had patience and technical expertise in the 11th hour.

Last, but most of all, my deepest love and appreciation to Mandy Hockey, my fiancée, for she offered me undying love, encouragement, and when needed, a swift kick in the pants.

TABLE OF CONTENTS

ABSTRACT v

LIST OF ABBREVIATIONS vii

I. INTRODUCTION 1

I.1. Background 1

I.2. Approaches 3

I.3. NMR Spectroscopy 5

I.3.1. General 5

I.3.2. Relaxation 13

I.3.3. Fourier transformation 16

I.4. Quantitation of metabolites 18

I.5. Choice of test system 24

II. STATEMENT OF PURPOSE 28

II.1. Objectives 29

III. MATERIALS AND METHODS 30

III.1. Treatment of animals 30

III.1.1. General 30

III.1.2. Dietary regime 31

III.1.3. Anaesthesia 31

III.2. Dry to wet weight ratios 33

III.3. Biochemical techniques and assays 33

III.3.1. General 33

III.3.2. Protein determination 39

III.3.3. Acid hydrolysis 39

III.3.4. Determination of total creatine 39

III.3.5. Determination of guanidino containing compounds: ß-guanidinopropionic acid, and phosphorylated ß-guanidinopropionic acid 40

III.3.6. Determination of ATP and CrP 40

III.3.7. Corrections and analysis 41

III.4. Flame Photometry 42

III.5. Nuclear magnetic resonance spectroscopy 42

III.5.1. Probe design 44

III.5.2. Spectrum aquisition parameters 53

III.5.3. Pulse sequences 56

III.5.4. Quantitation of metabolites 57

III.5.4.1. General 57

III.5.4.2. Correction of calculated phosphorus-containing metabolite concentrations using intracellular sodium concentration and intracellular volume 60

III.5.5. Standard NMRS rat insertion protocol 62

III.5.6. Maintenance of physiological conditions during NMRS experiments 63

III.5.7. Nuclear magnetic resonance data processing methods 64

III.5.8. Resolution of the peaks of creatine phosphate and guanidinopropionate phosphate 69

III.5.9. Sample calculation of the concentration of CrP from an in vivo spectrum of rat hind limb 72

IV. RESULTS 75

IV.1. Rat growth 75

IV.1.1. Weight 75

IV.1.2. Leg cross sectional area 77

IV.1.3. Volume as measured by NMRS 80

IV.1.4. Fat to water ratio of hind limb....81

IV.2. Dry to wet weight ratios....81

IV.3. Weight loss due to muscle storage....82

IV.4. Flame photometric analysis of the sodium and potassium contents of rat muscle....83

IV.5. Biochemical assays and calculation of metabolite concentrations....85

IV.6. Nuclear Magnetic Resonance Spectroscopy....91

IV.6.1. Standard solutions....91

IV.6.2. Receiver gain....93

IV.6.3. Sodium concentrations....94

IV.6.4. Concentrations of phosphorus-containing metabolites....96

V. DISCUSSION....105

V.1. NMRS and biochemical analysis....105

V.1.1. The rates and extents of PCM depletion....105

V.1.2. Comparison of the results of NMRS and biochemical analysis....108

V.1.3. Comparison of the capabilities of NMRS and biochemical analysis....111

V.1.4. Technical considerations....113

V.1.5. Comparison of the currently used methods of quantitating NMRS spectra....115

V.2. Animal Growth....118

V.2.1. Weight and Cross Sectional Area....118

V.2.2. NMRS Measurements of Volume....119

V.2.3. NMRS Measurements of Fat Content....120

V.3. Muscle Sodium and Potassium Determination....121

V.4. Anaesthesia....123

V.5. Concluding Remarks 124

VI. APPENDICES 125

VI.1. Sodium 23NMR Spectroscopy 125

VI.2. Components of an NMR spectrometer.....126

VI.2.1. The magnet.....126

VI.2.2. The probe: coil and circuitry design.....126

VI.3. Pulse sequences 133

VI.4. Schematic diagrams of early probes.....139

VI.5. Schematic diagrams of the tension transducer 141

VI.6. Estimation of the metabolite concentrations of rat hind limb muscles 150

VII. REFERENCES 152

ABSTRACT

In vivo quantitation of the phosphorus-containing metabolites in rat hind limb by Nuclear Magnetic Resonance Spectroscopy during four weeks of creatine depletion induced by feeding B-guanidinopropionic acid.

Male weanling, Sprague Dawley rats (Charles River, Montreal) were divided randomly into one of four groups: Control Biochemical Analysis, Control NMR examination, Experimental Biochemical Analysis, or Experimental NMR examination. Rats were fed 10g of rat chow per day (control) or 10g of chow plus 1% B-guanidinopropionic acid (experimental) for four weeks, after which time both groups were placed on control diet for two weeks. Both groups of animals were anaesthetized using sodium pentobarbital (0.65 mg/kg). The animals studied by NMR were placed weekly in a specially designed NMR probe (solenoid coil) within a Bruker 300 MHz, wide bore magnet in order to quantitate muscle metabolites of right hind limbs using the method of Ackerman (Thulborn and Ackerman, 1983). The right hind limb of the animals of the groups studied biochemically were dissected and the gastrocnemius muscles was quickly frozen between liquid nitrogen-cooled aluminum blocks, removed and analyzed by conventional biochemical techniques for their content of creatine phosphate, ATP, and guanidinopropionate phosphate.

Results indicate that (i) NMR can provide a non-invasive and accurate method of quantitating time-dependent changes in muscle metabolites which occur during creatine depletion and (ii) depletion occurs at a much faster rate than repletion (50% depletion in four days, compared to 50% repletion in two weeks).

At four weeks, the overall decrease of the CrP concentration from normal levels (18.3 mM/L tissue fluid) in the experimental group observed by NMRS was

approximately 80% (90% using conventional biochemical assaying techniques). Refeeding brought the CrP levels of these animals to 44% of control.

Analogue feeding lowered the ATP concentration to 66% of normal levels (5.8 mmoles/l tissue fluid) at the end of four weeks. The return to normal diet raised ATP levels to 73% of control values.

Concomitant with the decreases in the concentrations of ATP and CrP was an increase in the concentration of GPP from undetectable levels to over 10 mmoles/l tissue fluid at the four week point. Withdrawal of the analogue from the experimental groups' diet precipitated a fall in GPP concentration to 9.2 mmoles/l tissue fluid as found by both NMR and biochemical analysis.

NMR provides a comparatively accurate yet expensive means by which to monitor changes in muscle metabolite concentrations. Although it is a costly technique to implement, there can be no effective substitute for NMRS in instances where serial determinations in a living animal are required.

LIST OF ABBREVIATIONS

[ATP], [Pi]	= intracellular concentrations of corresponding phosphates
[ATP]t, [Pi]t	= apparent concentrations seen by NMR from the ratio of phosphate signal to total water signal
[Na]i	= intracellular sodium concentration
[Na]o	= extracellular sodium concentration
[Na]t	= apparent sodium concentration seen by NMR
A	= area
AH	= area under the proton signal without the lipid component
AHL	= area under the proton signal before removal of the lipid peak
AN	= area under the sodium signal
AP	= area under the phosphate signal
ATP	= adenosine triphosphate
bfg	= biochemistry flame photometry group
°C	= Celsius
CrP	= creatine phosphate
D	= proportionality constant
dietary regime	= feeding the animals according to the method outlined in the materials and methods ie. Rats from the experimental group receive 10g of ground rat chow supplemented with 1% GPA for a 4 week period. Subsequently these animals receive 10g of unsupplemented (normal) ground rat chow per day for two weeks. Rats from the control group receive 10g of ground rat chow daily for the entire six week period.
eV	= electron volts
E	= fractional extracellular volume (Ve/Vt)
EM	= electromagnetic radiation
F	= Fahrenheit
FG	= fast glycolytic
FID's	= free induction decays
FOG	= fast oxidative glycolytic
g6p	= glucose-6-phosphate
GPA	= guanidinopropionic acid
GPP	= phosphorylated guanidinopropionic acid
h	= Planck's constant

Icor.	= corrected integrals
Ih	= angular momentum
IV	= intracellular volume
Ivf	= height of the Lorentzian peak
K	= phosphorus
K_N	= coefficient giving equivalent total sodium concentration from the ratio of A_{Na}/A_H
K_P	= coefficient giving equivalent total phosphate concentration from the ratio of A_P/A_H ie $[P]t = K_P[A_P/A_H]$
L	= inductance
L	= litres
M	= magnetic field (direction specified in subscripts
M	= Molar
MHz	= Megahertz
mL	= milliliters
mM	= milli molar
N	= Normal
N	= number of nuclei
N	= number of spins in a given orientation
n	= number of acquisitions
Na	= sodium
nad	= nicotine adenine dinucleotide
nm	= nanomoles
NMR	= nuclear magnetic resonance
NMRS	= nuclear magnetic resonance spectroscopy
NS	= number of scans
pc	= printed circuit
PCM	= phosphorus-containing metabolite
ppm	= parts per million
Q	= quality factor
rf	= radio frequency
RG	= receiver gain
S	= signal intensity
SO	= slow oxidative
T1	= spin-lattice relaxation time
T2	= spin-spin relaxation time
TR	= transmit receive network

v	= frequency
Ve	= extracellular volume inside the field
Vi	= intracellular volume
VO	= extracellular volume
Vo	= frequency of the reference peak
VT	= total volume
Vt	= total tissue volume in the magnetic field
W	= Watts
w0	= larmour frequency x 2π
ø	= chemical shift
†	= time
∞	= fraction of total volume held by extracellular volume
μ	= magnetic moment
μL	= microliters
∂	= gyromagnetic ratio proportionality constant
ΔE	= energy difference
ΔV	= line width

1. INTRODUCTION

1.1. Background

In order to maintain the dynamic state of living systems, a continuous input of energy is required. Phosphorus-containing metabolites (PCM) are involved in these biosynthetic/metabolic reactions. They can act firstly as the energy currency in many processes involved in cell action and maintenance; second as the progenitors of phosphoenzyme intermediates necessary in reaction catalysis; and finally in the processes of energy conversion involving cellular infrastructure (Arnold 1984).

Of primary interest to this work are the energy currency functions of adenosine triphosphate (ATP), adenosine diphosphate (ADP), creatine phosphate (CrP), inorganic phosphate (Pi), and the sugar phosphates. Since the discovery of creatine in 1911 (Thunberg), creatine phosphate (Eggleton, 1927) and ATP in 1929 (Lohmann, 1929) many advances have been made in the elucidation of the uses of these and other PCM in the processes of muscle function.

Unequivocally established as the primary energy source of muscle contraction CrP levels decrease (Arnold, 1984) while ATP concentration is normally maintained at a constant level (Cain, 1962; Lipmann, 1930). Once hydrolysed, creatine phosphate is rapidly rephosphorlyated by the enzyme creatine kinase (Lundsgaard, 1930; Lohmann, 1934).

CrP is believed to serve both as an energy reservoir (a temporary pool) of phosphate for ATP (Meyer, 1982) and as a carrier of phosphate from the mitochondria (energy source), to the myofibrils (energy sink) (Bessman, 1985; Jacobus, 1985). Many of the details surrounding these potential roles of CrP remain clouded by conflicting information. This controversy is especially apparent in the light of

experiments with creatine-depleted animals in which muscle contraction is hindered very little by a near complete removal of creatine phosphate from the available energy pool (Mainwood, 1982b; Petrofsky, 1980; Fitch 1978). These experiments lend importance to the role of creatine phosphate as a "dynamic energy reserve during brief bursts of activity" (Totosy de Zepetnek, 1984).

Meyer (1984) proposed that the two functions of creatine phosphate, energy buffering and energy transport, are inseparable, and that they depend on the same properties of creatine kinase; namely the near equilibrium nature of the reaction and the maintenance of a high ATP to ADP ratio. The dual roles have been termed "spatial" and "temporal" buffering to differentiate the energy transport from the energy buffering effects.

Recent advances in the use of Nuclear Magnetic Resonance Spectroscopy (NMRS) with living muscle have made it possible to monitor all these metabolites simultaneously, and to relate changes in them to concomitant changes in the mechanical performance of muscles. Yet, several questions still remain. These include: How does muscle adapt to maintain tension even in conditions where its energy stores are depleted? How important is the proposed CrP transport system to muscle activity? What are the precise importances of CrP and creatine kinase (CK) in muscle activation and contraction? What are the energy sources and absolute costs of muscle contraction?

A meaningful interpretation of the metabolic responses of contracting muscle will only arise out of a knowledge of the energy costs of muscle contraction. This understanding must be achieved through a reliable and analytical technique to investigate these processes. Two approaches to this problem are currently being used; 1. chemical analyses of muscle biopsies after quick freezing using conventional spectrophotometric

or high pressure liquid chromatographic methods and 2. performing ^{31}P NMR spectroscopy of muscle in vitro or in vivo.

To date, there has been no quantitative NMR performed on muscle under what could be termed "stringent"[1] conditions. For this reason, the comparison of these two techniques has often been less than satisfactory (Doyle, 1982; Keller, 1985; Bevington, 1985; Helzberg, 1987). The need to resolve the myriad of questions concerning the absolute energy costs of muscle contraction has prompted this study. Towards this end the following questions are investigated by this study. " Can NMR be used to measure absolute quantities of intracellular metabolites in vivo?" and subsequently "How do the results obtained by NMR spectroscopy compare with biochemical determinations of the absolute quantities of phosphorus-containing, energy carrying metabolites of rat hind limb?"

I.2. Approaches

Biochemical analysis of muscle metabolites has long been the only method of analyzing muscle biopsies to determine their PCM composition (Ennor, 1952; Fiske, 1929). The basic procedure for the biochemical determination of ATP, ADP, CrP and Pi requires the freezing of the muscle sample (in vitro or in vivo), and subsequent acid extraction and biochemical analysis. Although reliable, sensitive, specific and relatively inexpensive, the method is plagued by three major shortcomings. First, the technique is totally destructive to the specimen. A muscle sample is obtained (usually 50 mg), and then quickly frozen, preferably in liquid nitrogen. The surgery performed on the animals renders follow up investigations impossible. Second, there is often the danger of some metabolite hydrolysis occurring during the freezing and extraction of the

---

1 Conditions wherein no assumptions are made concerning the resting concentrations of the metabolites of the specimen at any time prior to or during experimentation.

muscle sample, rendering results inaccurate. Third, the procedure is extremely time consuming, as relatively few experiments of a given type can be performed in a given time period and these analyses cannot be performed simultaneously.

Recently, Nuclear Magnetic Resonance Spectroscopy (NMRS) has been used with much success as a method of examining PCM in vivo (Shoubridge, 1985 , Helzberg, 1987). The non-invasive nature of NMRS makes it possible to extract information from living tissue without perturbing it in any way. Anaesthesia is often the only necessary infringement on the truly physiological state of the specimen (Kushmerick, 1985; Idstrom, 1985). In contrast to these advantages, NMRS is inherently insensitive (with millimolar sensitivity[1] limits compared to micromolar limits for chemical assays), and does not readily yield absolute concentrations (Ackerman, 1980; Gadian, 1982).

The information accessible to NMRS concerns the chemical environments and relative amounts of specific atomic nuclei within a sample. As its name implies, this knowledge is acquired by observing the phenomenon known as "magnetic resonance" of these nuclei. The properties of these nuclei (discussed below) allows them to interact with the magnetic portion of applied electro-magnetic radiation and to change their energy state. It is the decay of the high energy state of these nuclei which when monitored and amplified, provides information (in the form of a spectra) of the chemical environment, state of ionization, and pH surrounding these nuclei.

---

1 The term sensitivity, when used in reference to an atom with a magnetic moment, refers to a physical constant. This constant is a function of the a) natural abundance of this isotope in a sample of the the most common element; b) the spin number of the nucleus in question; c) and the magnetic properties attributed to that nucleus. Comparison of relative sensitivities can only be made for equal numbers of nuclei at a constant field.

For certain types of information concerning some metabolites or nuclei, the negative aspects of NMR spectroscopy are by far out weighed by the positive features of this technique. For example, in the case of phosphorus NMR of living tissue, the peaks of creatine phosphate, ATP, ADP, the sugar phosphates, and inorganic phosphate are all present in the same spectrum. This provides a wealth of fundamental, simultaneously obtainable information concerning glycolysis and the free energy state of the tissue, unmatched by any other technique. Although the sensitivity of the phosphorus nucleus is only about 1/15 of that of protons, its spectra are much simpler and therefore easily assigned and interpreted.

Some of the recent applications of NMRS have permitted the simultaneous observation of: sodium, carbon, hydrogen and phosphorus (Shinar, 1984; Radda, 1986); muscle metabolites and tension during muscle fatigue (Dawson, 1980; Shoubridge, 1984; Kushmerick, 1985); and intra and extra-cellular muscle lactate (Mainwood, 1987). The simultaneous observation of these compounds permits the correlation of metabolite use not easily followed by conventional chemical determinations.

I.3. NMR Spectroscopy

I.3.1. General

The first NMR experiments were the continuous wave experiments by Bloch, Purcell and their co-workers (1946) on "nuclear induction" of "atoms with odd spins", for which they received a Nobel prize. The first pulse experiments[1] were performed shortly thereafter. Hahn performed the first spin echo experiment[2] in

---

1 signal intensity is monitored at certain time intervals after the application of an excitation pulse of energy at a specific radio frequency

2 signal intensity is monitored after the application of an excitation pulse of energy at a specific radio frequency, a small wait, and an application of a second excitation pulse of approximately twice the duration of the first

1950. It was not until the late 1950's that the Free Induction Decay was analyzed by Fourier transformation to yield a spectrum. Odeblad of Sweden was the first to use NMR for a biomedical application (1956). His work on "living" tissues (liver, muscle, fat, cartilage and blood) was instrumental in promoting NMR as a tool for biological research and as a diagnostic technique in medicine. Despite the rapid advances in the technology behind this form of spectroscopy, it was not until 1973 that Moon and his colleagues were able to obtain phosphorus spectra from blood. Their five hour experiment is now performed in approximately five minutes using modern high-field superconducting magnets.

Magnetic resonance spectroscopy is essentially analogous to other forms of absorption spectroscopy in that it is the investigator's intention to raise a low energy ground state to a high energy excited state somewhere within a molecule. Not unlike other forms of spectroscopy it uses electromagnetic (EM) radiation to achieve these results. NMR differs from other forms of spectroscopy in that its interaction is with the magnetic rather than the electric component of the electromagnetic radiation, and that the input energy, a radio frequency (rf) pulse, is not used to probe the bonding energies of the molecules but rather to provide the much smaller amount of energy needed to induce a change in spin orientation of a nucleus within the specimen (Foster, 1983).

In its most basic form an NMR spectrometer consists of a magnet, a radio frequency (rf) transmitter, a suitable rf detector, and a probe (Figure I.3.1.a.). When a sample of a material having nuclei with certain magnetic properties is placed within a probe in the magnet pole gap and subjected to the rf field of the transmitter, absorption of the rf energy occurs at particular frequencies. The subsequent loss of this absorbed EM energy results in a measurable emission from the sample, this "signal" is amplified and then measured by the rf detector.

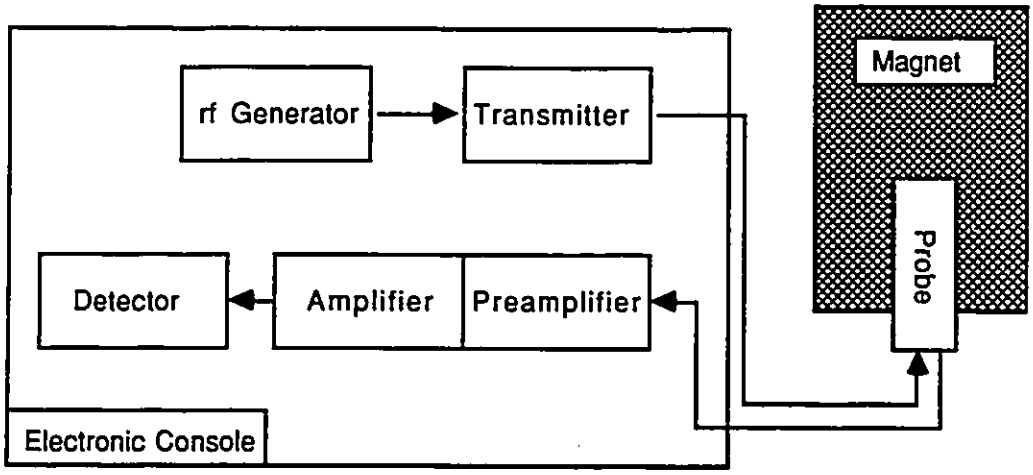

Figure I.3.1.a. Schematic diagram of an NMR spectrometer. Note the vertical orientation of the NMR probe within the superconducting magnet.

In all forms of spectroscopy, the system under investigation, in order that it may be characterized, must release energy. Energy is released and absorbed in quanta related to the differences in energy between ground and excited states of energy.

If a transition between the ground and the excited states of energy is to occur then the incident/applied quantum of radiation (hv) must be the same as the energy difference (ΔE) between those states: $hv = \Delta E$ (Foster, 1983). The quantum of applied energy (hv) is related to the frequency of applied energy (v) by Plank's constant (h). In NMR spectroscopy this energy is usually measured in Hertz.

In NMR , ΔE and v are in the range of 10^{-7} to 10^{-11} eV and 10^{3} to 10^{8} Hz respectively (Beall, 1984). This places NMR in the microwave and radio wave portions of the electromagnetic spectrum which penetrate deeper into biological material than do

the infra-red and ultra-violet portions. This capability provides NMR investigators with the possibility of investigating internal chemistry of much larger tissue samples, whole organs or even whole bodies (Gadian, 1981).

NMR is possible because nuclei of certain atoms possess a special property: they have an odd number of protons or neutrons. As a direct result of this characteristic they also possess net magnetic moments and angular momenta. A static magnetic field will interact with this moment in such a way as to force that moment to line up along it in specific directions and hence into different populations (Figure I.3.1.b.). The small difference in energy levels between the different orientations of the magnetic moments means that there is a chance that some nuclei will go into low and high energy orientations when the field is applied. The majority enter the low energy state but this distribution is affected by such factors as temperature and ΔE. The proportion of the two can be calculated from the Boltzman expression:

$$\frac{N_{low}}{N_{high}} = e^{(h\nu \,/\, kT)} \qquad (I.3.1.i)$$

where N_{low} is the number of nuclei in the low energy state and N_{high} is the number of nuclei in the high energy orientation, k is Boltzman's constant and T the temperature in K (Fukushima, 1981).

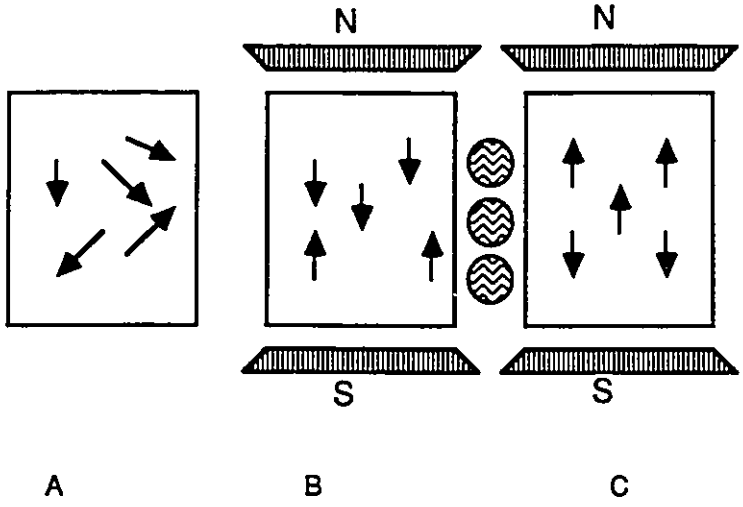

Figure I.3.1.b. Spin orientation. (A) Classical picture of random spin orientation in the absence of a magnetic field, (B) Quantum picture of spin alignments in an external magnetic field and (C) Spin orientations inverted after application of Electromagnetic radiation at the Larmor frequency (Power, 1983).

It is the difference in the size of these two populations which determines the effective fraction and the sensitivity of an absorption spectroscopy experiment. The ΔE ($h\nu$) in NMR is extremely small; as a consequence, the difference in the size of these two populations (effective fraction) is small. For this reason NMR is a relatively insensitive technique (Power, 1983). High magnetic fields and special techniques have been developed to overcome this insensitivity.

Insensitivity is a great disadvantage in biological and in vivo NMR, as sample size or concentration cannot be increased at will. The minimum observable concentration for ^{31}P in living tissue is about 0.2 mM (Fukushima, 1981). This accuracy is only obtainable with several hundred acquisitions and (often related) long waiting periods between signal averaging.

If a nucleus within a magnetic field (Figure I.3.1.c.) has angular momentum, it will precess around the magnetic field in response to the torque of the field acting on the

moment (Beall, 1984). The frequency of this precession is proportional to, and uniquely determined by, the gyromagnetic ratio ∂ and the strength of the magnetic field H_0. The speed of precession is given by the Larmor relation:

$$W_0 = \partial H_0 (1- \sigma), \qquad \text{I.3.1.ii}$$

where W_0 is 2π times the Larmor frequency ν_0, ∂ is the proportionality constant between the moment μ and the angular momentum $\hbar$ and σ is the chemical shift due to environmental shielding (Meyer, 1982). Therefore, in a given magnetic field, the precession frequency is different for every distinct nucleus as each has a uniquely defined ∂ (Foster, 1983).

The molecular environment of the nucleus can cause local modifications of the static magnetic field strength (Meyer, 1982). For example, the bonding one atom makes with another, the electron distribution which results from that bonding, and any other electronic shielding that may be taking place, will cause a field alteration which will often effect a slight "shift" in the resonance frequency of the nucleus under study pushing it slightly "up" or "down" field. This chemical shift is normally quoted as p.p.m. shift from the resonance of a particular nucleus standard (Gadian, 1982). This convention has the advantage of enabling a direct comparison between results from instruments operating at different frequencies. The p.p.m. shift of a chemical species can be derived from:

$$\text{P.P.M.} = \frac{\partial \times \nu_R}{\Delta \nu}, \qquad \text{I.3.1.iii}$$

where ν_R is the frequency of the reference substance and $\Delta\nu$ is the frequency difference in Hertz between the reference substance and the nucleus of interest in Hertz (Fukushima, 1981).

The sum of all of the magnetic fields of each individual spin, is normally referred to, rather than to the quantum state of each individual spin. The aggregate of the spins of all the nuclei involved in the process of relaxation is held to obey the laws of classical dynamics. The direction and magnitude of spin orientation of this aggregate is referred to as the magnetization vector, as it represents the vector sum of the magnetic field of each individual spin (Figure I.3.1.c.). If we regard our system in three dimensions with the Z axis being equivalent to the main field axis and X and Y its corresponding orthogonal axes, then in the absence of any EM radiation the magnetic moment would exist only in the Z direction. If radiation is applied at the Larmor frequency for a time †, the spin population will continue to precess freely; however, the magnetization vector will be rotated by an angle $\partial H_1 †$. In this case the magnetization in the XY plane would increase at the expense of the magnetization in the Z direction. When sufficient radiation is applied to "eliminate" the Z component of the magnetization the precession angle would be equivalent to 90°. At this point the magnetization in the XY plane (M_{xy}) would reach a maximum value, equivalent to the original value of M_z. The amount of power required to maximize Mxy is known as a 90° pulse. Similarly, a 180° pulse would eliminate M_{xy} and maximize M_z in the negative direction.

In order to induce a change in orientation of the magnetic moment a small external magnetic field is applied to the sample. This is necessary to donate a quantum of energy ($h\nu$), to the spinning nucleus. If the applied incident radiation is of sufficiently short duration, the sample will absorb an amount of radiation related to the effective difference between the high and low energy states, after which time it will precess, without friction, in its new energy level.

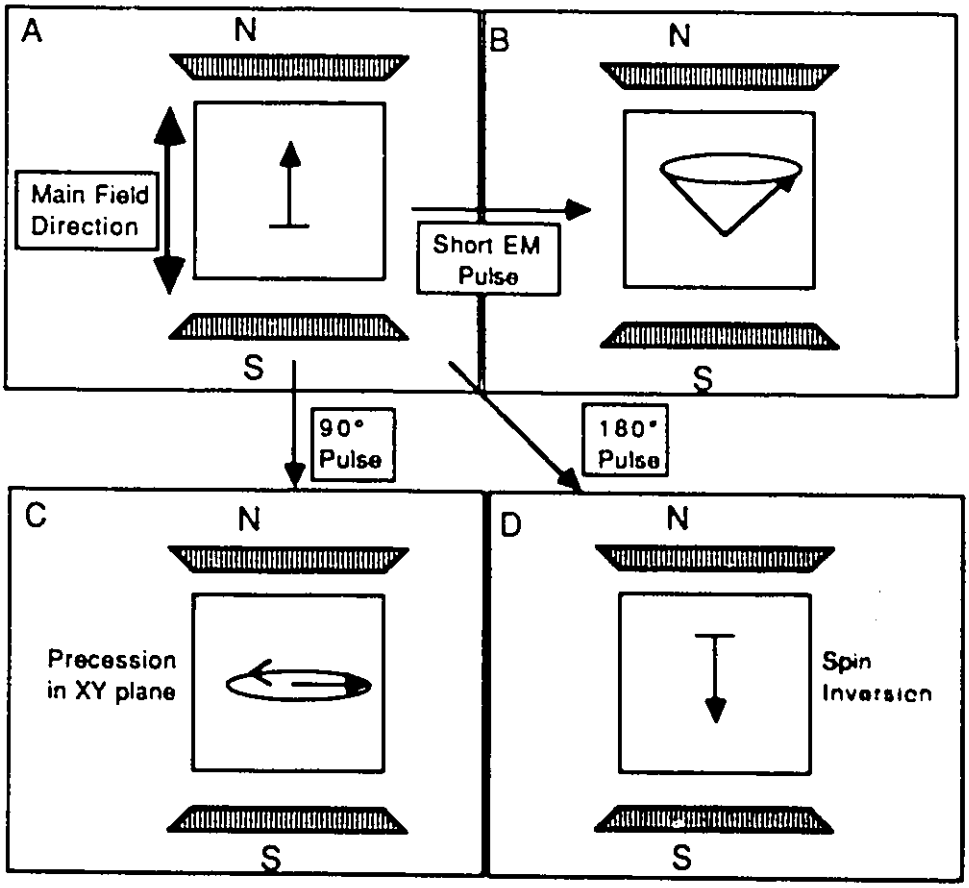

Figure I.3.1.c. Effect of EM pulses of different size on the direction of the net magnetization of a spin population. (Population is depicted as an arrow between magnet poles) A:M_Z has a value G, M_{XY} = zero; B:M_Z < G, M_{XY} > zero; C:M_Z = zero, M_{XY} = G, D:M_Z = -G, M_{XY} = zero (Foster, 1983).

I.3.2. Relaxation

Any excited spin population undergoes processes of energy loss known as relaxation, which results in a return of the population to its equilibrium state (Foster, 1983). The two main methods of relaxation are thermal vibration and loss of spin orientation (Fukushima, 1981). No energy is lost from the system during either of these processes.

Energy lost as a result of thermal vibration, also known as spin-lattice relaxation, is the result of coupling between the spin of the nucleus and its surroundings (lattice). The lattice includes both the surrounding molecular and atomic matrix. This process depends on diffusion, molecular rotation, and lattice vibration. The time required for a spin population to relax (re-establish itself along Mz) using this method alone is know as T_1 (spin-lattice relaxation time or longitudinal relaxation time depicted in Figure I.3.2.a.). This is an exponential time constant that characterizes the growth or decay of the component of magnetization parallel to the external field.

Energy lost as a result of the interaction between the spin of the nuclei and the spins of its neighbouring nuclei is known as spin-spin relaxation. The time required for a spin population to relax (re-establish itself along Mz) using this method alone is know as T_2 (spin-spin relaxation time or transverse relaxation time). This is an exponential time constant that characterizes this decay of confinement of magnetization perpendicular to the external field. The process may be thought of as a fanning out of the individual dipoles of Mxy as they spin around the Z axis (Figure VI.3.a).

In solutions (biological systems) relaxation is a complex process involving both methods of relaxation. For a single Lorentzian1 line (the predominent lineshape of most nuclei in solution) the decay of the magnetization in the XY plane, following a 90° pulse, will be exponential with time constant T_2^* (T two star) (Fukushima, 1981) Magnetization will re-establish itself along Mz with time constant of T_1. The decay rate for the magnetization in the XY plane is usually larger than or equal to the decay rate of the magnetization in the Z direction.

The decay rate constant in the XY plane $1/T_2^*$ consists of a term related to the recovery rate constant for magnetization along Z, $1/T_1$, as well as other mechanisms which give rise to a dispersal of the magnetization only in the XY plane eg. $1/T_2$ and $\partial\Delta H0$ (due to magnetic field inhomogeneity).

In a typical solution T_2^* is predominently determined by T_1 (reorientation and diffusion). In a typical solid T_2 is much more likely to determing T_2^*, as a result of the effects of these fields from neighbouring spins do not cancel as they do in liquids

Both T_1 and T_2 can affect the shape of a spectral line In cases where T_1 is especially short, line broadening occurs; when very long, power saturation can occur, resulting in signal loss When T_2 is very short, and spin orientation redistribution occurs between surrounding spins, the absorption line is broadened This phenomena is obviously enhanced in solid or more concentrated samples

The disruption of the magnetization by the incident 90° rf pulse produces a sinusoidally decaying electromotive force (EMF) in the detector coil The original height of this is related to Mxy (ie proportional to the effective number of spins in the

---

1 Lineshape wherein the full width at half height of the the line is $2/T_2^*$

sample). This signal is known as the Free Induction Decay (FID) (Fukushima, 1981). The decay rate for magnetization in the XY plane is usually larger than or equal to the recovery of the magnetization along the Z direction.

If the spin system were at equilibrium when the 90° incident pulse was applied to the magnetization, the spectral signals will be proportional to the number of nuclei in the sample. If the magnetization is re-perturbed and re-sampled before all of the spin isochromats have returned to equilibrium they will not contribute their maximum potential to the magnetization in the XY plane at the time of signal sampling. In the absence of refocussing pulses, a waiting period of 3-5 times the length of the T_1 period of the nuclei of interest should be used between successive applications of excitation pulses and their subsequent acquisition periods (Meyer, 1982). As the T_1's of nuclei in various molecules may be different, the relative degree of saturation for each signal may differ, and therefore signal amplitudes measured under partial saturation conditions will not be proportional to the number of nuclei in each species.

Due to the insensitive nature of the NMR experiment and the preponderance of random distributions known as "noise", it is often necessary to repeat and average signal aquisition many times if a sufficiently large signal is to be acquired so as to permit its measurement (Fukushima, 1981). The accumulation of the non-random signal is proportional to the number of experiments, while noise accumulates at a rate proportional to the square root of the number of experiments. For this reason, the ratio of signal to noise (the ratio which determines whether or not an experiment can be successfully conducted), increases as $\sqrt{n}$ where n is the number of acquisitions. Each acquisition requires a finite amount of time for completion, thus it can also be said that the signal to noise ratio increases with time, or, more accurately, $\sqrt{t}$ (Meyer, 1982).

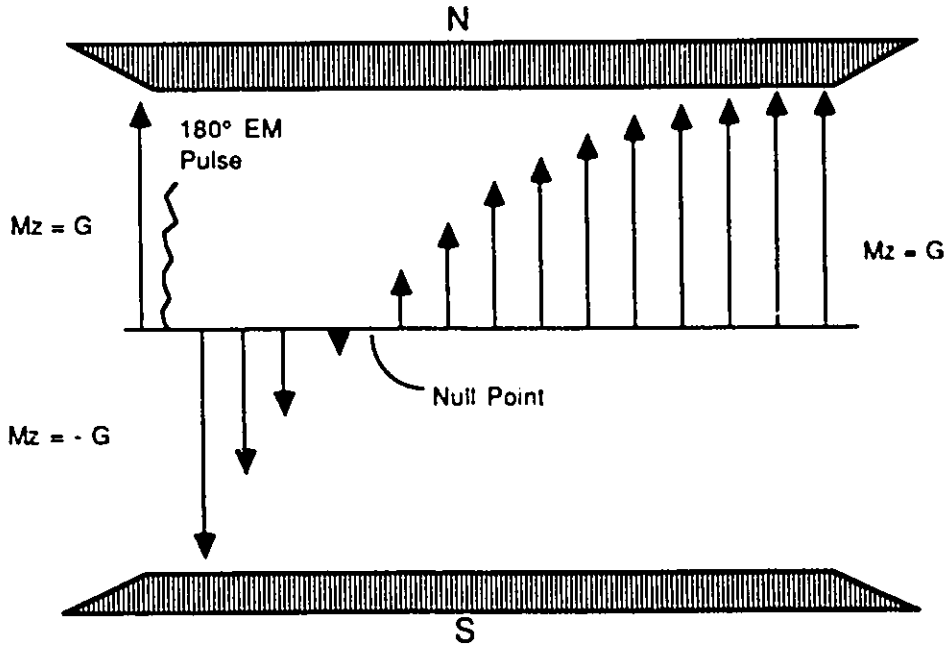

Figure I.3.2.a. Longitudinal relaxation after the spin system has received an inverting EM pulse. The arrows represent the magnetization vector at various times after spin inversion. The time constant of decay is T_1. T_{null} is the point at which the magnetization vector is zero (Foster, 1983).

I.3.3. Fourier transformation

If information concerning the time course of the decay of the signal averaged FIDs is to be of use in elucidating the amounts of certain nuclei and their respective chemical environments, a means must be developed which allows the translation of one type of information into the other. The mathematical operation decomposes the output pulse into its frequency components to permit plotting as a spectrum is called the Fourier transform. The application of this method of multiplexing was not used in NMR until 1966 (Foster, 1983).

Simply stated, any function (f(t)) can be expressed as an infinite series of cosine and sine waves or Fourier series as suggested below (Fukushima, 1981).

$$f(t) = \sum_0^{\infty} An \cos\left(\frac{n\pi}{T}\right)t + \sum_0^{\infty} Bn \sin\left(\frac{n\pi}{T}\right)t \qquad \text{I.3.3.i}$$

This expression is valid over the region -T< t< T. When we carry out the mathematical operation of Fourier analysis we deal not with the Fourier series but with the related integral in which the variable t is not restricted to the region T to -T but spans from ∞ to -∞. One representation can be readily transformed to the other using the following formula

$$A(w) = \frac{1}{2\pi}\int_{-\infty}^{\infty} A(w)e^{iwt}\,dt \qquad \text{I.3.3.ii.}$$

The translation from time space to frequency space requires that the amplitude of a wave A(t) is multiplied by a sinusoidal wave of unit amplitude, exp (iwt), and this product is added over all times at frequency w; where w is equivalent to the angular frequency 2wf.

For example, a sine wave can be represented on graphs depicting amplitude vs. time or amplitude vs. frequency. Monochromatic by definition, the spectrum on the latter graph would be a single peak located at the sine wave frequency. The width of the peak would be inversely proportional to the duration over which the sine wave exists. If two such sine waves were superimposed, the resultant amplitude vs. time graph would relate an interference pattern with a simple series of beats. The amplitude vs frequency graph would relate two spikes, one at each of the appropriate frequencies.

In the NMR experiment, the simple monochromatic sine wave is replaced by a multichromatic exponentially decaying sinusoidal wave. When algebraically summed these waves result in a complex interferogram or FID, which is what is actually recorded during an experiment. The Fourier transform of this FID yields a the spectrum

of the sample under investigation. In the case where two lines of different frequency lie close together, the ability to distinguish between them is determined by how long the FID is sampled, the concentration of the respective nuclei and their sensitivity.

The advantage of Fourier Transform (FT) NMR in the characterization of a complex interferogram is immediately obvious if we consider the amount of time it would take to characterize the amount and frequency of certain nuclei using the amplitude vs time method of analaysis. The latter method would require as many experiments as there were nuclei in different environments whereas the FT method, a multiplexing technique, requires but one experiment.

1.4. Quantitation of metabolites

NMRS measurement of the concentrations of specific tissue metabolites presents a difficult application because the signal, although proportional to metabolite concentration, is critically dependent on tissue state, volume, and geometry each of which is often ill-defined and not easily estimated. For this reason the issue of absolute concentrations has often been avoided (Thulborn and Ackerman, 1983; Wray and Tofts, 1986).

As previously discussed, NMR provides information on the relative amounts of nuclei in different chemical environments. If this information is to be translated into quantitative information of absolute metabolite concentrations *in vivo* or *in vitro* three problems must be overcome:

1. The volume of tissue within the effective magnetic field must be determined
2. The NMR signal giving relative differences in phosphate metabolites must be converted into an absolute value with some appropriate calibration method

3. The volume of the particular compartment, within the whole tissue volume, in which the metabolite is contained in must be estimated.

In order to resolve these problems, attention must be given to tissue geometry, tissue composition, and the chemical and physiological stability of the specimen. Disregard of these considerations can yield inconclusive results. For example, the metabolite composition of liver, sampled from the exterior of a rat, will harbour contributions from overlying muscle tissue. (Geoffrion, 1987; Helzberg, 1987). Similarly, coils designed for the examination of muscle metabolites of mouse hind limb sample the entirety of the heterogeneous muscle population of the leg.

The first problem (tissue volume sampled) has physical and physiological components which are very complex and show considerable interrelations. It must be recognized that NMR spectroscopy is not suitable for all investigations into metabolite measurement. The sample must be accessible to the coil or vice versa, fit into a probe, and its constituents must be concentrated enough to be measured spectroscopically (Gadian, 1982; Helzberg, 1987).

If the sample meets all of these requirements then an appropriate spectrometer, as well as spectroscopic apparatus including probe and coil must be selected. In addition to these hardware considerations, much attention must be given to the selection of appropriate pulse sequences with which to examine the specimen. Pulse sequences now exist which make possible the localization of specific volumes of tissue from within animals or their organs (Bendall, 1984). Such factors must be taken into consideration when decisions concerning coil and probe are made. Similarly, the longevity of the sample must be considered when selecting such parameters as the length of the experiment, the recycle time and pulse angle (Dawson, 1978). For example, if the stability and concentration of the metabolites of the sample permits, it is possible to

obtain sufficient information from a sample by waiting for all magnetization to return to equilibrium before pulsing and sampling again. In other instances, the time may not be afforded and rapid recycling times between acquisitions may be necessary (Dawson, 1978; Billadello, 1984).

Presently two approaches are used to resolve the second problem of conversion to absolute values. They fall into two categories which we will call the "ratio" method (Doyle and Barany, 1982) and the "assumption" method (Dawson, 1982; Meyer, 1986; Bevington, 1986).

The ratio method, simply stated, relates the ratio of the peak areas of metabolites of interest to the peak area of a standard solution, included with the sample at the time of the experiment, of known volume and concentration. For example, in a phosphorus spectrum the ratio of the peak areas of an internal standard capillary of phosphoric acid to CrP can be used to determine the concentration of creatine phosphate. Specifically if the phosphoric acid peak area is 5 units when at a concentration 50 mM and volume 0.2ml then CrP, peak area 2 units, must be present at a concentration of 4 mmoles if it is contained in a volume of 1ml.

In order for this method to be accurate, one must assume that the signal intensities wrought from any and all of the sampled portions of the standard must be equivalent to any and all of the sampled portions of the specimen. For this assumption to be true, the sensitive volume of the coil must be fully characterized and there can be no uncertainty as to what portion of the standard is being examined (Thulborn and Ackerman, 1983). These are stringent if not impossible conditions to meet for most in <u>in vivo</u> or <u>in vitro</u> NMR experimental conditions, especially if a surface coil is being used for observation (Bendall, 1984). If suitable conditions could be found for this method it would be advantageous to have a standard which was visible at two frequencies.

in order that concentration measurements at one frequency could be checked against the concentrations of an invariant metabolite at another frequency.

The "assumption" method, currently the most used, assumes a concentration of one metabolite in a spectrum and subsequently compares the peak areas of other metabolites to the peak area of this first metabolite (Meyer, 1982; Shoubridge, 1985,1984; Meyer, 1986). The concentrations of the other metabolites are established according to their peak areas relative to the "reference" metabolite (ie a doubling in peak area represents a doubling in concentration). The most common reference metabolite used in ^{31}P NMR is the ß peak of ATP (Shoubridge, 1984; Bevington, 1986). This metabolite is used because it has been found that this peak is free from contributions from other metabolites, and because the chemically measured ATP concentration is thought to be entirely NMR visible (Dawson, 1980 and Meyer, 1982).

In comparison to the "ratio" method, the "assumption" method is more readily implemented as it does not require the use of any external standards. There are, however, two major disadvantages to the latter approach. Firstly, in tissues for which no prior measurement of the metabolite of interest has been made, making an assumption regarding its concentration could have grave consequences. Secondly, in tissues that are undergoing changes in concentration of the reference metabolite, this method is of little use. In instances where the concentration of the reference metabolite is changing, as in the case of creatine depletion (Shoubridge, 1984), the "assumption" method has been applied after setting the values of the metabolites equal to those from the biochemically determined concentrations at rest. In other instances, for example, during muscle contraction (where the concentrations of all the metabolites are changing), concentrations are determined by making comparisons to the resting spectra. This

method makes many obvious assumptions which could easily lead to errors in measurement.

An alternative to these methods was recently recommended by Thulborn and Ackerman (Thulborn and Ackerman, 1983). Simply stated, the proton signal, which is determined by the number of water molecules in the field (which is in turn directly related to fat free tissue volume) provides a reference for the phosphate signal. Thus the ratio of phosphate signal: proton signal effectively gives the moles: volume ratio. Absolute concentrations can then be obtained from the signal given by a set of standard solutions.

Ackerman's thesis is based on the assumption that in instances where the alternating magnetic field distribution, B1, is determined predominantly by coil geometry, the magnitude of B1 for a multiply-tuned coil will map equally over space for each coil frequency. This allows the matching of flip angles over space for each nuclide of interest. Since the homogeneity of the B1 distribution is not critical, non-uniform B1 fields, such as those generated with surface coils, can be used for NMR quantitation by either a spin imaging or chemical shift approach (Thulborn and Ackerman, 1983)

Consider the case where the resonances under consideration are ^{1}H from H_2O and ^{31}P of CrP and the other PCM of muscle. When the ratio of signal intensities for these two nuclides is obtained, it can be used to calculate the individual concentrations of each metabolite. This is achieved simply by the obtained ratio and a standard curve, which is established by plotting the relative signal intensities of the same nuclei under identical conditions from a "mock" sample. Solutions of a variety of volumes and concentrations are used to produce this curve, which contains the ratio of signal intensities on the ordinate axis and concentration of the nuclear species of interest on the abscissa (Thulborn and Ackerman, 1983)

Furthermore Thulborn (Thulborn and Ackerman, 1983) hypothesizes that ^{23}Na NMR when used in conjunction with ^{1}H NMR can provide accurate intracellular concentrations of other NMR visible metabolites. The basis of this proposal is outlined below.

A more complete examination of the "Ackerman method" has been made by Tofts and Wray (1985). Tofts states that in order to develop a practicable method for measuring concentrations, three NMR effects must be taken into account. These are: 1) the effect of sample electrical conduction losses on the flip angle, 2) the effect of sample losses on the coil sensitivity, and 3) the time dependent changes in the spectrometer.

In order to correct for this first modifier of signal intensity, the doubly tuned probe used in her experiments is tuned and matched using a tank circuit containing a variable capacitor and an impedance bridge. The effects of sample conduction losses are then related to the change in the 90° pulse length found for "dummy samples" and the differing amounts that the variable capacitor is tuned in or out using a standard curve and the equation $T_{90°} = K_2\ 90°\ c\ (t)$ (where $T_{90°}$ is the 90° pulse length, t is the number of turns of the capacitor, c is the capacitance at that number of turns and K_2 is the slope of the standard curve relating $T_{90°}$ and the number of turns used to tune the capacitor) (Tofts and Wray, 1985).

As previously mentioned, matching the pulse widths less difficult using solenoid coils than with surface coils. For this reason, the pulse widths can be standardized in each experiment by making an accurate determination of both 90° and 180° pulse widths (Thulborn and Ackerman, 1983; Tofts and Wray,1985).

Any effects of sample electrical losses on the coil sensitivity this are corrected for by using the method outlined above; ie determining the ratio of signals of two nuclei gives the ratio of concentrations which in turn accounts for differences in sample conduction.

The third concern raised by Toft's and Wray regarded effects of time dependent changes in spectrometer sensitivity (a.k.a. gain) on signal measurement. These effects are monitored by applying a known input voltage to the pre-amplifier and measuring its output before and after each experiment. If the changes in amplification are greater than a predetermined amount (ie. 10% in Wray's experiments), the experiment is repeated repeated/redone as it was thought to be invalid/inaccurate. If the amplification change is less, then the change in the ' gain' can be used to correct the peak areas by using it as a multiplicitive factor applied against the resulting values in order that they might be compared to the starting values.

As a hypothesis I propose that, when used in conjunction with one another (as proposed by Thulborn and Ackerman), ^{31}P, ^{1}H and ^{23}Na NMRS can provide quantitative measurements of intracellular metabolite concentrations of rat hind limb muscles in vivo.

1.5. Choice of test system

The choice of an appropriate system for testing an hypothesis is critical. Central to the purposes of our experiments (see Section II), the appropriate test system must undergo large changes in NMRS measurable metabolite concentrations. These changes must also be independently measured by another reliable technique. Other important criteria to consider when choosing a test system are its relevance and reliability (Gadian,

1982; Green, 1979). A third, and less important criterion is convenience, a factor which should include an examination of cost.

The creatine-depleted rat was chosen as the system in which to perform our experiments, as it fulfils all of the requirements outlined above. The following paragraphs affirm the match between these criteria and describes some of the characteristics of the rat hind quarter.

The use of the isolated perfused rat hind quarter has become an important and widely accepted means of studying muscle metabolism in vitro. This is a result of the advantages afforded by the hind limb over analogous preparations. Firstly the preparation is composed of skeletal muscle of one predominant fibre type (type IIb). Second, it possesses similar anatomical construction to that of man, more specifically similar number, distribution and sizes of muscles (Armstrong, 1984). Third, in the in vitro situation the contents of the perfusion medium can be well controlled, the delivery of nutrients to muscle can occur via normal vascular channels, and substrate uptake or metabolite output is easily measurable (Hood 1986). The use of in vivo NMRS gives the experimenter all of the advantages of the in vitro preparation without detracting from the physiological relevance of the experiment. Although primarily used for the study of resting metabolism, NMRS has been increasingly used for the study of muscle metabolism during contraction when the rate of energy expenditure is greatly increased.

The rat hind limb has been used as a model for the study of muscle metabolism for over half a century. It is a very relevant test system as its muscle fibre types, metabolism, mechanics and biochemistry are similar to those of other mammals including man. The rat is of an very appropriate size for NMR spectroscopy, initial purchasing and maintenance costs are low, and it is quite easily managed in captivity (Green, 1979).

Creatine analogue feeding was chosen as a means by which to induce continuous changes in muscle metabolite concentrations in order to fully test our method of NMR quantitation. The chemistry of creatine synthesis and analogue substitution has been fully reviewed by Totosy de Zepetnek (1984). In brief glycine and arginine are condensed to form guanidinoacetate and ornithine via the catalysis of amidinotransferase. Subsequent N-methylation transforms guanidinoacetate into creatine. Although the highest concentrations of creatine and creatine phosphate occur in the heart, skeletal muscle and brain, the reactions involved in creatine synthesis occur primarily in the liver (Bessman, 1985). Creatine is transported by the plasma (concentration ~ 0.40 mM) to the aforementioned tissues, where it is actively concentrated (~ 5 mM), and simultaneously phosphorylated (Walker, 1979).

Studies on creatine uptake by muscle led to the discovery of ß-guanidinopropionic acid as an inhibitor of creatine entry into muscle. Guanidinopropionate inhibition is competitive, the Km being 0.2 mM (Fitch 1968). As a result of this inhibition, the free plasma creatine (as well as intramuscular creatine phosphate) of animals fed creatine analogues are rapidly and significantly depleted. In these instances creatine production does not cease, rather its entry into muscle is impaired and it is subsequently excreted in the urine.

The molecular weight of creatine and its analogue, GP, are identical. The only difference in their composition lies in the location of a methyl group (Figure 1.5 a). The similarity of structure and nature of inhibition of these compounds suggests a substrate specific transport site for creatine (Shields and Whitehair, 1973). This specificity was exploited by Shields in order to deplete muscles of their creatine by feeding mature rats the analogue as part of their daily diet. In his experiments a fifty day depletion period reduced muscle creatine by 75%. Fitch (1974) found 75% depletion of free (plasma)

creatine after a 42 day feeding trial. In addition, Fitch found a 93% depletion of CrP compared to control animals of the same age, and a concomitant phosphorylation of GP. The ATP levels of these animals decreased by 52%.

More recently Shoubridge (1984) and Meyer (1986), obtained results concerning the pH and phosphagen changes of creatine-depleted rat muscle. In these experiments, Meyer fed a 2% GPA (guanidinopropionic acid) enriched diet ad libitum to mature rats (150-200g) for a 3 month period. CrP decreased by 92% and the ATP decreased by 44% of control values. Simultaneously GPAP (guanidino propionic acid phosphate) increased to 25.3 µmol/g wet weight. Shoubridge reported a 90% and a 50% reduction in the concentrations of CrP and ATP respectively, following feeding weanlings a diet enriched with 1% GPA. Creatine and Pi concentrations were similar in both groups. The total phosphagen content was about 25 µmol/g in both control and analogue fed animals.

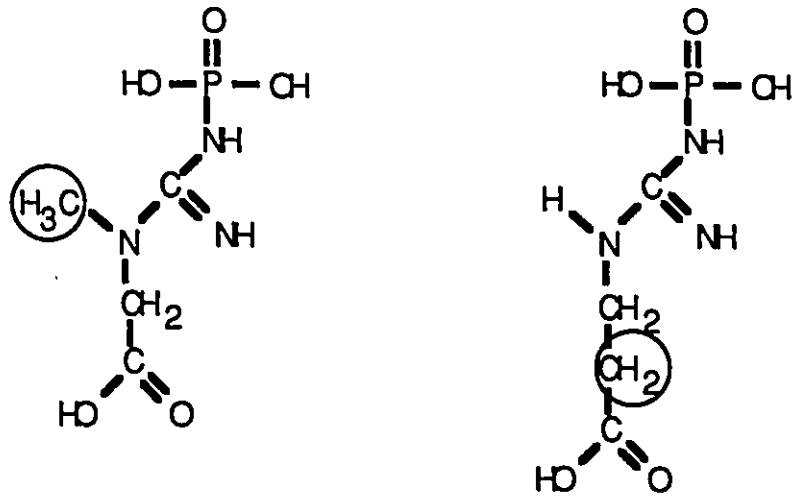

Creatine Phosphate

Guanidinopropionate Phosphate

Figure I.5.a. Chemical structure of creatine phosphate and guanidinopropionate phosphate

II. STATEMENT OF PURPOSE

In order for a technique to be truly useful in monitoring the energetics of a dynamic physiological system it must be sensitive, selective, non perturbing and quantitative.

Previously, authors have used freeze extraction and subsequent biochemical analysis to quantitate metabolites in physiological preparations (Crow and Kushmerick, 1983; Beis and Newsholme, 1975; McGilvery and Murray, 1974), however, this technique is invasive. Only recently has it been possible to examine metabolites in these preparations in their truly resting state (Hoult et al.,1974 and Barany et al 1975) Yet, NMRS provides us with information of the relative amounts of visible metabolites not their absolute concentrations (Crow et al, 1983).

Only within the last five years have attempts been made to establish effective procedures to quantitate phosphorus-containing metabolites in vivo This report uses the recently proposed methods of quantitation of Ackerman (Thulborn and Ackerman, 1983) and compares this with results obtained from biochemical assays, to monitor changes in CrP and ATP in rat hind limb resulting from the inclusion of a creatine analogue in their diet .

As discussed above (section I.4), static or equilibrated physiological environments facilitate the use of NMRS as a means of quantitation of metabolite levels This is due to the feasibility of inter-technique comparisons of metabolite concentration between NMRS and another suitable quantitation method (eg biochemical analysis and the concentration of ATP) Continuously changing levels of the metabolites of CrP GPP (guanidinopropionate phosphate) and ATP in the depleted skeletal muscle provides a very rigorous system in which to compare the abilities of these quantitation techniques

because the previously accepted constant standard (the beta peak of ATP) can no longer be used as a point of reference. Consequently, any truly quantitative NMRS technique will be adequately tested in such a dynamic physiological system.

Weanling rats were monitored using the "Ackerman NMRS quantitation method" while being depleted of their creatine, using the presently accepted depletion technique for four weeks. Subsequently they were re-fed a normal diet for two weeks. Simultaneously, biochemical assays were performed on another population of rats treated identically, and the results of the two techniques were compared.

II.1. Objectives

The questions we addressed while examining these techniques included:

1. Can ^{1}H and ^{31}P NMRS be used as a method of determining the absolute concentrations of metabolites, whose amounts are known to be fluctuating, and of following the time course of these changes in concentrations in vivo?

2. What are the rates and extent of depletion and repletion of creatine phosphate and ATP and the rates of appearance and disappearance of guanidinopropionate phosphate during the six weeks the rat is on the depletion/repletion diet?

3. Does the information provided by ^{23}Na NMRS or flame photometric analysis of sodium and potassium of rat hind limb provide an improved means of quantitating intracellular metabolites by providing a reasonable estimate of extracellular volume?

III. MATERIALS AND METHODS

There are two distinct parts to this investigation: the NMR spectroscopy and the biochemical analysis. They differ only in the ultimate experimental destination or use of the animals in this study. These differences are reflected in all sections of the methods

III.1. Treatment of animals

III.1.1. General

The animals used in this study were weanling (23 day old), male, Sprague Dawley rats obtained weekly from Charles River Canada Incorporated of Montreal

After arrival and during feeding the rats were weighed 1-2 times weekly to monitor their continued growth. The animals of the NMR group had their right leg circumference and diameter measured weekly at the ankle, calf and knee to monitor the change in volume of their leg. The cross sectional area of the leg at the height of the calf was determined by assuming that the calf is either (a) elliptical and that the measured lateral and longitudinal thicknesses of the calf were the diameters of the ellipse or (b) a circle and that the circumference would in turn provide a radius. Equation III.1.1.i relates the measured parameters to the cross sectional area using assumption (a)

$$\text{Cross sectional area} = \pi \frac{a}{2} \frac{b}{2} \qquad \text{III.1.1.i}$$

where a and b are the lateral and longitudinal thicknesses respectively

III.1.2. Dietary regime

Upon arrival the rats were separated randomly in pairs into one of two groups; control or experimental (Figure III.1.2.a.). The rats in all groups were fed 10 grams of ground Purina Rat Chow a day for the period the rats were on the diet as per the protocol of Totosy-de Zepetnek (1984). The feed of the rats in the experimental group was supplemented, for the first four week period, with 1% GP which was synthesized in our laboratory from ß-alanine and cyanamide according to the method of Rowley (1971) and tested for purity by measuring melting point depression. The depression was never more than three degrees, and for this reason it was assumed that the impurity of the prepared GP was minor (Totosy de Zepetnek, 1984). The paired rats were further divided (Figure III.1.2.a.) into either the NMR group or Biochemistry/Flame photometry (BF) group. The rats remained on the described diet for a total of six weeks if in the NMR group, or between zero and six weeks if in the BF group.

III.1.3. Anaesthesia

All anaesthetics were administered intra-peritoneally. The anaesthetic used for all documented experiments was fresh sodium pentobarbital (Somnotol, MTC Pharmaceuticals), and was given in undiluted form at a dose of 65 mg per kg body weight. A combination of Ketamine (Roche Products Ltd.) and Xylazine (Haaver-Lockhart Ltd.) was used on some rats of the NMR group for some preliminary equipment tests (Green, Knight, Precious, and Simple, 1981).

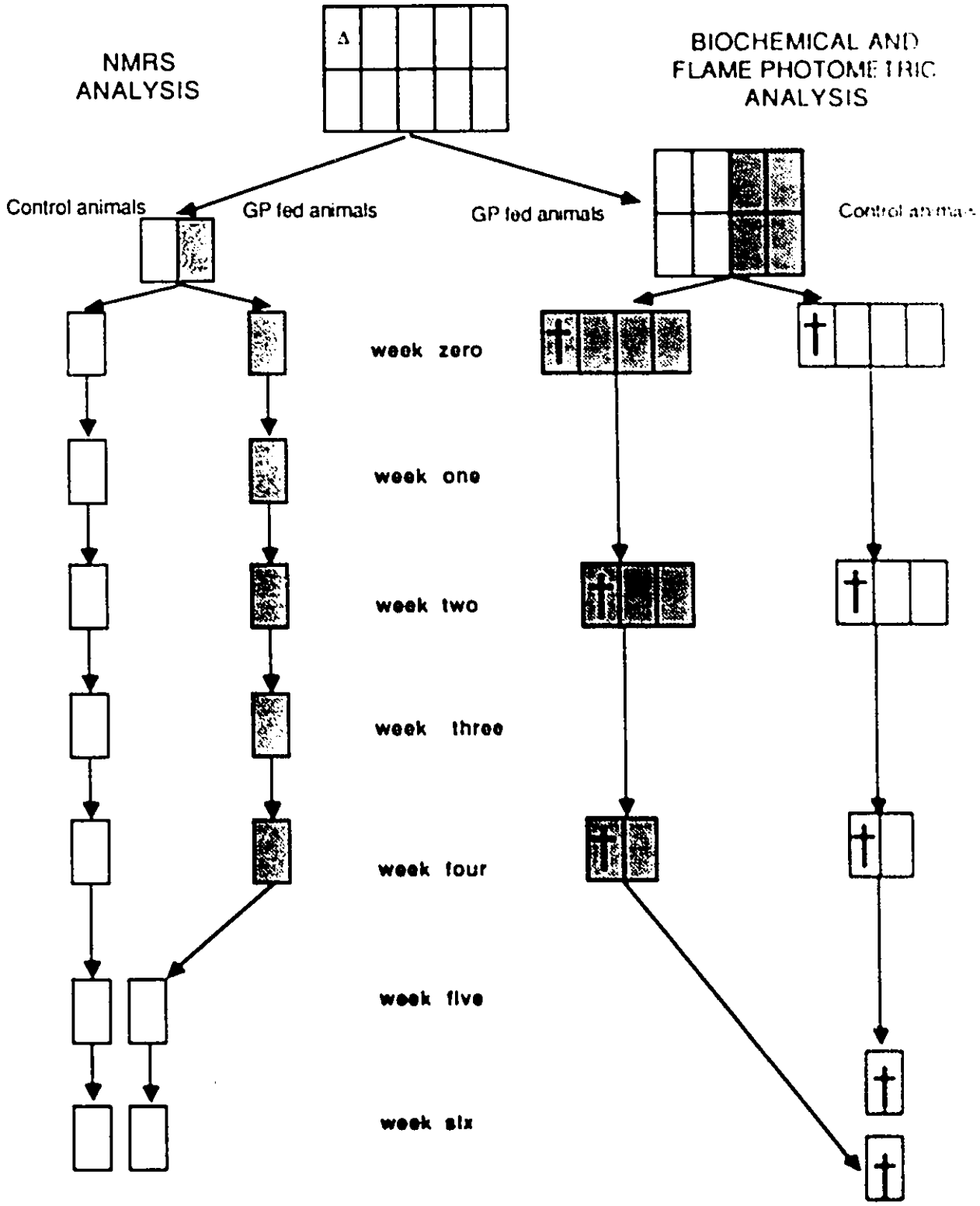

Figure III.1.2.a. Time course and ultimate use of rats placed on dietary regime
Δ each small rectangle represents 6 animals † represents the sacrifice of that group of animals.

III.2. Dry to wet weight ratios

Simultaneous to the removal and freezing of the right gastrocnemius for biochemical analysis, the left gastrocnemius was removed for the determination of the dry to wet weight ratio of this muscle group. Three pieces of approximately 50 mgs were removed from each gastrocnemius and dried to constant weight at 42° C in a vacuum oven.

The weight loss or gain during storage was tested by removing 0.2 -0.01g pieces of left gastrocnemius muscle and placed in a -90° C freezer and weighed weekly for a three week period.

III.3. Biochemical techniques and assays

III.3.1. General

Sections of the gastrocnemius (G_M, Figure III.3.1.a.) muscles from at least 4 normal and 4 GP-fed rats at each of 0, 2, 4 and 6 weeks of feeding were used for biochemical analysis (see Figure III.3.1.a. and Table III.3.1.a.). This region was selected for a number of reasons. Firstly, the gastrocnemius (40% of the total volume of the hind limb) is comprised of 93% fast twitch fibre (28±5% F.O.G. (fast oxidative glycolytic), 65±5% F.G. (fast glycolytic), 7±1% S.O. (slow oxidative)[1]), hence it is generally representative of the muscle fibre type composition of whole rat hind limb which is 95 % fast twitch fibre (18.7% F.O.G., 76.2% F.G. and 5.1% S.O.). This parallel is of import as the entire hind limb is examined by the NMRS experiments as such, a suitable point of comparison for the two experimental techniques must be determined. Second, despite the fact that quick freezing and analyzing the entire gastrocnemius would be more representative of the whole hind limb, only the first

---

1 The concentration of fast fibres at the surface of the gastrocnemius is thought to be greater than that of the average for the entire gastrocnemius (Armstrong, and Phelps, 1984).

millimetre of surface muscle muscle is frozen sufficiently rapidly to provide accurate estimations of CrP.

Muscle or muscle group	Fibre type	Proportion (%)[f]
hind limb	FOG	18.7
	FG	76.2
	SO	5.1
gastrocnemius (mixed)	FOG	28
(61 % of the total mass	FG	65
of the hind limb)	SO	7

$$f \text{ Proportion} = \frac{\text{estimated mass for each fiber type}}{\text{total estimated masses for all fiber types}} \times 100$$

Table III.3.1.a. Estimated total proportions of each of the fibre types of the hind limb muscles of the rat (taken from Armstrong and Phelps, 1985). The gastrocnemius occupies 61 % of the total mass and area of the hind limb of the rat. FOG=fast oxidative glycolytic, FG=fast glycolytic, SO=slow oxidative

After the rat had reached the appropriate level of anaesthesia both hind limbs were shaved and the sciatic nerve of the right leg was severed at the level of the upper thigh. After a ten minute waiting period to allow spontaneous muscle contractions and tension generated as a result of the severing of the nerve to subside (Tolosy de Zepetnek, 1984). The skin surrounding the right calf was removed. Subsequently, the biceps femoris and semitendinosis muscles which encapsulate the gastrocnemius and underlying soleus and plantaris were retracted and excised (Figure III.3.1.a). The achilles tendon was then attached to a silk thread, severed and the gastrocnemius separated from the leg with gentle tension. The gastrocnemius and underlying attached muscles were then frozen back to front between aluminium blocks pre-cooled in liquid nitrogen and severed

at the level of the knee. The flattened muscles were then placed in liquid nitrogen. The entire freezing procedure took less than 2 seconds to complete.

Thin slices of muscle were removed from the medial-posterior portion (Armstrong, 1984) of the gastrocnemius group with a razor while the rest of the muscle was held in a bath of liquid nitrogen with frozen forceps. Thin slices (0.5-1mm, 25-70 mg), were removed from the 2 to 3 millimetre thick gastrocnemius with a razor and transferred to pre-cooled screwcap, plastic tubes for storage at -70° C for subsequent enzymatic determination of energy metabolites, or for flame photometric determination of sodium and potassium content. This portion was chosen since its fibre type population is very similar to the total fibre type composition of the hind limb (76% F.G., 19% F.O.G., 5% S.O.) (Armstrong, 1984), and because it is free of contaminating slow twitch soleus (see Figure III.3.1.a. and Table III.3.1.a.). This portion was also the first to contact the aluminium blocks and therefore assumed to be the portion of the gastrocnemius most quickly frozen (Olgin, 1985).

Prior to extraction, the sample muscle weight was determined in an insulated styrofoam vessel, then transferred to pre-weighed plastic tube to be ground to powder with a pre-cooled stainless steel rod in a stainless steel block.

After grinding, the tubes were placed on ice and 2 mLs of 6% perchloric acid was added, followed by vortexing, and the tubes were allowed to stand for fifteen minutes. Following vortexing and centrifugation at 10,000 g for ten minutes, the supernatant was decanted into a cold fresh tube leaving a protein precipitate. The supernatant was neutralized with 300 µL of 2.5 M potassium bicarbonate. The resultant mixture was centrifuged at 10,000 g for 10 minutes. The supernatant was either refrozen immediately at -70°C for future use or assayed immediately.

The expected concentrations of the PCM (phosphorus-containing metabolites) of the hind limb and the gastrocnemius can be predicted by using estimations of the PCM concentrations (Mainwood, 1987) of soleus (predominantly slow twitch) and extensor digitorum longus (predominantly fast twitch), combined with information, provided by Armstrong (1985), about the relative masses of each of the muscles of hind limb and the percentages of slow and fast twitch in each. The PCM concentrations of these muscles and the estimated concentrations of gastrocnemius and the entire rat hind limb are shown in Figure III.3.1.b. Note the small difference between the predicted PCM concentrations of hind limb and gastrocnmemius. Estimates were obtained using the method outlined in Appendix VI.6.

An error in the sampling of the gastrocnemius, although highly unlikely, might include contributions from the white or red gastrocnemius. Sample biasing, if as great as 20% could change the obtained gastrocnemius PCM concentrations by up to 14%. Such an error, although significant, would not preclude the use of the gastrocnemius as representative of the entire hind limb musculature or vice versa.

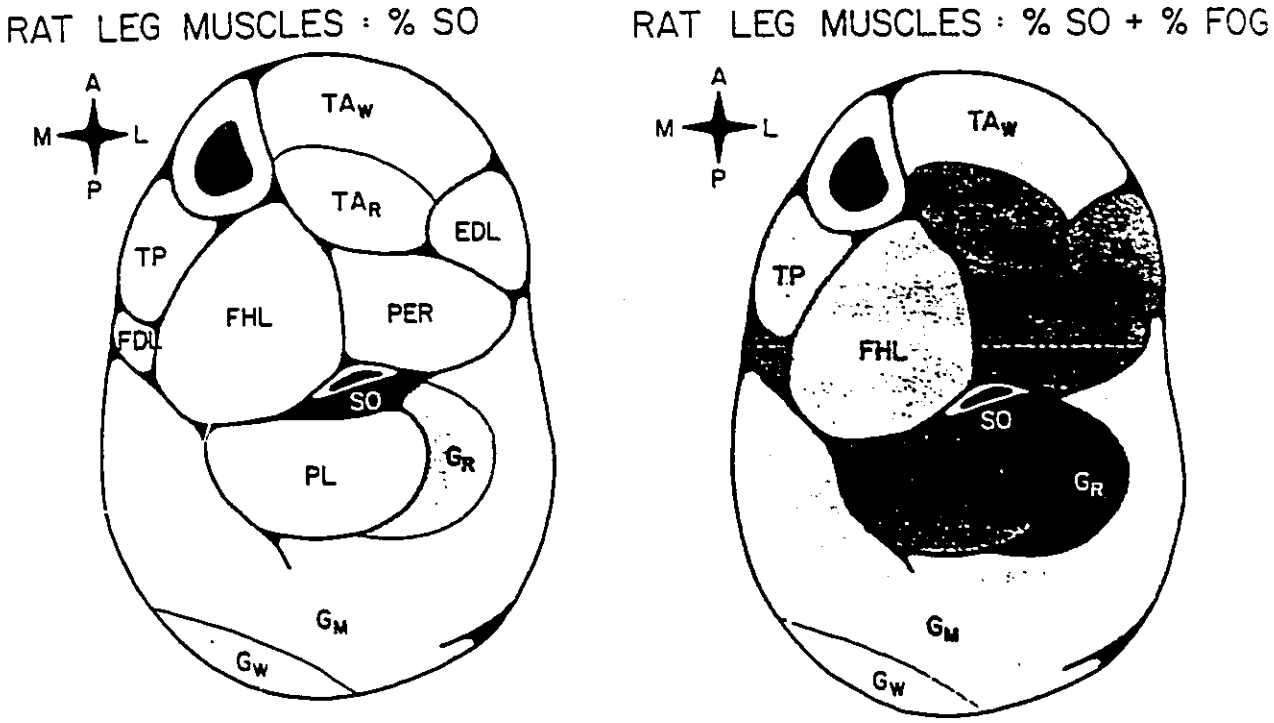

Figure III.3.1.a. Cross sectional view of the rat leg muscles depicting the position of the individual muscles. R depicts red, W white, and M middle. The shading intensity is proportional to the percent slow oxidative fibres. The directions are indicated are anterior (A), posterior (P), medial (M) and lateral (L). The muscle name abbreviations are gastrocnemius (G), plantaris (PL), soleus (SO), tibialis anterior (TA), extensor digitorum longus (EDL), tibialis posterior (TP), flexor digitorum longus (FDL), flexor hallicus longus (FHL), and peroneals (PER). (Taken from Armstrong and Phelps, 1984)

Muscle or muscle group	Metabolite	Concentration Normal (mmol/ kg wet weight)	Gp-fed[f]	Concentration Normal (mmol/ L tissue fluid)	Gp-fed[f]
soleus*	CrP	11.7	1.0	15.7	1.3
	ATP	3.9	2.6	5.2	3.4
	GPP		35.5		47.0
	Cr	21.2	3.9	28.0	5.2
extensor*	CrP	21.7	0.5	28.7	0.66
digitorum	ATP	6.0	1.7	7.9	2.2
longus	GPP		36.2		47.9
	Cr	26.7	5.2	35.3	6.9
gastrocnemius(M)[£]	CrP	20.9	0.5	27.7	0.7
	ATP	7.2	1.8	9.5	2.4
	GPP		30.0		39.7
	Cr	24.9	5.1	32.9	6.8
hind limb[£]	CrP	20.8	0.5	27.5	0.7
	ATP	7.4	1.8	9.7	2.4
	GPP		30.0		39.7
	Cr	24.7	5.1	32.6	6.8
gastrocnemius	CrP	18.6	0.7	24.6	0.8
(assuming a 20%	ATP	10.7	2.0	14.1	2.7
missampling ie. an	GPP		31.4		41.5
increase in slow	Cr	19.6	4.8	25.9	6.4
oxidative fibres)					

f "fully" depleted rat (minimum 4 weeks of GPA feeding)
* observed concentrations
£ predicted concentrations

Table III.3.1.b. Observed concentrations(*) of PCM of the soleus and extensor digitorum longus muscles of rat hind limb. Predicted concentrations(£) of the PCM of gastrocnemius and the entire hind limb muscle group. The factor used to convert the molarities presented in mmol/ kg wet weight to mmol/ L tissue fluid (0.756) was derived from the dry to wet weight ratio experiments.

III.3.2. Protein determination

All protein assays were performed by the Hartree modification of the method of Lowry (Hartree, 1972).

III.3.3. Acid hydrolysis

Total creatine, the sum of creatine and creatine phosphate, was determined after acid hydrolysis of the muscle extract (50 µL in the case of control and 100 µL in the case of experimental, Gp-fed, animals). Hydrolysis of creatine phosphate was performed at 65°C for 8 minutes with 0.5 N HCl (10 µL for control and 20 µL for experimental animals) followed by neutralization on ice with 0.4 N NaOH (18 µL for control and 34 µL for experimental animals).

III.3.4. Determination of total creatine

Total creatine was determined by a modification of the colourimetric assay of Ennor and Rosenberg (1952). Briefly, a solution of 1.0 mL distilled water, 500 µL 17-å-napthol (Kodak) in alkali, 100 µL of muscle extract, and 50 µL of a 1% butane-2,3-dione solution (J.T. Baker) diluted 1:20 in distiled water was allowed to react for thirty minutes then read spectrophotometrically at 510 nm.

The recorded readings were compared to those obtained from a standard curve containing 0-100 nmol of creatine per sample volume. It was determined that samples contained between 25 and 35 µmol of creatine per gram wet weight of muscle tissue in agreement with previously reported literature values (McGilvery and Murray,1974; Beis and Newsholme,1975).

III.3.5. Determination of guanidino containing compounds: ß-guanidinopropionic acid, and phosphorylated ß-guanidinopropionic acid

The Sakaguchi colour reaction (Sakaguchi, 1925) was used to assay for guanidino compounds in the muscle extract and hydrolysate. More recently, Bonas, Cohen, and Natelson (1963), described the reaction mixture for this colourimetric reaction. It contains 100 µL of sample, 1 mL of distiled water, 250 µL of a thymine-â-napthol mixture (B.D.H., AnalR), 100 µL of NaOCl (J.T. Baker), and 100 µL of 2% Na-thiosulfate (J.T. Baker). A spectrophotometric reading is taken of this mixture at 510 nm at 10° C after a five minute incubation on ice.

III.3.6. Determination of ATP and CrP

ATP and CrP content of the unhydrolysed muscle samples was determined by the combined enzymatic assay method of Lamprecht and Stein (1965). In brief, a series of three reactions occurs in the following sequence:

$$\text{1. Glucose-6-phosphate} + \text{NADP}^+ \xrightarrow[\text{i}]{} \text{6-phosphogluconate} + \text{NADPH} + \text{H}^+$$

$$\text{2. Glucose} + \text{ATP} \xrightarrow[\text{ii}]{} \text{Glucose-6-phosphate} + \text{ADP}$$

$$\text{3. Creatine phosphate} + \text{ADP} \xrightarrow[\text{iii}]{} \text{Creatine} + \text{ATP}$$

providing a stepwise quantitative analysis of the contents of G6P (glucose-6-phosphate), ATP, and CrP within the muscle extract. The enzymes represented by 1, 2, and 3 are i. glucose-6-phosphate dehydrogenase (E.C. 1.1.1.49); ii. hexokinase (E.C. 2.7.11.3); and iii. creatine kinase (E.C. 2.7.3.2.). Endogenous G6P is removed by

reaction 1. The increase in O.D. at 340 nm during reaction 2 and 3 is due to the increased formation of NADPH and is the direct result of the reactants of reactions 2 and 3, reaction 2 providing the content of ATP and reaction 3 the content of CrP.

III.3.7. Corrections and analysis

All of the biochemically assayed samples were corrected for the following.

1. The loss of creatine or guanidino propionic acid due to hydrolysis during and prior to the assay. The correction factor made for this loss is determined by assaying a non-hydrolysed and a hydrolysed standard after each series of hydrolyses were performed.

2. The apparent increase of creatine due to the interfering presence of the creatine analogue guanidino propionic acid in the assayed muscle hydrolysate. As the misdetermination of the creatine concentration is proportional to the concentration of GP in the sample, the empirical factor used to correct for this was 0.15 x [guanidino propionic acid]. The constant was determined by independent assays performed in our laboratory.

3. The residual amounts of ATP, CrP, Cr, GPP and Gp that can be found in the minute volume of extract which is not decanted after the first spin of the muscle hydrolysate. This residual volume is found by weighing the tubes before the addition of muscle and after decanting. The scaling factor used to correct our assays were determined by assaying this residual volume on a number of test muscles. The amount of loss in percent for ATP, CrP, phosphate, Gp, creatine was found to be 5, 5, 13, 10 and 7 respectively.

Corrections were not applied for muscle weight loss between the time of excision and the time of assay. This loss amounted to less than one percent of the muscle weight at the time of excision and was not considered significant (see section IV.3.a.).

III.4. Flame Photometry

Samples (between 0.04 - 0.1 grams), as discussed in section III.3., were taken from the right limb of at least 4 normal and 4 GP-fed rats at each of the four periods of interest. These pieces were weighed, vacuum dried to constant weight, digested in 2 mls of 4M Nitric acid ([Na] 1 p.p.m., [K] 1 p.p.m.), and filtered through 0.22 micron Sartorius filters. Subsequently the sodium and potassium contents of the muscles were determined either by flame photometry or by atomic absorption spectroscopy.

The Corning 480 flame photometer was used for flame photometric determinations. Sodium was sampled manually in undiluted form while potassium was sampled using an auto-dilution of 1:200. The standards used for the determination of sodium were 5, 15, and 45 mM and 1 and 5 mM for potassium. Calibration, using a lithium chloride internal standard, was performed prior to any determinations. The wavelengths of observation were 590, 768, and 672 nm for sodium, potassium and lithium respectively.

III.5. Nuclear magnetic resonance spectroscopy

All NMRS experiments were performed using a Bruker-MSL 300 spectrometer equipped with a vertical, wide bore magnet, using the protocol outlined in Figure III.5.a. Proton experiments were performed at 300.16 MHz, sodium experiments at 79.36 MHz and phosphorus at 121.5 MHz. Experiments which used standards in place of animals followed identical protocols.

Nuclear magnetic resonance spectroscopy experimental protocol

1. Anaesthetize rat
2. Adjust rat foot support
3. Insert rat leg into coil from top (non-electrical/physiological side) towards bottom (non-physiological/electrical) side of the probe
4. Attach rat to probe with velcro
5. Place and attach probe to aluminum housing (can) for stability and grounding
6. Place probe in magnet
7. Attach moistened oxygen supply
8. Tune and match probe to 300.13 MHz (proton frequency)
9. Shim magnet
10. Determine 90° pulse on protons
11. Acquire proton spectra
12. Measure the temperature of the preparation
13. Tune and match probe to 79.37 MHz (sodium frequency)
14. Determine 90° pulse on sodium
15. Acquire sodium spectra
16. Tune and match probe to 121.5 MHz (phosphorus frequency)
17. Determine 90° pulse on phosphorus
18. Acquire phosphorus spectra
19. Remove probe from magnet and rat from probe

Figure III.5.a. Experimental protocol for NMRS experiments. For experiments which used standards in place of animals replace the word "rat" with the words "standard solution" and omit steps 1 and 2.

III.5.1. Probe design

Probe III, the probe used for all experiments, was a specially constructed to transmit and receive at the frequencies of protons (300.13 MHz), sodium (79.37 MHz), and phosphorus (121.5 MHz) and to accommodate rats weighing between 50 and 175 grams.

The probe body housing (can) was built from aluminium. The probe body was made of copper rods 5 mm in diameter, Teflon, and a two sided, copper coated printed circuit board 2 mm in thickness (see Figures III.5.1.a and b). The body was divided by the PC (printed circuit) board (copper two sides) into upper and lower halves. All physiological apparatus was mounted on the upper/top half of the probe, while electrical circuitry was confined to the lower/bottom half.

The rat is secured belly-down to the topside of the probe. His leg traverses the plane of the probe from top to bottom. The rat faces towards the grounding discs (figure III.5.I.a., item (j)) at all times, hence is upside down upon insertion into the magnet

The three turn receiver coil was a solenoid, 15 mm in diameter and 8 mm in height, constructed of a high conductivity copper strap 0.9 mm in thickness and 2.7 mm in width (Figure III.5.1.c.). The coil was shielded from its environment, on its inner and outer surface, by a Teflon housing (Figure III.5.1.a. and c.). The top lead of the coil was alternatively grounded to the probe body (figure III.5.I.a., item (j)) or connected in series with a fixed value capacitance. The other lead was attached to the transmit/receive (TR) network (Figure III.5.1.a and b). The coil and circuit arrangement was designed to optimize filling factor and quality factor, Q, of the receiver coil following the design suggested by Hoult and Richards (1976) and personal communications with Paul Morris of Morris Instruments of Ottawa

The TR (transmit/receive) network used in transforming the impedance of the receiver coil at resonance to 50 ohms resistive was constructed from non magnetic, high-quality, high-voltage fixed capacitors (American Technical Ceramics) and variable air tuned capacitors (Voltronics). The Q's of the loaded and unloaded coil at its different frequencies of operation are given in Table III.5.1.a.

The Q's were determined by measuring the half power 3 dB band width (Δf) at its resonant frequency (f_0) and applying equation III.5.1.i (Beall,1984).

$$Q = \frac{f_0}{\Delta f} \qquad \text{III.5.1.i}$$

The high Q requires the probe be tuned for all samples (Gadian, 1982) in order to achieve optimum performance. Typically the 90° pulse widths for all three nuclei were 13 µs at an average power of 50 W (Watts) for protons, 240 W for sodium and 120 W for phosphorus.

The circuit, a diagram of which is presented in Figure III.5.1.g., has several modes of operation:

1. if the switch at **C** and **D** is connected to **D** and neither **A** nor **B** are closed the probe may be tuned for protons,
2. if the switch at **C** and **D** is connected to ground and **A** is closed then the probe may be tuned for sodium,
3. if the switch at **C** and **D** is connected to ground and **B** but not **A** is closed the probe may be tuned for phosphorus.

In all instances all capacitors were electrically connected directly to the copper base of the PC board in order to provide a satisfactory earth. Insulation, where required, was provided by using Teflon.

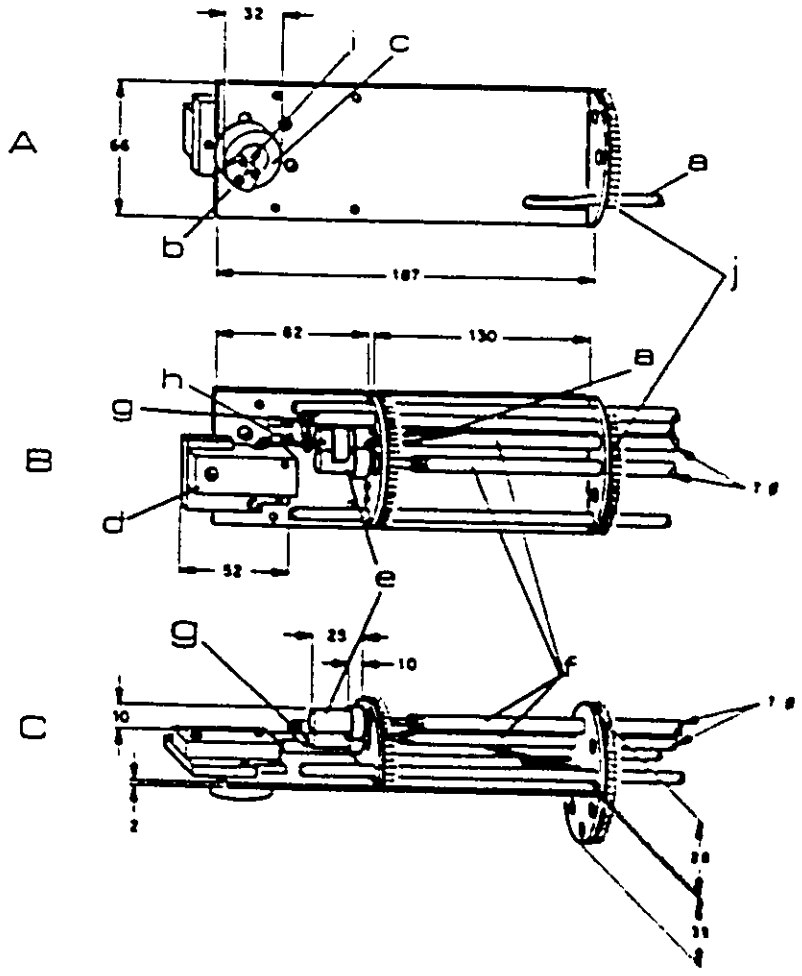

Figure III.5.1.a. Top (A), bottom (B) and lateral (C) views of NMRS probe III. The rat is secured to the topside of the probe and faces towards the right in all cases. During the observation the hind limb traverses the centre plane of the probe via the hole labeled (i). The foot is secured in the support (d) (spatial facsimile of the tension transducer to be used in future experiments). The other major components include (a) the rf input, (b) standards capillaries, (c) Teflon shield (assures that the rat does not touch the the rf coil and /or influence tuning), (d) foot support, (e) tune and match circuitry including variable air tuned capacitors by Voltronics, (f) tuning rods, (g) switch used to change tuning frequency, (h) capacitors involved in frequency change (high-voltage fixed capacitors by American Technical Ceramics), (i) hole traversing the rf coil, (j) grounding discs. All measurements are in millimetres.

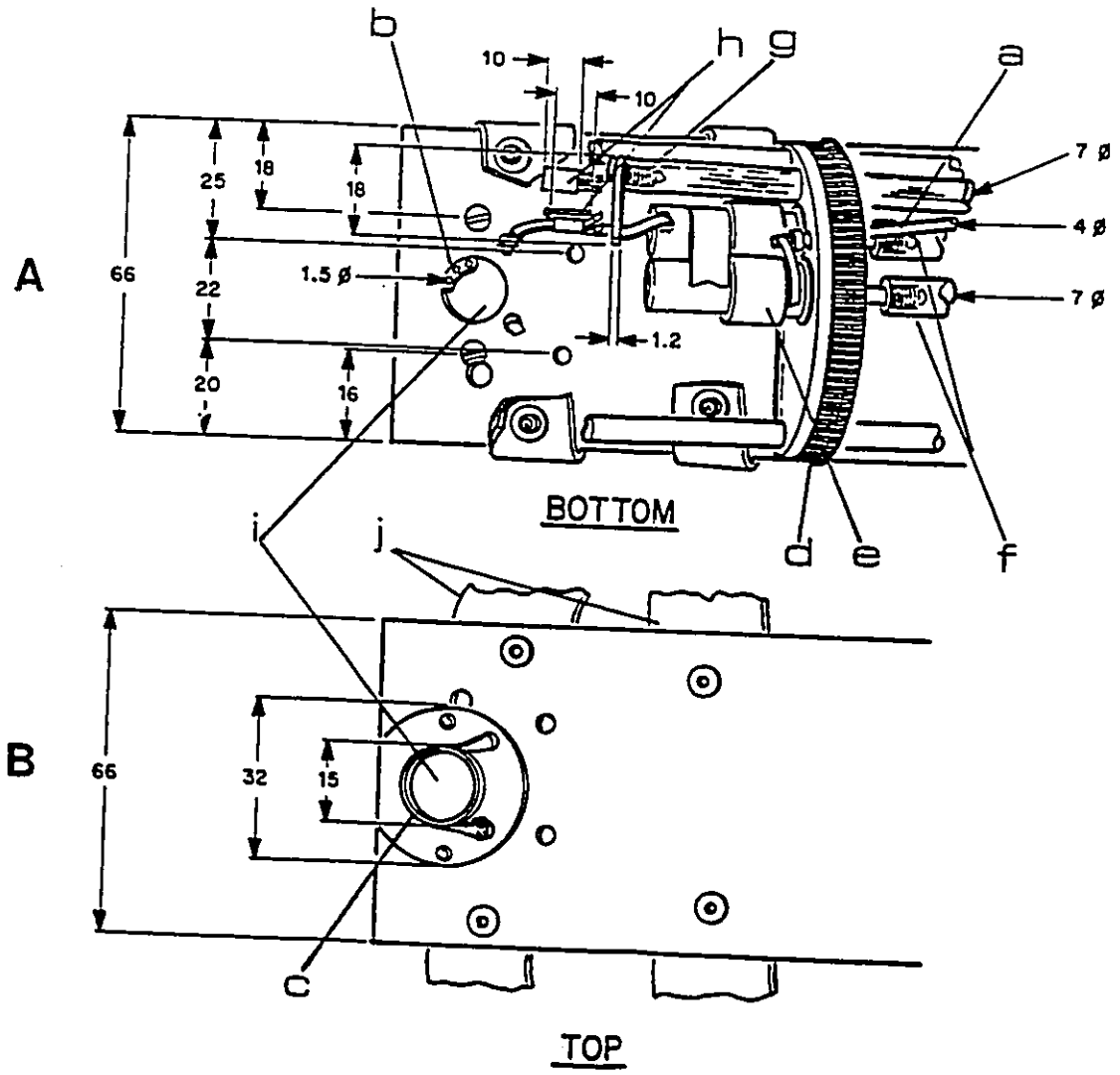

Figure III.5.1.b. Bottom (A) and top (B) view of probe III without foot support. Labeled parts include (a) the rf input, (b) standards capillaries, (c) rf coil, (d) grounding disc, (e) tune and match circuitry, (f) tuning rods, (g) switch used to change tuning frequency, (h) capacitors involved in frequency change, (i) hole traversing the rf coil, (j) velcro straps used to safely secure the rat to the probe. All measurements are in millimetres. "ø" denotes outer diameters in all cases. The rat is secured to the topside of the probe and faces towards the right in all cases.

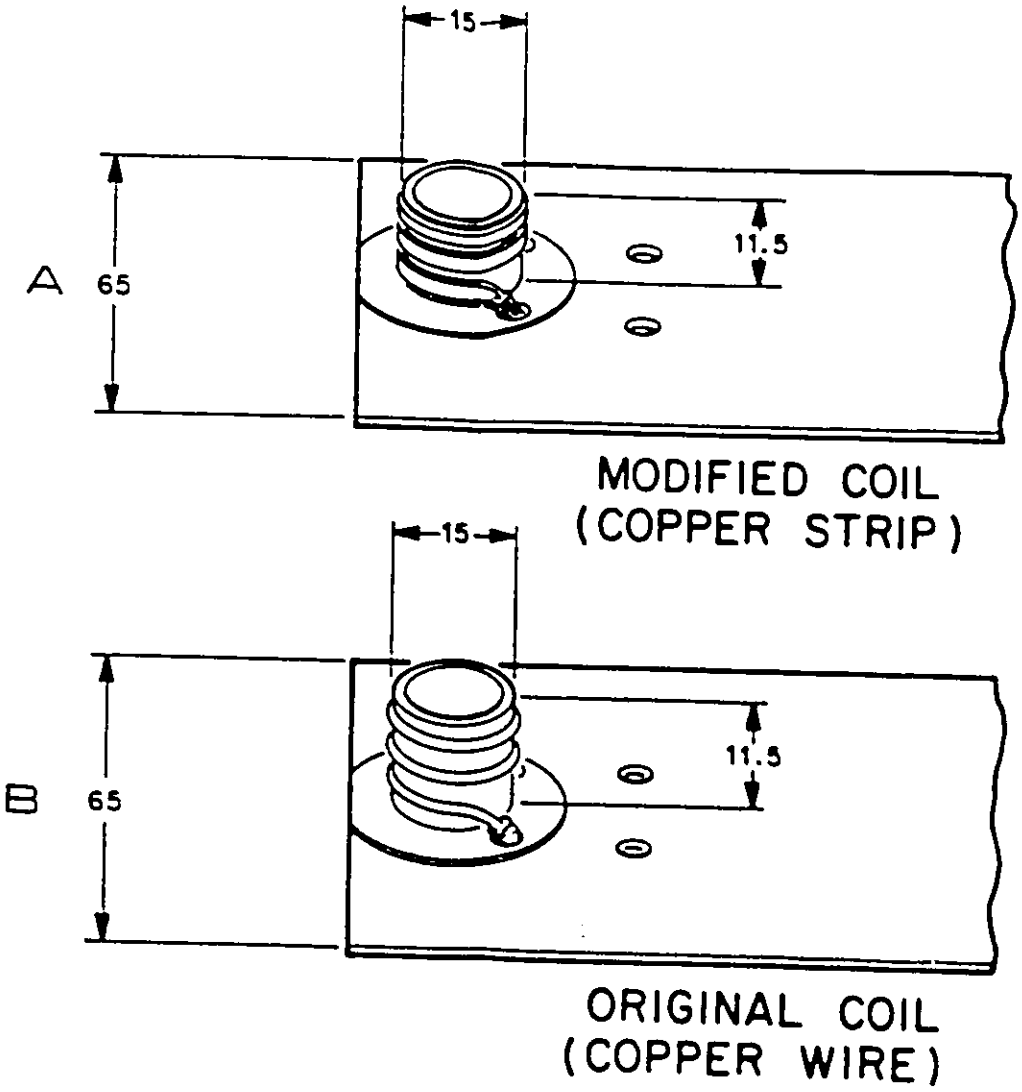

Figure III.5.1.c. Lateral view of NMR coils used in the described experiments. (A) coil used in probe III (actual probe used in all experiments). Coil (A) is constructed of high conductivity copper strap 0.9 mm. in thickness and 2.7 mm. in width. (B) coil (constructed of copper wire) used in probes I and II (predecessor probes). All measurements are in millimetres. Diameters shown represent inner diameters only. The rat is secured to the topside of the probe and faces towards the right in all cases.

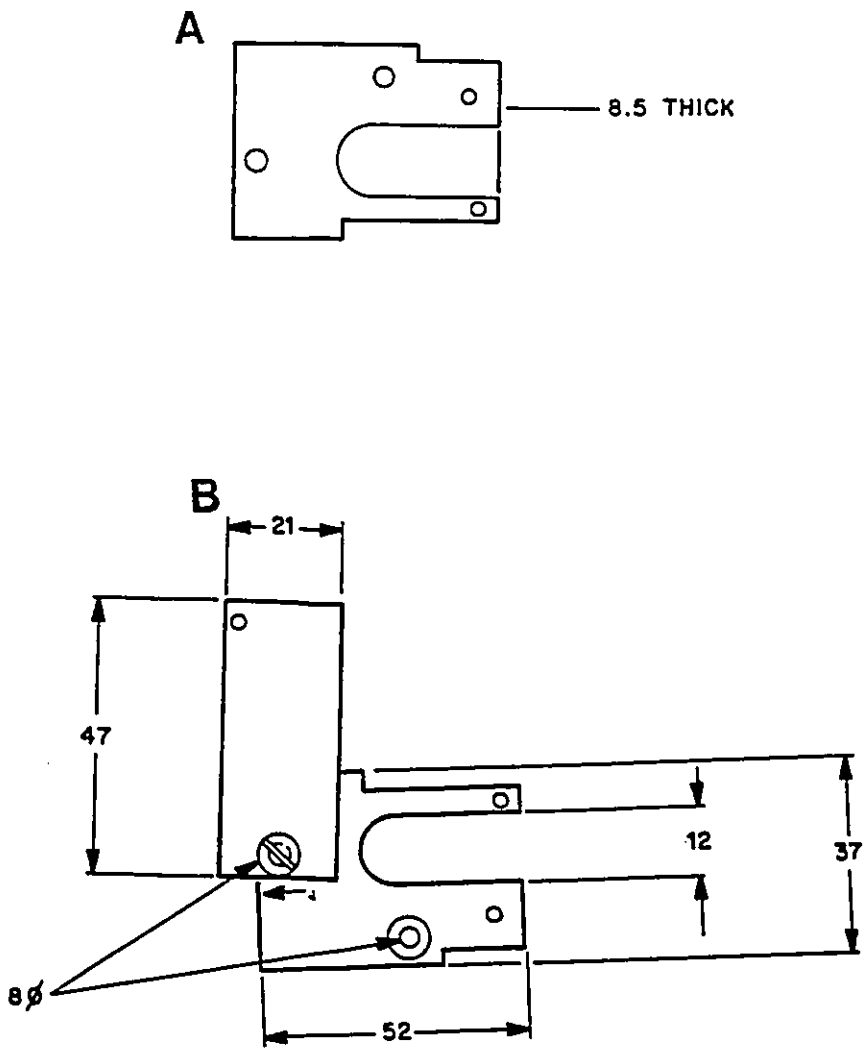

Figure III.5.1.d. Top (A) and bottom (B) view of foot stabilizer (used in lieu of the tension transducer) on the bottom side of probe III. The bottom view depicts the support (facsimile of the foot pedal of the tension transducer) drawn out to the side as it would be while the rat is being secured to the probe. The toes of the foot point towards the right in all cases. All measurements are in millimetres. "ø" denotes inner diameters only.

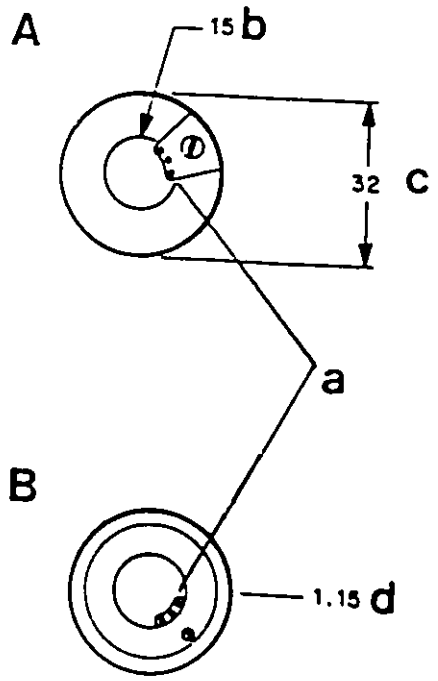

Figure III.5.1.e. Top (A) and bottom (B) views of the topside Teflon shield used to assure that the rat does not touch the rf coil and/or influence tuning. This shield is mounted over the rf coil and attached with plastic screws to the probe pc board base. Glass capillaries, containing standard solutions, are placed and held within the coil by a Teflon holder (a). Labelled measurements include (b) inner diameter of Teflon shield, (c) outer diameter of Teflon shield, and (d) thickness of the wall of the Teflon shield. All measurements are in millimetres.

Probe III	Phosphorus	Sodium	Protons
Empty coil	243	99.2	375
"Ackerman standards"$^{\pi}$	173.6	79.4	333.5
Rat hind limb	151.9	94.4	375

Probe II	Phosphorus	Sodium	Protons
Empty coil	11.1	3.8	20
"Ackerman standards"	7.0	3.3	16.6
Rat hind limb	5.8	3.7	18.8

Probe I	Phosphorus
Empty coil	7.2
"Ackerman standards"	6.1
Rat hind limb	6.1

$^{\pi}$ Standards used to calibrate and test the probes ability to quantitate

Table III.5.1.a. Quality factors of NMRS probe III, II and I at the frequencies of phosphorus, sodium and protons with various types of samples. Q is derived using the equation $Q=f_0 / \Delta f$. Probe II was the probe used during all documented experimentation. Probe I was the probe used during its developmental stages.

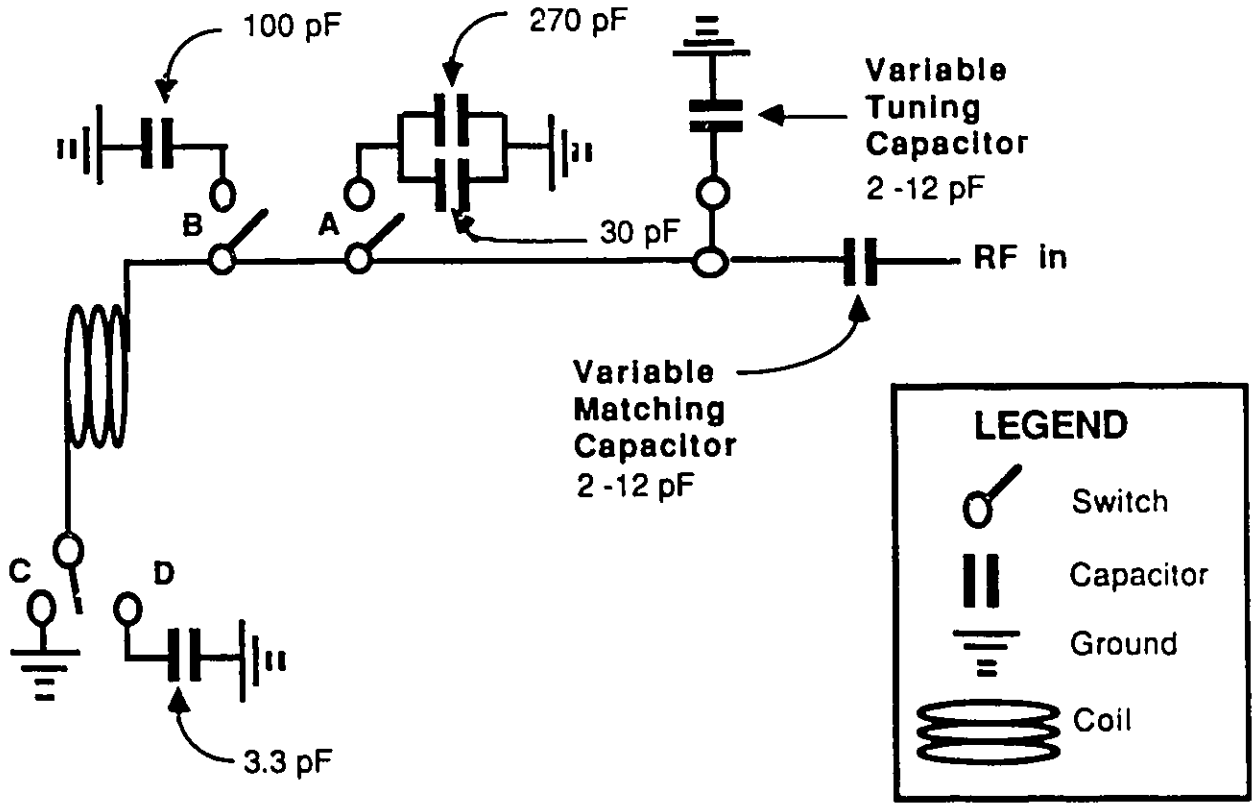

Figure III.5.1.g. Circuit diagram of the triple tuning NMR probe. Protons are examined when the switch at C and D is connected to D and neither A nor B are closed. If D is connected to ground and A is closed, then the probe may be tuned for sodium. When D is connected to ground and B is closed the probe may be tuned for phosphorus.

III.5.2. Spectrum aquisition parameters

Table III.5.2.a. illustrates the spectrum aquisition parameters for the quantitation experiments.

In brief, all samples were "shimmed" and the 90° pulse widths for each nuclei of interest were determined prior to spectral acquisition. Shimming is the process wherein the main magnetic field of the NMR apparatus is made more homogeneous in the area of the sample. This is accomplished by adjusting the current in the coils which surround the probe. In biological NMR experiments the samples are normally shimmed on the most prevalent and sensitive nucleus, the proton, prior to the acquisition of any other spectra (Ackerman, 1981). This assures the largest possible signal to noise ratio for the experiments involving other nuclei.

The 180° pulse widths for all nuclei were determined prior to FID acquisition by setting the transmitter on resonance and finding the pulse width at null signal. The 90° pulse width was subsequently determined by dividing the 180° PW by two as suggested by Hoult (1978). Subsequently all of the FIDs for all nuclei were acquired using phase cycling and quadrature detection, with pulse recycle times of five times T_1 (see Figure III.5.2.b.) in order to allow for the full recovery of the nuclei of interest back to H_0 (Becker,1979; Gadian, 1982).

The FIDs for proton and sodium spectra were acquired using pulse sequence 1 (section III.5.3.). The phosphorus FIDs were obtained using pulse sequence 1 to obtain complete ^{31}P spectra and sequence 2 (section III.5.3.) to obtain ^{31}P spectra after a refocussing pulse to rid the spectra of its phospholipid components (Figure III.5.7.a.). The relative sensitivity and abundance of the nuclei of interest determines the number of scans (FIDs) needed for each experiment (see Table III.5.2.a.). Three spectra were

taken for protons and sodium using four and sixteen scans respectively. Consecutive spectra of multiples of 20 scans were taken for phosphorus.

Nucleus	Phosphorus	Sodium	Protons
Signal frequency	121.5 MHz	79.37 MHz	300.13
Sweep Width (Hz)	20,000	5,000	10,000
Spectrum size	4 K	4 K	4 K
90° Pulse width	11 - 15 µsec	11 - 15 µsec	11 - 15 µsec
Number of FIDs	20 - 200$^{\infty}$	16	4
Recycle time	15 sec	5 sec	10 sec
Quadrature detection	yes	yes	yes
Phase cycling	yes	yes	yes
Pulse program	Cyclops or $(90°_x - t - \text{acquire})_n$	Cyclops	Cyclops
O1	- 1078 Hz	1345 Hz	N/A
O2	N/A	N/A	6131 Hz
RG	20 (in vivo)	30	50
	30 (std. solutions)		
Power 120 Watts	240 Watts	50 Watts	
Peak width	0.4 p.p.m. (CrP)	0.4 p.p.m.	0.4 p.p.m.

Table III.5.2.a. Spectral acquisition parameters used in obtaining phosphorus, sodium and proton spectra from rat hind limb and associated standards. $^{\infty}$ phosphorus spectra were taken on a base of 20 scans; if more were taken they were corrected back to 20 using equation III.5.4.1.iii.

	T_1 value	T_1 value	T_2 (measured)
CrP	2.7 s≈	3.5 ± 0.5 s¥	0.25 s†
ß- ATP	1.2 s≈	1.3 ± 0.4 s¥	unavailable
P_i	4.6 s•	6.0 ± 0.5 s¥	unavailable
H (H_2O)	642 ms†	not measured	45-52 ms†
Na	unavailable	0.54 ± 0.05 s¥	12-16 ms†

† taken from Beall et al. 1984 (32 MHz)
≈ Evelhoch 1985 (145 MHz)
• taken from Meyer et al 1985 (121 MHz)
¥ n= 5 (121 MHz ^{31}P, 300 MHz ^{1}H)

Table III.5.2.b. Relaxation times for phosphorus-containing metabolites, sodium and water in the rat hind limb.

Nucleus	Spin	Percent Abundance	Relative Sensitivity
^{31}P	1/2	100	0.066
^{23}Na	3/2	100	0.093
^{1}H	1/2	99.98	1.000

Table III.5.2.c. Spins, abundances and sensitivities of the nuclei under study (Beall, 1984).

III.5.3. Pulse sequences

The pulse sequence applied to the hind limb for the aquisition of the ^{1}H, ^{23}Na and ^{31}P spectra was sequence 1 below. In all cases a cyclops routine of pulse application was used to assure that any residual dephasing of the magnetic moment left in the XY plane was removed or made negligible. A cyclops pulse routine pulses along the first the X, then the Y, then the -X, and finally the -Y axis. During the ^{31}P experiment a Hahn spin echo pulse sequence (sequence 2), was used to remove the T_1 effect/contribution of phospholipid to the spectra.

Pulse sequences

1.	$(90°_x - t - \text{acquire})_n$	Pulse acquire (Beall, 1984)
2.	$(90°_x - t - 180°_y - t - \text{acquire})_n$	Hahn spin echo (Beall, 1984)

The sweep width and number of computer points (size) selected for each nucleus provides close to maximal signal to noise per unit time for all nuclei, as determined by the method of Becker, Ferretti, and Gambhir (1979).

A capillary tube containing dimethyl methyl phosphonate (DMMP) (-32 .5 p.p.m.) and a relaxation agent was used as an external standard in the phosphorus experiments. The capillary was mounted inside the coil alongside all samples in a Teflon support. This capillary was present and unchanged for all experiments. This compound has a minimal chemical shift change with temperature over the physiological range.

III.5.4. Quantitation of metabolites

III.5.4.1. General

The method of quantitation used by Ackerman makes no assumptions about the content of specific metabolites in vivo. By obtaining the ratio of peak intensities (areas) of the metabolite of interest and of the proton signal from the water surrounding that metabolite, concentrations of these metabolites can be obtained. The method is based on the mapping of B1 spatial distributions at the frequencies for which the coil is tuned. By making the assumption that the area of a peak of interest is proportional to the number of spins present for that nuclei, Ackerman proposes equation III.5.4.1.i.

$$\frac{S_a}{S_b} = D\frac{C_a}{C_b} = D\frac{N_a}{N_b} \qquad \text{III.5.4.1.i}$$

Where S_a and S_b are the signal intensities, C_a and C_b are concentrations and N_a and N_b are the total number of spins, for nuclei a and b respectively. D is the proportionality constant or slope relating the ratio of $S_a/S_b : C_a/C_b$ which is irrespective of B1 inhomogeneities and sample volume geometry.

In the case where the protons of water are nuclei b then the equation III.5.4.1.i can be simplified to equation III.5.4.1.ii.

$$S_a \approx S_{H_2O}\frac{D}{111}C_a \qquad \text{III.5.4.1.ii}$$

where C_b is molarity of water protons or 111 M.

If Ackerman's formulation is correct, to obtain concentrations of sodium or a phosphorus-containing metabolite (PCM) from a physiological sample, standard curves must be made in order to characterize D. Standard curves are obtained by plotting the

ratio of the areas of the sodium or phosphorus peaks to that of the proton peak against the concentration of sodium or phosphorus within that standard solution. The standard solutions were made using two fold dilutions of a stock of 200 mM sodium chloride and 80 mM potassium phosphate. The standard solutions volume and concentration were changed independently and the curves replotted in order to mimic the in vivo situation. The volumes of the standard solutions were changed by the insertion of Teflon rods into the centre of the sample which extended beyond the ends of the coil. The volumes used were 1.25, 1.02, 0.91 and 0.65 ml

After acquisition the peak integrals of the phosphorus spectra of the physiological experiments were corrected back to standard (calibration) acquisition parameters, using empirical scaling factors derived from the equations III.5.4.1.iii and III.5.4.1.iv below.

Correction for the number of scans (NS) taken:

$$\text{area for a given NS} \times \frac{20}{NS} = \text{area if 20 scans were taken} \qquad \text{III.5.4.1.iii}$$

Correction for the the receiver gain (RG):

$$\text{area for a given NS} \times \Upsilon^{1} = \text{area}_{RG} \qquad \text{III.5.4.1.iv}$$

---

1 The constant Υ was found to be 0.31622 for this spectrometer for a RG (receiver gain) change of 10 units (from 30 for standards to 20 for the in vivo experiments) as derived from the equation IV.6.2.i.

For example the correction for the number of scans if 100 scans were taken and the area was found to be 25 units, then the conversion applied to normalize this experiment to those where only 20 scans were taken would be $25 \times \frac{20}{100} = 5$ units.

After the correction of each integral back to standard acquisition parameters the area for each peak of interest (subsequently known as $I_{corrected.}{}^{31}ATP$, $I_{corrected.}{}^{23}Na$) was divided by the proton peak area ($I_{corrected.}{}^{1}H$). In so doing the ratio of the peak of interest (eg. ATP or Na) to that of water was produced. When applied to the calibration curves (IV.6.1.a.) obtained from the preliminary experiments (described above), these ratios translate directly into a millimolar concentration using equations III.5.4.1.v and III.5.4.1.vi. It is assumed that the mean NMRS visible concentration is proportional to the product of the slope of the calibration curve and the ratio of the peak area of the nucleus of interest to that of the proton peak.

Concentration determinations

for sodium

$$[Na]_{mean} = \frac{\frac{I_{corrected.}{}^{23}Na}{I_{corrected.}{}^{1}H} - 0.000124}{0.0029}$$

III.5.4.1.v

for phosphorus

$$[PCM]_{mean} = \frac{\frac{I_{corrected.}{}^{31}PCM}{I_{corrected.}{}^{1}H} - 0.000172}{0.0018} \qquad \text{III.5.4.1.vi}$$

It should be noted that the proton peak area used for the determination of the above concentrations does not include any contribution from fat present in the rat hind limb. The need to discount this peak area in the determination of the true peak area

attributable to water is substantiated by the works of Yoshikawa (1979), Siefkin (1986), and Lederman (1982). Although the entire proton peak area was measured, only the peak area attributable to free water was used for the determination of $I_{cor.}{}^{1}H$. This area (invariably >95% of the total area) was integrated from the upfield to the downfield side of the major peak, stopping at the base of the upfield side of the second peak in the proton spectrum. The peak area of this second peak, that attributable to fat, was taken as that portion which when summed to the free water integral totaled the total proton integral.

III.5.4.2. Correction of calculated phosphorus-containing metabolite concentrations using intracellular sodium concentration and intracellular volume

The amount and concentration of extracellular sodium is comparatively large and constant (≈140mM), while intracellular sodium concentration, approximately 50% of which is bound to intracellular proteins, is a factor of ten smaller in concentration (≈8mM) (Ganong, 1977).

Assuming that the mean sodium concentration of the muscle could be described by equation III.5.4.2.i

$$[Na]_{mean} = \frac{V_O [Na]_O + V_i [Na]_i}{V_T}. \qquad \text{III.5.4.2.i}$$

where V_T is the total muscle volume, V_O is the extracellular volume, V_i is the intracellular volume and $[Na]_O$, and $[Na]_i$ are the extra and intracellular concentrations of sodium respectively. Then intracellular muscle volume can be

estimated by subtracting a volume/fraction, determined by the partitioning of sodium between the interior and exterior of the muscle cells, from the total muscle volume.

Suppose too that ∞ is the extracellular volume as a fraction of total volume and (1- ∞) is the intracellular volume of the rat hind limb under investigation during NMRS. If these are substituted into equation III.5.4.2.i. above it yields the equation III.5.4.2.ii. below.

$$[Na]_{mean} = (\infty \quad [Na]_o + (1-\infty)[Na]_i) \qquad \text{III.5.4.2.ii}$$

If we solve for ∞ ignoring the small Donnan correction (effect of an impermeant ion on the diffusion of other ions) (Ganong, 1977), and substitute the estimations of intra and extracellular sodium concentrations, VT is elimated as a common factor and equation III.5.4.2.iii. results.

$$[Na]_{mean} = 132\infty + 8 \qquad \text{III.5.4.2.iii}$$

When equation III.5.1.v. (below) is equated to equation III.5.4.2.iii (above) then equation III.5.4.2.v. results (assuming that the minor contribution of the Y intercept of this standard curve is ignored).

$$[Na]_{mean} = \frac{\frac{I_{corrected}{}^{23}Na}{I_{corrected}{}^{1}H} - 0.000124}{0.0029} \qquad \text{III.5.4.1.v}$$

$$= \frac{I_{corrected}{}^{23}Na}{I_{corrected}{}^{1}H} \times \frac{1}{K_{Na}} \qquad \text{III.5.4.2.iv}$$

$$\infty = \frac{\left\{\frac{I_{corrected}{}^{23}Na}{I_{corrected}{}^{1}H} \times \frac{1}{K_{Na}}\right\} - 8}{132} \qquad \text{III.5.4.2.v}$$

This correction factor ∞, is used in our experiments to correct all of the obtained whole limb PCM concentrations to their intracellular values as shown in equation III.5.4.2.vi. below.

$$[PCM]i = \left(\frac{1}{1 - \infty}\right) [PCM]Total \qquad \text{III.5.4.2.vi.}$$

It can be mathematically shown that even 50% errors in the estimation of $[Na]_i$ will result in comparatively much smaller percentage errors in the estimation of intracellular volume. This is due to the relatively low and oftentimes ignored (Thulborn and Ackerman, 1983) concentration of Na inside the cell and its meagre contribution to the mean sodium concentration. Recent reports have shown that approximately 62% of intracellular sodium is invisible to NMRS (Cope, 1970; Chang and Woessner, 1978; Gupta, 1982), this would not significantly alter the calculated extracellular volume or the corrected calculations of the PCM concentrations. If, for example, $[Na]_T$ was 30 giving an ∞ of 0.17 with an assumed value of $[Na]_i$ of 8 then if $[Na]_i$ had been in reality 50% greater than assumed ∞ would have had a value of 0.14 and $[P]_i$ would have been overestimated by 3.6%.

III.5.5. **Standard NMRS rat insertion protocol** (Figure III.5.a.)

Subsequent to the rat being adequately anaesthetized, its right hind limb was placed within the Teflon protected coil of the NMR probe, juxtaposing the gastrocnemius to the DMMP external standard reference capillary. The position of the leg/foot support beneath the plane of the probe was simultaneously adjusted to accommodate the length of the leg and to assure that the final position of the support placed the largest part of the

calf at the centre of the volume of the coil. This section of the leg is approximately two thirds of the distance from the heel to the knee.

Before securing the rat to the probe, final checks were made to assure that the rat body was entirely on the physiological side of the probe, and that the rat was in a natural position.

After the final adjustments to the leg position were made the rat was secured using Velcro straps to the probe, the can (aluminum housing) was attached to the probe base, the probe was placed within the magnet, and the humidified oxygen attached. The rat remained in this position for approximately one and a half hours while all spectra were acquired.

III.5.6. Maintenance of physiological conditions during NMRS experiments

Every attempt was made to conduct experiments under physiological conditions. In this regard the rectal temperature of the rats and the temperature inside the can was routinely monitored by the use of non-magnetic thermistors. A circulating warm water bath, made of thin plexiglass and powered by a small pump, was used to maintain the rats body temperature on the rare occasions that the body temperature of the animal was found to drift more than 2° C below physiological (39° C). Early experiments demonstrated that the corneas of the rats placed in the magnet were prone to drying. This problem was solved by passing medical oxygen through water and subsequently into the probe. This procedure served two purposes: to prevent the drying of the corneas, and to maintain a constant atmosphere inside the can which would facilitate the oxygenation of the tissues of the preparation.

III.5.7. Nuclear magnetic resonance data processing methods

The summed free induction decay values for all spectra were multiplied by an exponential factor corresponding to 5 Hz for protons, 5 Hz for sodium and 10 Hz for phosphorus before Fourier transformation (Becker, 1979). Integrals were computed on an Aspect 3000 computer after a 2 point baseline correction routine and first order phase correction.

The integration of peaks in the phosphorus spectra of both control and experimental animals were conducted in a similar fashion. When the free induction decays of these spectra were acquired, using $(90°_x - \dagger - \text{acquire})_n$, the peaks were integrated after baseline correction by a spline fitting routine (Figure III.5.7.a). In cases when the spectra were acquired using the pulse sequence $(90°_x - \dagger - 180°_y - \dagger - \text{acquire})_n$ then no baseline fitting routine was needed other than the two point correction routine previously discussed (Figure III.5.7.b).

In the phosphorus spectra of muscles from GP-fed animals the total integral of the phosphorylated guanidinopropionic acid and creatine phosphate area (-1 to -4 p.p.m.) was calculated after 10 Hz line broadening. This summed area was apportioned between its component parts by the relative intensities of the two species after 2 Hz line broadening, allowing a greater resolution of the two line shapes.

Although the spectra acquired using the spin-echo pulse sequence yielded spectra of metabolites without the superimposed phospholipid spectra this sequence often affected the height and area of the ATP peaks (see Figure VI.3.d.). For this reason, only the spectra acquired using the $(90°_x - \dagger - \text{acquire})_n$ pulse sequence were used to determine the area of the beta peak of ATP (17 - 19 p.p.m.). Similarly, only the spin-echo pulse sequence was used to determine the areas of the peaks of CrP and GPP.

The integrated areas of the phosphorus spectra were normalized to 20 scans for the purpose of comparison. Markedly different abundances of phosphorus in the hind limb of the weanling animals compared to standard solutions necessitated the use of an alternate receiver gain (30 vs 20) in the first week of experimentation. A standard curve (Figure IV.6.2.a), plotted using a wide range of receiver gains, was established in order to normalize the PCM integration areas obtained in in vivo conditions to those used to establish the standard phosphorus concentration curve.

The frequency width used for the integration of the sodium spectra was 4000 Hz (± 2000 from resonance) while that for the proton spectra was 8000 Hz (± 4000 from resonance). Subsequent to the integration of the entire proton spectrum the area was measured to the upfield base of the peak attributed to the protons of fat (Figure III.5.7.c.). This area (+4000 - -3300 Hz) was used as the area attributable to the protons of water for the determinations of PCM and sodium concentrations.

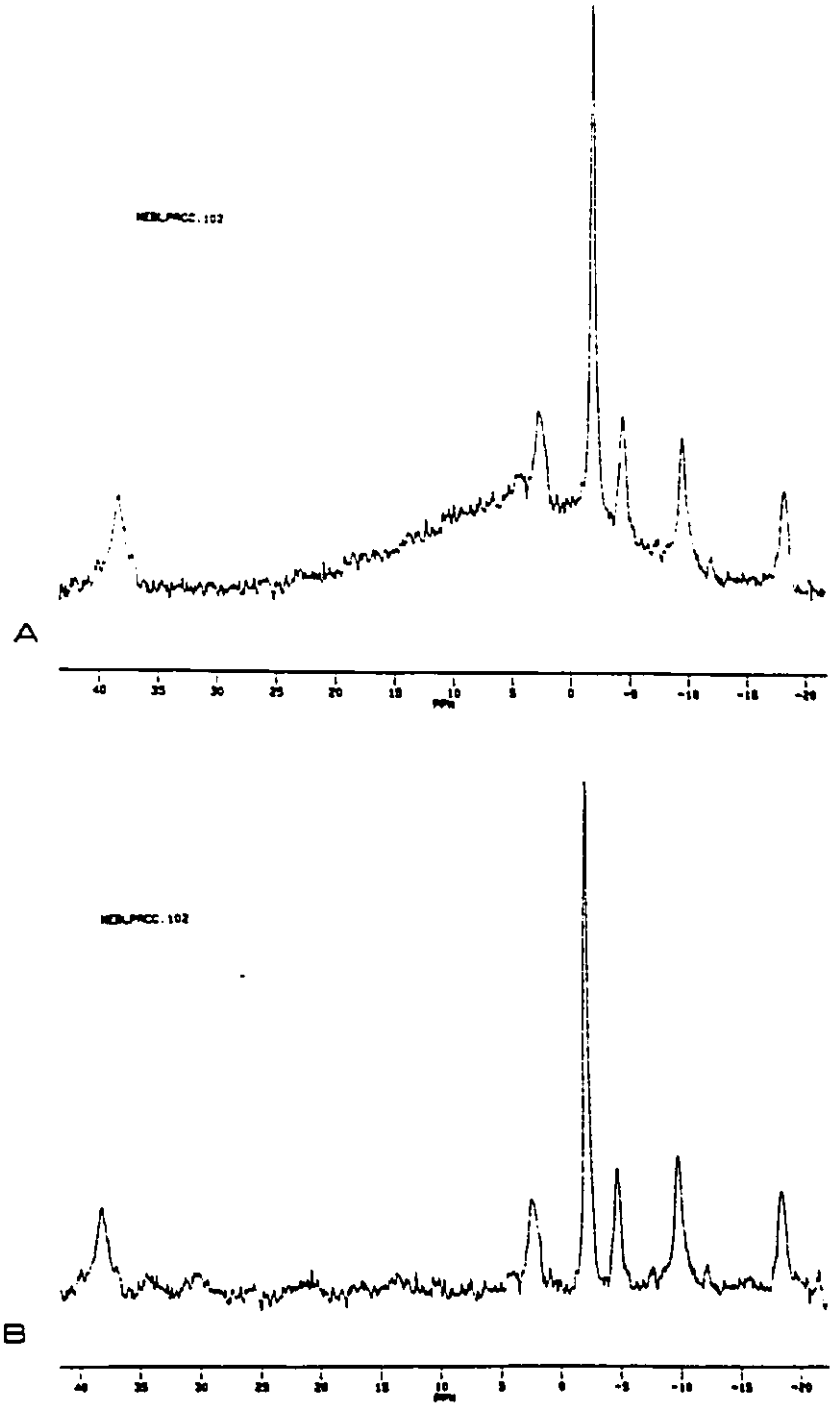

Figure III.5.7.a. ^{31}P in vivo spectra of the hind limb of a control rat obtained using (A) $(90°_x - t - \text{acquire})_n$ pulse sequence and (B) using the same $(90°_x - t - \text{acquire})_n$ pulse sequence and by superimposing a spline curve (baseline fit) to remove the contribution of the phospholipid (broad underlying peak). Note the predominance of the uneven baseline and the concomitant disturbance of the peak heights.

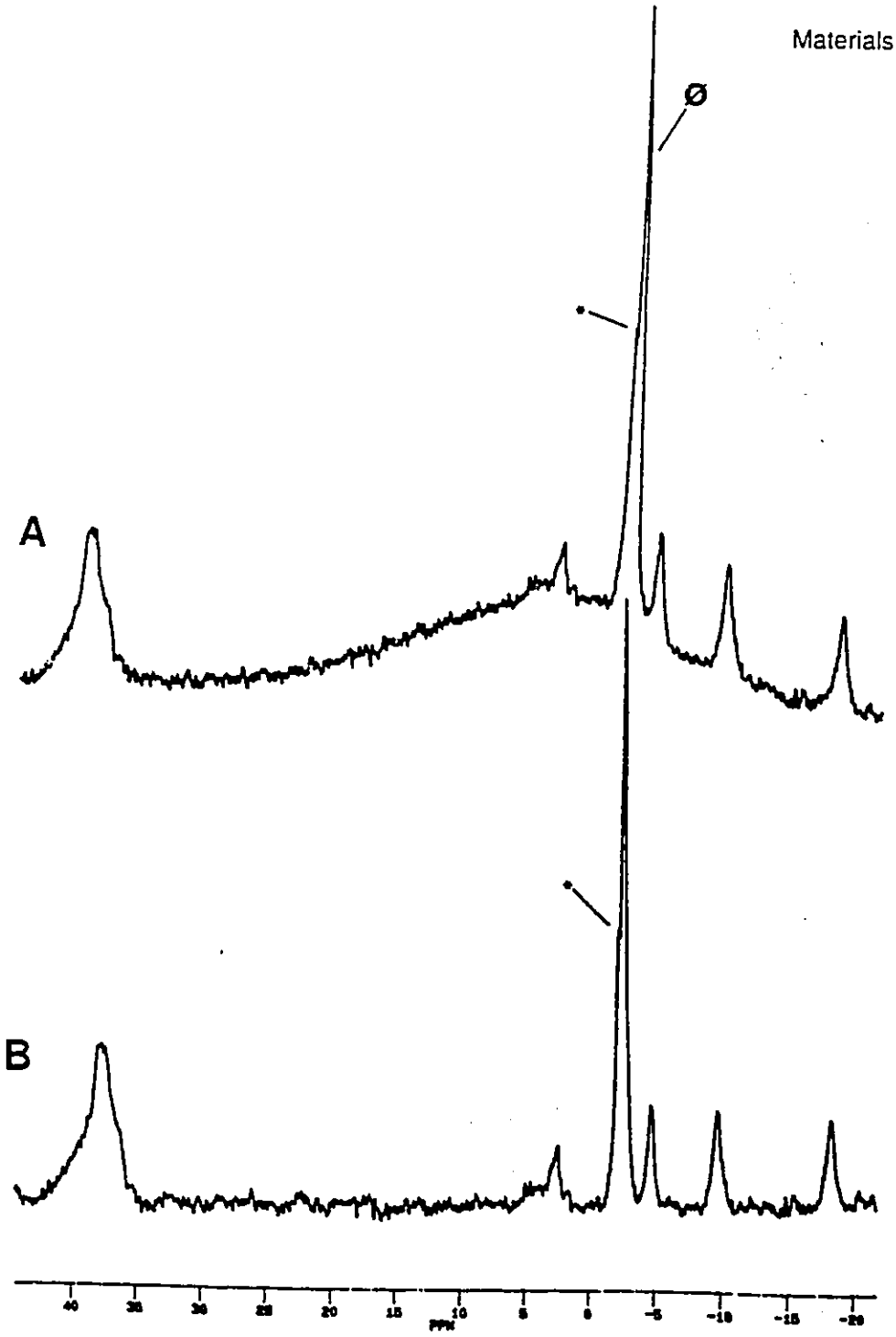

Figure III.5.7.b. ^{31}P in vivo spectra of the hind limb of a Gp-fed rat obtained using (A) $(90°_x - \tau - \text{acquire})_n$ pulse sequence and (B) a $(90°_x - \tau - 180°_y - \tau - \text{acquire})_n$ pulse sequence. Note that the peak heights are not disturbed by this process. The * indicates the peak of CrP, the adjacent peak (@) is that of GPP. No baseline fitting routine was needed other than the two point correction routine.

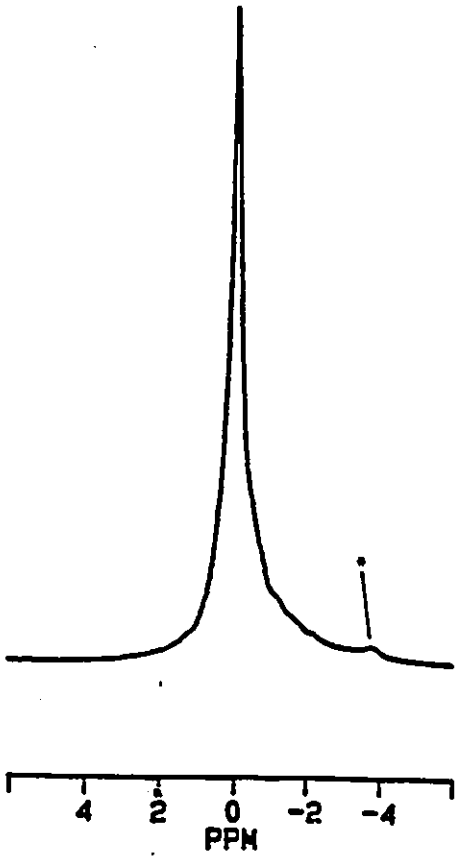

III.5.7.c. 1H <u>in vivo</u> spectra of the hind limb of a Gp-fed rat obtained using a $(90°_x - \tau - \text{acquire})_n$ pulse sequence. The peak attributed to the protons of fat is labeled with an *.

III.5.8. Resolution of the peaks of creatine phosphate and guanidinopropionate phosphate

Magnetic field inhomogeneity within the observe coil caused an increase in the peak width of CrP and GPP, resulting in decreased separation of these peaks. For this reason, a standard curve (Figure III.5.8.a.) was constructed to isolate the contribution of the minor peak area to that of the major peak or vice versa.

The standard curve was formed using the equation of a Lorentzian line (Pople et al, 1959) (III.5.8.i)[1] along with the assumptions that a) the average separation of the peaks (V_0 - V) of CrP and GPP frequencies is 58 Hz (n = 12), b) the line width at half height ($\Delta V_{1/2}$) of both CrP and GPP is 36 Hz (n =12) and c) peak area is directly proportional to peak height. I_{vf} is the height of the Lorentzian peak at its resonant frequency.

$$g(v)= I_{vf} = \frac{\frac{2}{\pi \Delta V_{1/2}}}{1 + \frac{4 (V_0 - V)^2}{(\Delta V_{1/2})^2}}. \qquad \text{III.5.8.i}$$

Using this information, a new function, the ratio of the sums of the contribution (intensity) of the GPP peak to the intensity of the CrP peak at its resonant frequency (vf_1 (eg O Hz)) to the sums of the intensity of the CrP peak to the intensity of the GPP peak at its resonant frequency (vf_2 (eg -58 Hz)), was developed (III.5.8.ii). Substituting this equation with a series of possible peak intensities (ie relative peak areas) results in a standard curve (Figure III.5.8.a).

---

1 The Lorentzian line shape of these two peaks was substantiated by separate investigations (Brady, 1986).

$$\text{Ratio of peak heights} = \frac{I(vf_1\ CrP) + I(vf_1\ GPP)}{I(vf_2\ GPP) + I(vf_2\ CrP)}. \qquad \text{III.5.8.ii}$$

Using this correction curve, the fraction of the total area of the CrP-GPP peak attributable solely to CrP or GPP could be interpolated (Figure III.5.8.a.), provided the ratio of peak heights was known. For example, if the ratio of GPP:CrP peak heights was 0.6, the percentage of the total CrP-GPP peak which is attributable to GPP would be 65% while the percentage attributable to CrP would be 35% (see graph for details).

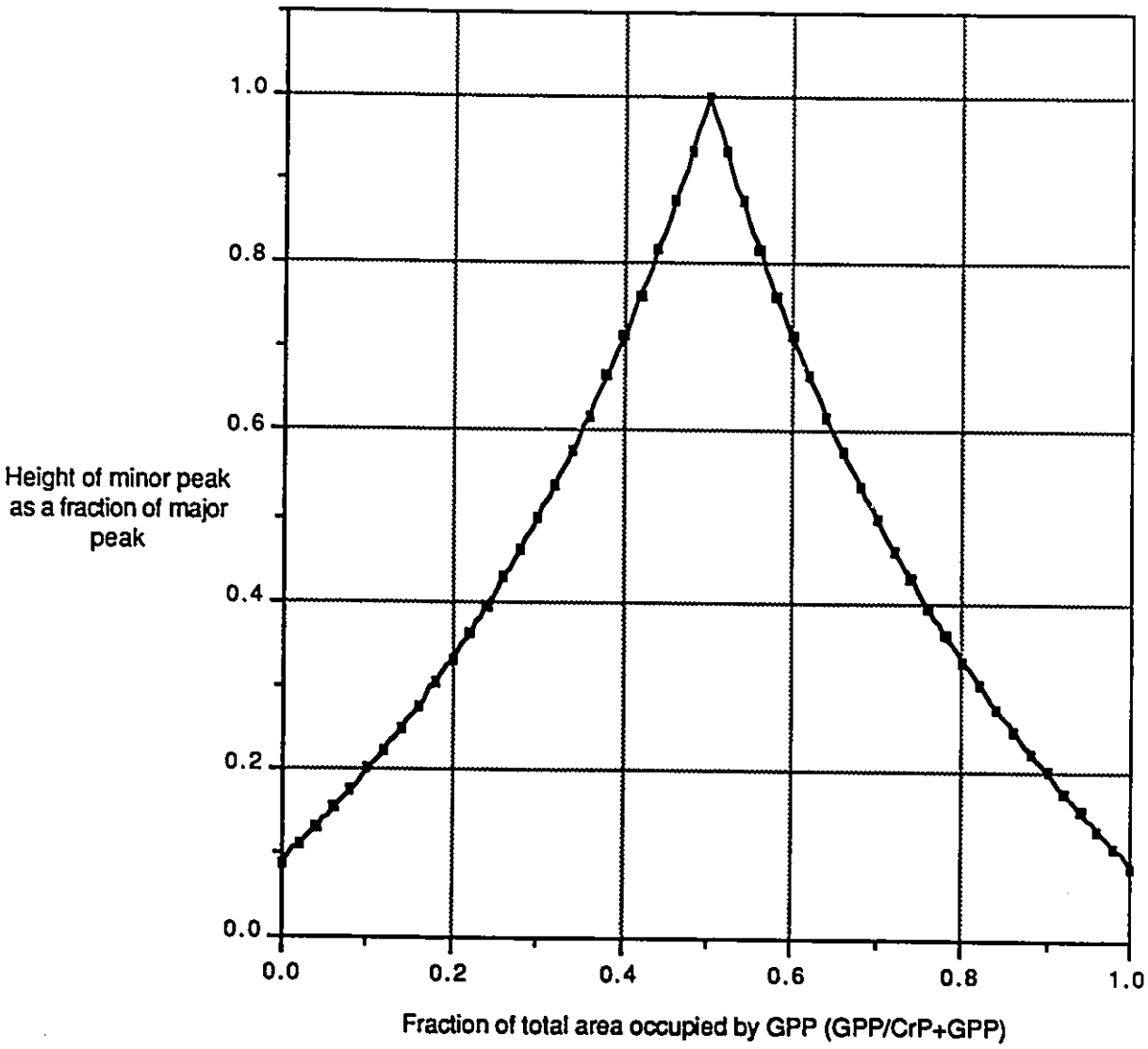

Figure III.5.8.a. Correction curve derived using the equation of a Lorentzian line and the lineshape characteristics and separation distance of the CrP and GPP peaks. The fraction of the total peak area of CrP and GPP occupied by GPP (ordinate) is obtained using the ratio of peak heights (abscissa) taken from the spectra of interest. The left hand arm of the curve is used when the minor peak is to the left of the major one. The right hand arm is used when the minor peak on the spectrum is to the right. For example, if the ratio of GPP:CrP was 0.6, this would indicate that GPP occupies 65% of the CrP/GPP peak. Line width is assumed to be 36 Hz.

III.5.9. Sample calculation of the concentration of CrP from an *in vivo* spectrum of rat hind limb.

Figure IV.6.4.a. depicts a typical ^{31}P spectra of a partially CrP-depleted (four weeks on diet) rat hind limb *in vivo*. The proton and sodium spectra taken during that experiment are not shown. Table III.5.9.a depicts the integrals (areas) of the peaks in each spectra. Note that the spin echo spectra were used for the determination of CrP and GPP concentrations while 90°-T-acquire spectra were used to determine the concentration of ATP.

Rat	^{1}H Area	^{1}H Area w/o lipids	^{23}Na Area
D	121.14	115.96	9.28

Spectra Type	Total Area CrP + GPP	Ratio of Peak Heights	Area ß-ATP
Spin Echo	34.55	0.46	n/a
90°-T-aq	n/a	n/a	6.64

Spectra Type	% of CrP-GPP peak which is GPP	Area Attributed to CrP	Area Attributed to GPP
Spin Echo	72	9.6	24.94
90°-T-aq	n/a	n/a	n/a

	mmoles/L tissue fluid			millimoles/L intracellular fluid		
Spectra	[CrP]	[GPP]	[ATP]	[CrP]	[GPP]	[ATP]
Spin Echo	4.95	12.69	n/a	5.81	14.90	n/a
90°-T-aq	n/a	n/a	3.39	n/a	n/a	3.98

Table III.5.9.a. Summary of NMRS findings for one rat fed the experimental diet for a four week period. 60 scans were taken in the ^{31}P experiment, 16 for the ^{23}Na and 4 for the ^{1}H.

The final values for the concentrations of CrP, GPP, and ATP were derived using the assumptions and equations previously described. For example, if the spectra of the molecule under investigation did not have any overlapping peaks, equation III.5.4.1.iii. was used to correct for the number of scans. In the case of depleted animals, it is first necessary to find the area under consideration that is attributable solely to CrP or GPP. The total area is divided between the two molecules using graph III.5.8.a. and the ratio of

peak heights. In this instance the ratio is 0.46 (determined after simple baseline correction of the spectra); using the graph to determine the fraction of the total peak area which is GPP we find that it is 0.72 or 72 percent. A quick check of the spectra reveals that this would seem to be approximately correct. Multiplication of this factor against the total area reveals that an area of 9.6 is due to CrP and 24.94 to GPP (see above).

To correct for the number of scans taken in this experiment relative to the standards, equation III.5.4.1.iiii. is used. This correction allows the comparison of all similarly acquired spectra by mathematically reducing the integrated area to that which would be obtained if a designated number of scans had been acquired, in this case 20 scans. Using the area attributed to CrP+GPP (Table III.5.9.a) as an example, the area is multiplied by 20 (the number of scans arbitrarily chosen as a point of comparison) and divided by 60 (the number of scans taken), resulting in an area corrected for scan number of 3.2. As the spectra were acquired using a different receiver gain from the standards, correction III.5.4.1.iv. is applied (multiply by 0.31622), giving 1.012.

Using equation III.5.4.1.vi., the scan and receiver gain corrected area is then divided by the corrected area associated with muscle water (115.96 after removal of the area associated with fat). This is then further corrected using calibration curves IV.6.1.a. to provide a "whole leg" CrP concentration using the standard equation of a line ($Y=mX + b$), where the slope of the correction curve is 0.0018 and the Y intercept is 0.000172. The concentration of CrP in this animal is thus 4.95 millimoles per litre tissue fluid.

To determine the intracellular CrP concentrations, information obtained from the ^{23}Na NMRS experiments is required. Briefly, the intramuscular concentrations are multiplied by a factor equivalent to the intra to extracellular ratio. This ratio (as

determined by the ^{23}Na experiments) increases the intramuscular concentrations by a factor equivalent to $(\frac{1}{1 - \infty})$. The fraction of the total leg which is extracellular volume (∞) is determined using equation III.5.4.2.v. as previously discussed. Resting state distributions and concentrations of sodium and potassium were taken from current literature. In a similar fashion to phosphorus, it is the slope and the intercept of the standard curve (figure IV.6.1.b.) that provides this final correction. The results are shown in table III.5.9.a.

IV. RESULTS

IV.1. Rat growth

IV.1.1 Weight

Forty rats were placed on the feeding regime to be used for muscle biochemistry; while twelve rats were placed on an identical diet for NMRS examination. The effect of analogue feeding on body weight of the NMRS animals and a subpopulation of the biochemistry group is shown in Figure IV.1.1.a and Table IV.1.1.a.

The mean body weight of the rats fed GPA is not significantly different ($p>0.05$) from that of the control group at any age during the time course of the experiment ($n\geq8$ in all cases), as determined by Student's t test (a method of estimating whether the difference found represents a chance or regular variation). The mean weight of weanling rats was 59.7 g; the mean weight of the 6 week old animals was 141.4 g.

	Body weight (grams)			
Weeks	Weanling	2	4	6
Control	58.3±1.9 (8)	114.0±7.7 (9)	124.5±3.8 (10)	144.3±8.9 (10)
GPA Fed	61.1±3.8 (8)	110.3±7.6 (9)	119.1±7.1 (10)	138.5±3.2 (10)

Table IV.1.1.a. Comparison of body weight in grams between rats fed ground chow (control) and rats fed ground chow plus 1% GPA for four weeks. Both groups were subsequently fed normal chow. Weights were not significantly different at any age ($p<0.05$, Student's t test). (The numbers in brackets denote sample size)

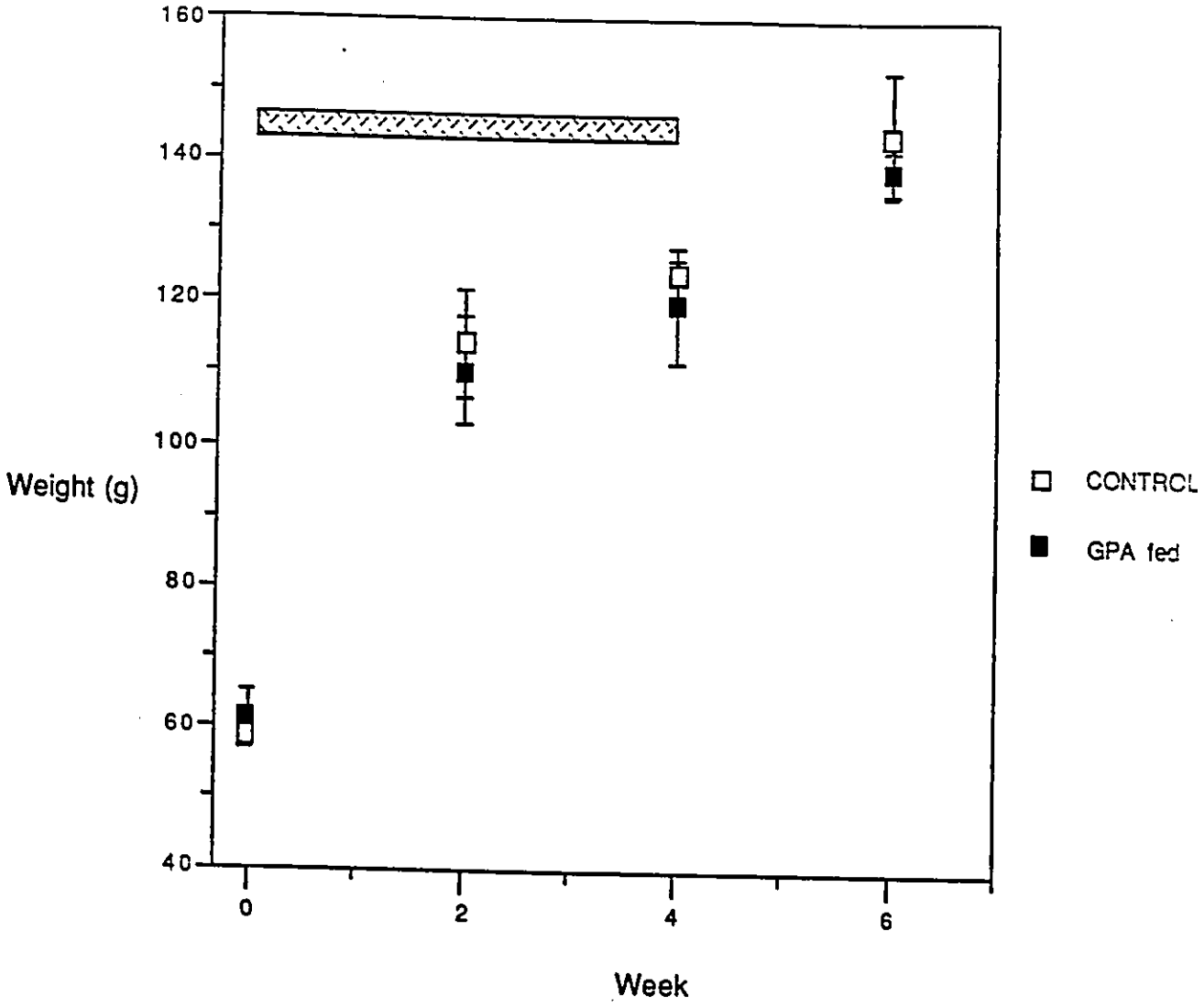

Figure IV.1.1.a. Growth curves of rats fed ground chow (control; open squares) or chow containing 1% GPA (experimental; filled squares) for four weeks (shaded area) from weaning (n≥8). Subsequently, the experimental animals were fed normal chow for a two week period in conjunction with the control animals. Standard deviations are indicated at each point.

IV.1.2 Leg cross sectional area

The effect of analogue feeding on calf cross sectional area of six control and six GPA-fed animals was monitored over the six week dietary regime and is displayed in Figure IV.1.2.a. Calf areas were derived using calf width (lateral measurement), diameter (shin to posterior calf), and circumference.

At weaning, the average elliptical cross sectional area of the hind limb of both groups was 0.49 cm^2. Although not exponential, the increase in cross sectional area of both the control and experimental limbs was rapid over the first four weeks of growth. The hind limb cross sectional areas of the two test groupsbecame significantly different at two weeks of age ($p<<0.05$, Student's one tailed t test). At four weeks, the mean cross sectional areas (elliptical) of the control and GPA-fed animals were 0.89 $\pm$.04 cm^2 and 0.73 $\pm$.08 cm^2 respectively; at six weeks of age the elliptical areas were 0.88 $\pm$ .09 and 0.78 $\pm$.11 cm^2.

The circular cross sectional areas averaged about twice those of the elliptically estimated areas. Hence, the circular representation of the leg appears to be an invalid model to apply to characterize leg area. Table IV.1.2.a. shows both both sets of this data.

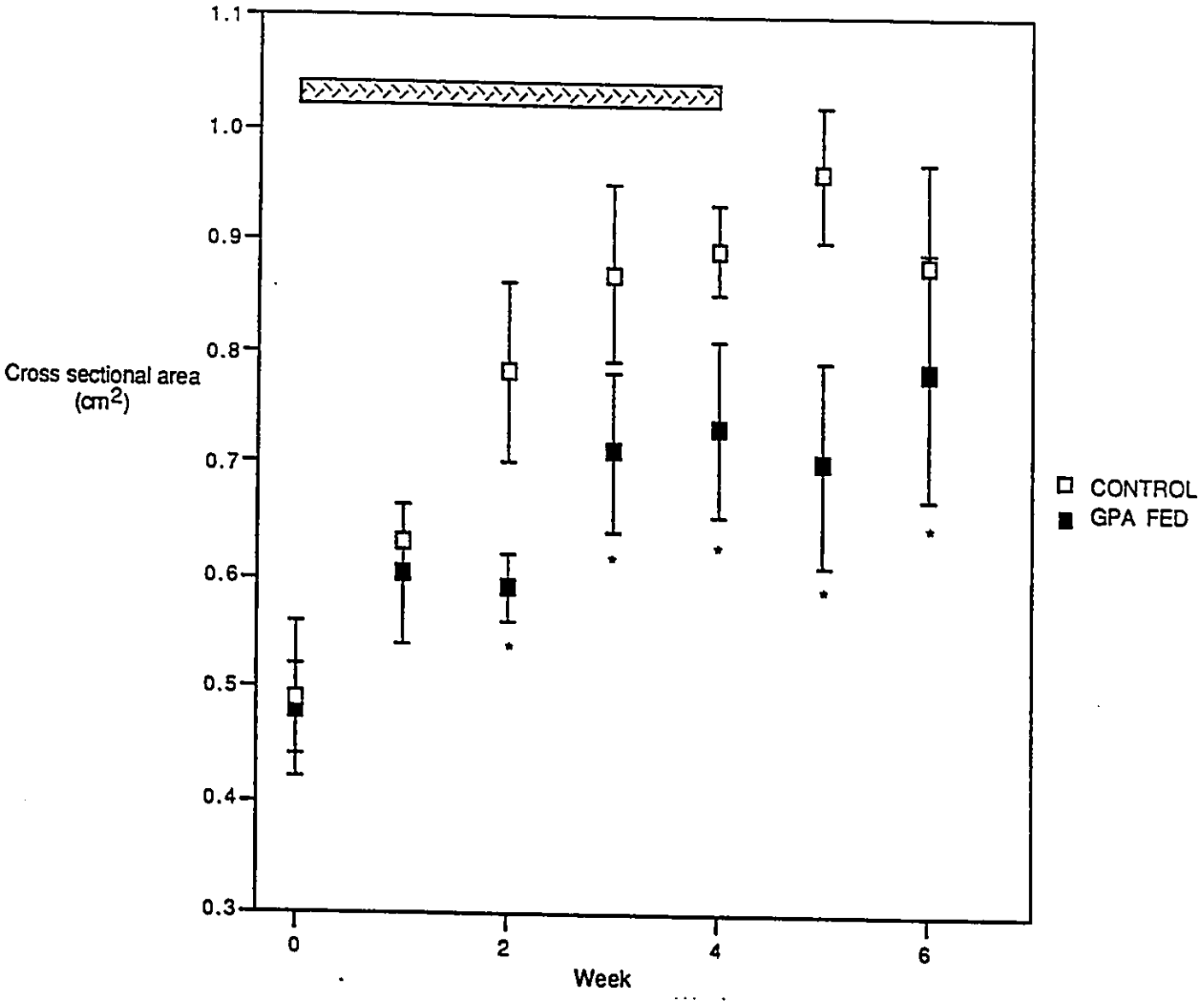

Figure IV.1.2.a. Growth curves of elliptically-estimated rat hind limb cross sectional area measured at calf height. Rats were fed ground chow (control; open squares) or chow containing 1% GPA (experimental; filled squares) from weaning to 4 weeks of age (n=6) (shaded area). Subsequently both groups were fed normal chow. Standard deviations are indicated at each point . The * indicates a significant cross sectional area difference at at least the 0.001 level (Student's one tail t test).

Elliptical cross sectional area estimate (cm^2)

$$(\text{Area} = \pi \frac{\text{width}}{2} \frac{\text{depth}}{2})$$

Weeks	0	1	2	3	4	5	6
Control	0.49±.07	0.63±.03	0.78±.08	0.87±.08	0.89±.04	0.96±.06	0.88±.09
GPA Fed	0.48±.04	0.60±.06	0.59±.03	0.71±.07	0.73±.08	0.70±.09	0.78±.11

Circular cross sectional area estimate (cm^2)

$$(\text{Area} = \pi (\frac{\text{Circumference}}{2\pi})^2)$$

Weeks	0	1	2	3	4	5	6
Control	0.78±.2	1.48±.13	1.52±.1	1.67±.15	1.79±.10	1.93±.13	1.97±.11
GPA Fed	0.75±.2	1.12±.08	1.2±.05	1.40±.08	1.64±.08	1.68±.10	1.67±.19

Table IV.1.2.a. Calf cross sectional area of rats fed ground chow (control) or chow containing 1% GPA (experimental) from weaning to 4 weeks of age (n=6). Subsequently both groups received normal chow. Areas were determined using the equations of an ellipse and a circle.

IV.1.3 Volume as measured by NMRS

Calf growth, in relative terms, was also examined by monitoring the changes in size of the proton NMR signal. The means of the results from these experiments are shown in Table IV.1.3 a. The mean proton area of control animals during any week was not significantly different from the corresponding GPA-fed animal proton area ($p>>0.05$ Student's one tail t test). This lack of linear increase (or decrease) in proton area of the hind limb over the 6 week time course of the experiment indicates that proton NMRS fails to monitor leg growth in an effective manner.

The most simple explanation for this apparent ineffectiveness might be attributed to the size of the coil relative to the size of the calf under observation. If the calf is sufficeintly large that upon insertion the thickest area of the leg does not penetrate the coil centre, then comparing leg volumes using proton signals would not be possible since the probe would not be sampling the same area for each rat.

	Proton area (arbitrary units)			
Week	Control	Control (without lipid)	GPA fed	GPA fed (without lipid)
0	100.0± 20.5	92.6± 18.3	103.7± 7.7	95.0± 8.4
1	110.2± 13.0	96.1± 13.0	102.8± 16.2	91.1± 18.4
2	85.2± 5.4	80.4± 4.5	91.2± 15.3	86.8± 15.7
3	96.9± 9.9	85.4± 9.3	93.3± 21.2	88.1± 21.0
4	90.6± 12.8	78.1± 16.1	107.9± 13.2	103.4± 13.7
5	106.3± 18.3	103.6± 19.0	109.1± 11.2	105.1± 9.9
6	105.1± 20.5	98.5± 20.6	110.3± 15.0	101.6± 9.6

Table IV.1.3.a. Mean proton signal areas as measured by ^1H NMRS of the hind limb of rats fed either ground rat chow (control) or ground rat chow supplemented with 1% GPA for four weeks. Subsequently both groups were fed control diet (n = 6 in all cases). There are no significant differences in intra group sequential signal area or mean inter-group signal area.

IV.1.4 Fat to water ratio of hind limb

Table IV.1.4.a. illustrates the ratio of the proton peak area attributed solely to water to that attributable to water plus fat. GPA-fed animals seem to become increasingly lean with their stay on the diet, while this is apparently not the case for contol animals. The mean final water to proton ratio (pooled results) for the control animals is 0.93 while that for the GPA-fed rats is 0.92. The statistically significant (Student's one tail t test, $p<0.05$) tendency towards leaness, exhibited between weeks 1 and weeks 4 and 5 may not be reliable considering the more variable volume measurements of section IV.1.3.

Ratio of proton signals

Week	Control	GPA fed
0	0.93	0.91
1	0.88	0.88
2	0.94	0.95
3	0.89	0.94
4	0.86	0.96
5	0.97	0.96
6	0.93	0.92

Table IV.1.4.a. Ratio of proton peak area without lipid component to total proton peak area with lipid component as determined by NMRS of rats fed according to the dietary regime.

IV.2 Dry to wet weight ratios

Table IV.2.a. contains the mean dry to wet weight ratios and standard deviations obtained from drying pieces of muscle from the right gastrocnemius of normal and GPA-fed rats to constant weight. The mean of the average of all four test periods is 0.2425 ± 0.0095 for the control and 0.2415 ± 0.007 for the GPA-fed animals. There was no significant difference found between the values of any of the ratios in either group at any age ($P>>0.05$, Student's two tail t test).

Dry to wet weight ratio

Weeks	0	2	4	6
Control	0.2336±.0058 (5)	0.2511±.0063 (5)	0.2454±.0044 (7)	0.2402±.0215 (9)
GPA Fed	0.2327±.0098 (6)	0.2417±.0033 (6)	0.245±.0036 (7)	0.2467±.0111 (9)

Table IV.2.a. Dry to wet weight ratios of the gastrocnemius muscle of control and GPA-fed rats after 0, 2, 4, and 6 weeks of GPA treatment. Rats were fed according to the dietary regime. The numbers in brackets denote sample size. There is no significant difference between obtained control and experimental ratios or between animals on similar diets at different ages (Student's two tail t test).

IV.3 Weight loss due to muscle storage

Muscle storage at -90 °C for prolonged periods of time did not significantly change the wet muscle weight of 0.1 - 0.02 g pieces of gastrocnemius (Table IV.3.a.) ($p>0.05$, Student's two tail t test). Repeated weighing and drying of these excised portions demonstrated a weight loss equivalent to 0.36% ±.62 after 3 weeks of storage (n=12).

Average loss in original weight (percent) after storage

Normalized original weight	1 week	2 weeks	3 weeks
100	0.40 ± .047	0.38 ±.064	0.36 ±.062

Table IV.3.a. Weight loss due to the storage of the muscle samples at -90° C prior to acid extraction and biochemical analysis (n=12). There is no significant total loss or gain in weight during the three weeks of storage (Student's two tailed t test).

IV.4 Flame photometric analysis of the sodium and potassium contents of rat muscle

Results from determinations of the total and intracellular sodium and potassium concentration from control and GPA-fed animals are shown in Table IV.4.a. The mean sodium and potassium concentrations (pooled results) for the control and GPA-fed groups were 39.5, 137.3 and 42.5, 137.8 millimoles / L tissue fluid respectively. There was no significant difference between the mean sodium and potassium concentrations of control and GPA-fed animals (matched age pairs) at any time during the 6 week experiment ($p>>0.05$, Student's unpaired t test). Similarly, the difference in the sum of the sodium and the potassium concentrations between the control and experimental group (176.5 millimoles/L tissue fluid (control), 179.8 millimoles/L tissue fluid (GPA fed)) was not significant as determined by Student's unpaired two tail t test ($p>>0.05$).

Control

Weeks on diet	[Sodium] a	[Sodium] b	[Potassium] a	[Potassium] b	[Sum] a	[Sum] b
0	35±4 (3)	47±5	100±6	133±8	135±3	179±4
2	27±3 (4)	35±4	110±4	145±5	136±2	180±2
4	27±5 (3)	36±6	103±2	137±3	130±4	173±5
6	30±4 (8)	40±5	102±13	134±17	132±12	174±15

GP-fed

Weeks on diet	[Sodium] a	[Sodium] b	[Potassium] a	[Potassium] b	[Sum] a	[Sum] b
0	35±2 (3)	46±2	104±11	138±14	139±10	184±14
2	28±5 (4)	37±6	111±7	147±9	139±9	184±13
4	31±5 (6)	42±6	102±12	137±16	134±11	177±14
6	34±4 (8)	45±5	98±14	129±19	131±11	174±19

Table IV.4.a. Sodium and potassium concentrations of gastrocnemius muscles of rats fed according to the dietary regime at 0, 2, 4, and 6 weeks of age expressed as a) millimoles/kg wet weight and b) millimoles/L tissue fluid. The numbers in brackets denote sample size.

IV.5 Biochemical assays and calculation of metabolite concentrations

Biochemical analysis of the metabolite concentrations of the left gastrocnemius of control and GPA-fed rats demonstrated the following:

Compared to pooled control (14.3 millimoles /L tissue fluid), free creatine[1] was depleted by 47 percent in two weeks and 60 percent in four weeks by the feeding of the creatine analogue GPA (Table IV.5.a). Matched age pair differences between the control and experimental groups creatine concentrations were 40 and 75 percent for weeks 2 and 4 respectively.

Creatine phosphate was depleted by 88 percent of pooled control values in GPA-fed animals after two weeks and 90 percent after four weeks of GPA feeding (see Figure IV.5.b and Table IV.5.a) (Control concentration equals 23.4 millimoles /L tissue fluid). Similar comparisons of control and experimental group matched age pairs yield decreases of 88 and 92 percent at weeks 2 and 4 respectively.

Refeeding normal chow to the experimental group for two weeks caused an increase in the concentration of creatine to the level of 6.3 millimoles /L tissue fluid or 45 percent of control. Matched age pair differences between the control and experimental groups creatine concentrations was 33 percent after 2 weeks of refeeding.

Creatine phosphate levels rose to 6.9 millimoles /L tissue fluid (30 percent of control) with the return of the experimental animals to normal chow (see Figure IV.5.b

---

1 The biochemical assays performed provide estimates of free creatine. Free creatine should not be confused with total creatine which is generally two fold larger. Please refer to section I.5.

and Table IV.5.a) for a two week period. Similarly matched age pair differences between the control and experimental groups creatine phosphate concentration was 30 percent.

ATP levels decreased to 6.2 millimoles /L tissue fluid from the pooled control concentration of 7.6 millimoles/L tissue fluid after two weeks, and to 4.3 millimoles /L tissue fluid after four weeks (see Figure IV.5.a and Table IV.5.a). Matched age pair differences in ATP concentration between control and experimental groups were 22 at 2 weeks and 50 percent at 4 weeks of GPA feeding.

Following 2 weeks of refeeding regular chow, there was a 60% increase in the ATP concentration of the previously GPA-fed animals.

The mean protein contents of control and GPA-fed animal muscles did not differ significantly between the two groups at any week ($p>0.05$). The mean percent protein for the control group was 14.03 ± 0.11 while that of the GPA-fed group was 13.4 ± 0.15. This small disparity was not found to be significant ($p>>0.05$). (see Table IV.5.b. and Table IV.5.b).

The difference in protein content between control weanling and any of the subsequent control animals is significant ($p<0.001$) (Table IV.5.b). Similarly there appears to be a significant difference between the protein content in 2 week controls and the 4 week control animals ($p<0.05$). This is perhaps due to a spuriously low value for the week zero control value. This is supported by the lack of any significant difference between the protein contents of any of the GPA-fed animals ($p>0.05$).

Significant differences in the concentration of ATP between control and GPA-fed animals exist at 2 and 4 weeks ($p<0.05$, Student's 1 tail unpaired t test). Similar differences between control and GPA-fed animals are apparent for CrP at 2 and 4 weeks.

At 6 weeks of age, CrP levels remain significantly different from normal, while ATP levels return to within normal range ($p=0.6$, Student's 1 tail unpaired t test) (see Figure IV.5.b. and Table IV.5.a).

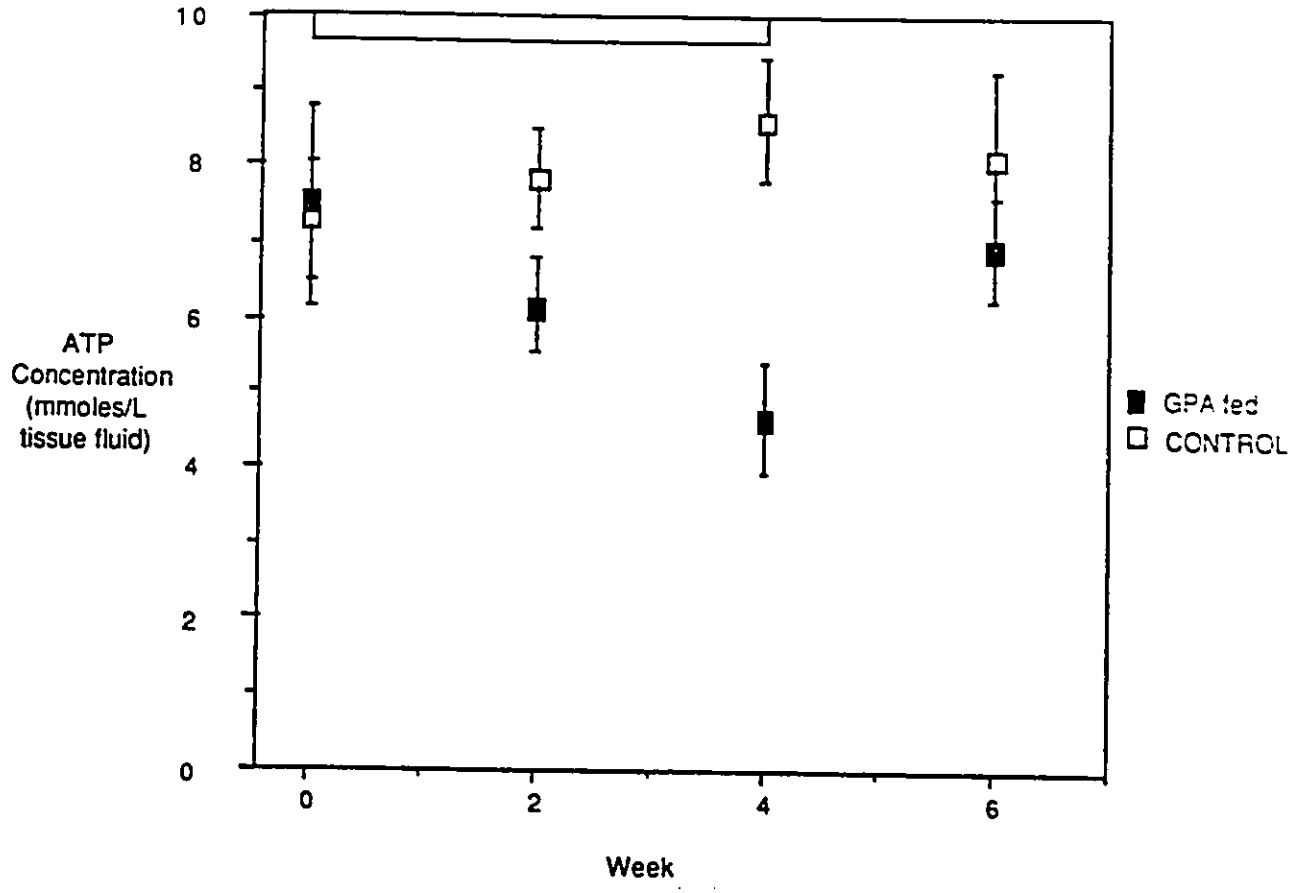

Figure IV.5.a. Intra-limb ATP concentration of rat hind limb as measured using biochemical assays from weaning through to 6 weeks of age. Unshaded bar indicates the time period during which the experimental animals were fed chow containing 1% GPA by weight. Open symbols denote control animals while closed symbols denote rats fed a diet containing 1% GPA.

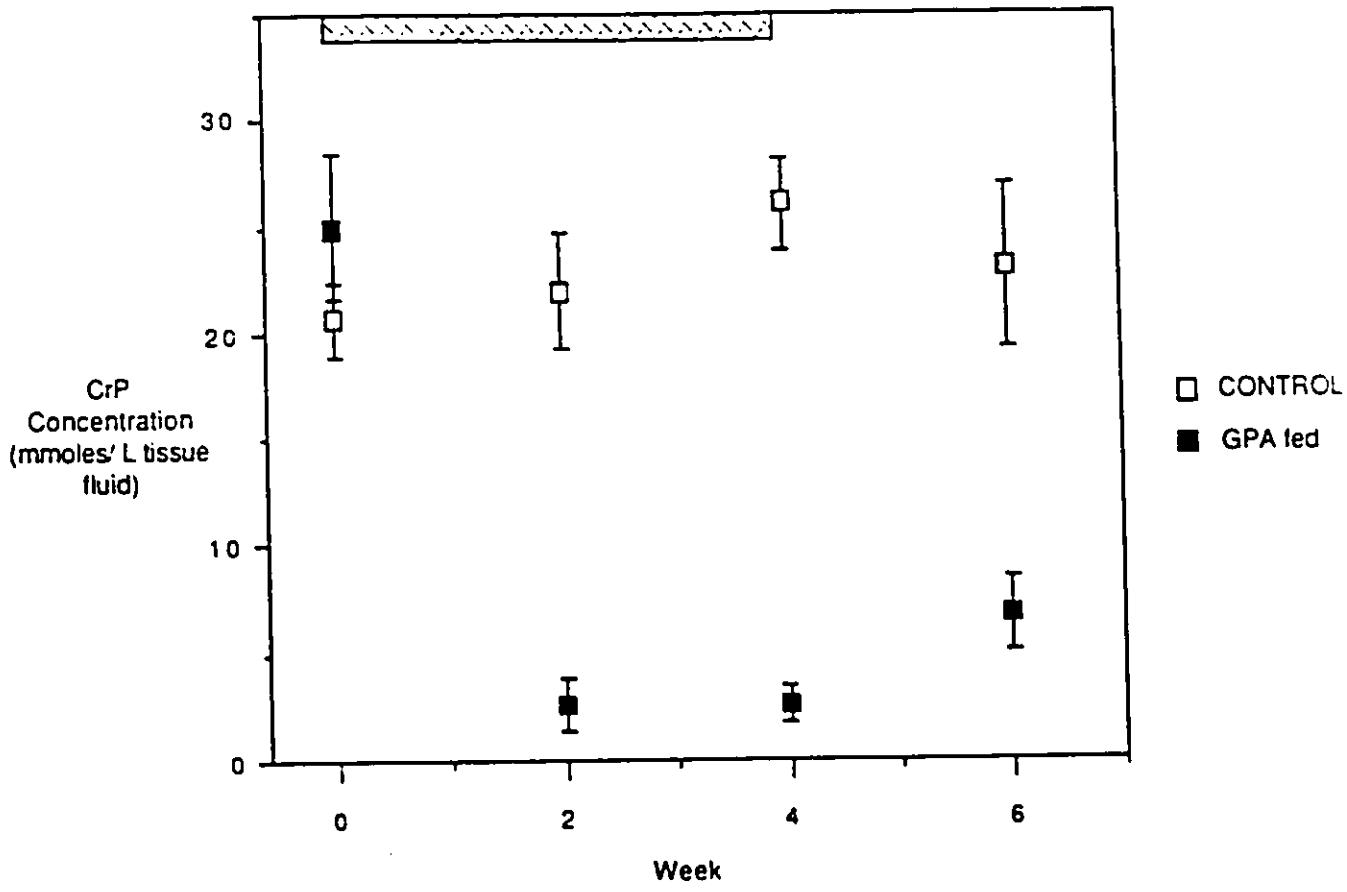

Figure IV.5.b. Intra-limb CrP concentration of rat hind limb measured using biochemical assays from weaning through to 6 weeks of age. Shaded area indicates the time period during which the experimental animals were fed chow containing 1% GPA by weight. Open symbols denote control animals while closed symbols denote rats fed a diet containing 1% GPA.

P.C.M. concentration (millimoles/ L tissue fluid)

P.C.M.	Week	0	2	4	6	mean
CrP	control	20.7±1.8 (5)	22.0±2.7 (9)	26.0±2.1 (11)	23.1±3.8 (8)	23.4
	GPA fed	25±3.4 (4)	2.7±1.2 (8)	2.1±.8 (8)	6.9±1.8 (6)	
Creatine	control	14.1±5.1	12.2±1.9	15.7±4.2	18.8±5.9	14.3
	GPA fed	13.8±4.9	7.5±1.4	4.2±1.7	6.3±3.7	
GPP	control	1.0±.3	0.5±.37	0.5±.5	1.1±.7	
	GPA fed	0.5±.4	14.9±.4	9.2±1.9	9.3±2.5	
ATP	control	7.3±.8	7.9±.7	8.7±.8	8.1±1.2	8.1
	GPA fed	7.5±1.3	6.2±.6	4.3±.7	6.9±.7	
Pi	control	10.5±4.0	12.1±7.4	11.2±3.7	10.4±3.5	11.2
	GPA fed	11.2±4.0	9.4±3.4	9.0±3.6	8.8±1.5	

Table IV.5.a. PCM concentrations of animals fed ground rat chow (control) or ground rat chow supplemented with 1% GPA as determined using biochemical assays. n for each group appears in brackets under the first group. GPA-fed animals revert to the control diet at 4 weeks of age.

Protein content of rat hind limb gastrocnemius

Weeks	0	2	4	6
control	10.8±1.2 (5)	13.5±.82 (9)	15.2±1.1 (11)	14.4±1.3 (8)
GPA fed	13±2.7 (4)	13±1.0 (8)	14.1±.67 (8)	13.5±1.6 (6)

Table IV.5.b. Protein contents as a percentage of muscle weight of animals fed ground rat chow (control) and rats fed ground rat chow supplemented with 1% GPA. n for each group appears in brackets. GPA-fed animals revert to the control diet at 4 weeks of age.

IV.6 Nuclear Magnetic Resonance Spectroscopy

IV.6.1 Standard solutions

Figures IV.6.1.a and IV.6.1.b present the calibration curves and the equations of their respective lines (obtained by linear regression) for phosphorus and sodium. These graphs are based on Ackerman's assumptions and his equation #7 (Thulborn and Ackerman, 1983; equation III.5.4.1.ii above), and relate the ratios of the areas of the peaks of ^{31}P or ^{23}Na and ^{1}H to that of the concentration of inorganic phosphate or sodium in a solution of sodium chloride and K_2HPO_4. The equations of the lines are depicted on the graphs below and in Methods and Materials (section III.5.4.1). Prepared using four different sample volumes and concentrations of sodium and phosphorus, the standard curves are linear and independent of both of these variables. A linear regression through the data points of both of these graphs yields the slopes (0.0018 for phosphorus, 0.0029 for sodium) and Y intercept (0.0001722 for phosphorus and 0.000124 for sodium).

Test solutions of various volumes, made on separate occasions, with a concentration of CrP of 25 mM and ATP of 10 mM in a 25 mM solution of NaCl gave results almost identical to the standards.

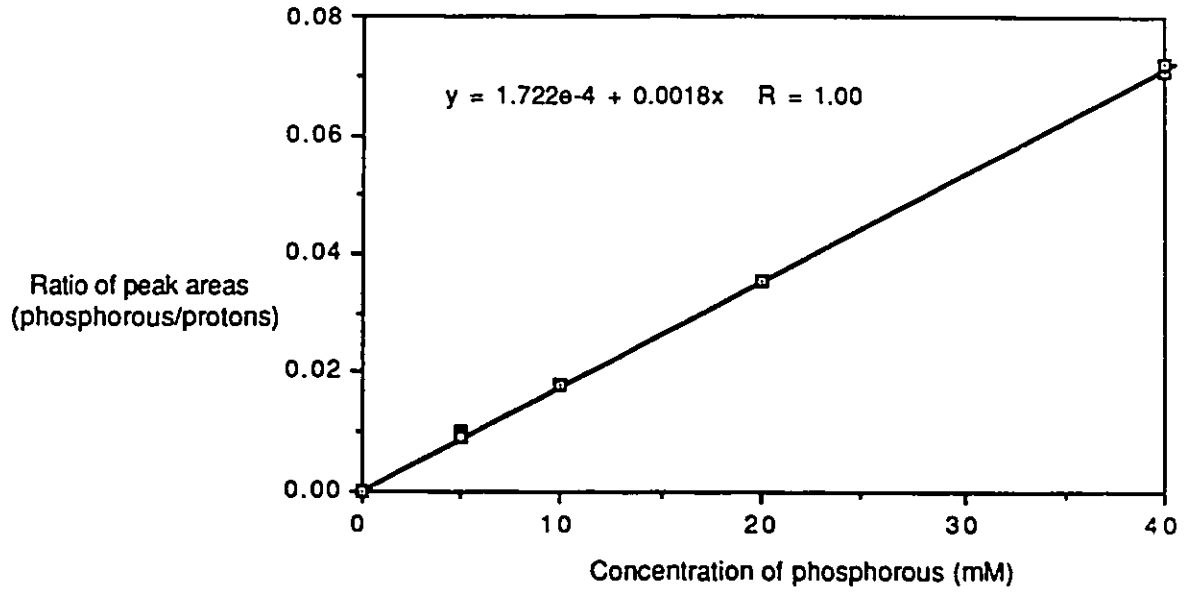

Figure IV.6.1.a. Phosphorus-containing metabolite calibration curve. Physiologically representative solutions of known volume (0.648 ml, 0.916 ml, 1.023 ml, 1.250 ml) and K_2PO_4 concentrations provide a ratio of phosphorus and proton NMR signals. The ratio can subsequently be used to obtain measurements of in vivo PCM concentrations.

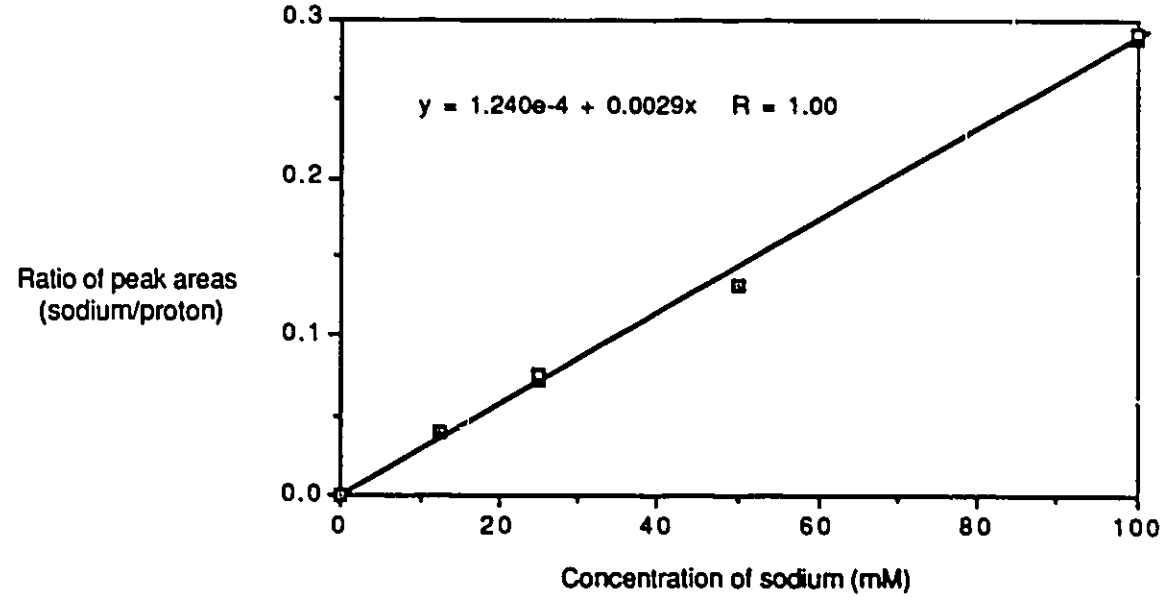

Figure IV.6.1.b. Sodium calibration curve. Physiologically representative solutions of known volume, K_2PO_4 and sodium concentrations provide a ratio of sodium and proton NMR signals. The ratio can subsequently be used to obtain measurements of in vivo sodium concentration.

IV.6.2 Receiver gain

Figure IV.6.2.a. presents the standard curve used to translate the in vivo PCM integration areas obtained with a receiver gain (RG) of 20 into areas at the receiver gain of 30 (the RG used to obtain the phosphorus standard curve). The equation of the polynomial is given below. The data points used to obtain this graph are given in Table IV.6.2.a.

$$\text{Peak area} = 236.8906 \times 10^{(-0.05\ RG)} \qquad \text{IV.6.2.i}$$

The graph data was obtained by taking a solution of known volume and concentration of NaCl and performing the previously described sodium NMR experiment (Methods III.5.2., III.5.3) at receiver gains between 10 and 60. The obtained signal areas were corrected to 4 scans (Table IV.6.2.a.) and plotted on a logarithmic scale.

Receiver Gain (Arbitrary Units)	Sodium Peak Area
10	74.264
15	41.755
20	23.625
25	14.623
30	7.320
35	4.222
40	2.189
50	0.735
60	0.247

Table IV.6.2.a. Data points used in the construction of the receiver gain calibration curve (Figure IV.6.2.a.).

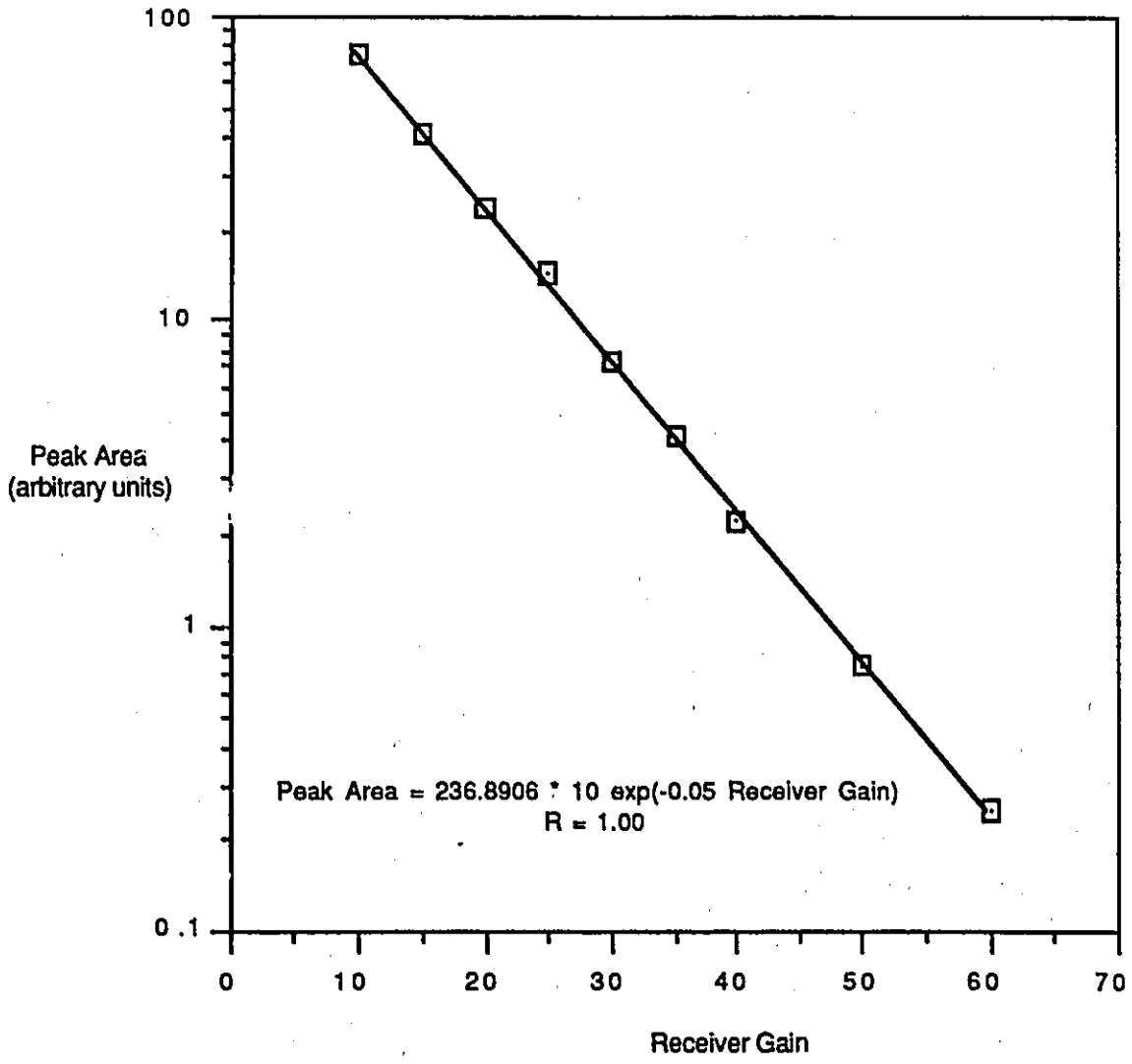

Figure IV.6.2.a. Bruker MSL-300 receiver gain calibration curve. (n≥3 in all cases)

IV.6.3. Sodium concentrations

There was no significant difference ($p>0.05$, Student's paired two tail t test) between sodium concentrations of control and GPA fed at any age as determined by ^{23}Na and ^{1}H NMRS (Table IV.6.3.a.). Nor were the grouped mean $[Na]_i$ values obtained for control and GPA-fed animals significantly different from each other; 31.6 ±6.9 millimoles/liter tissue fluid (control) and 30.5±5.8 millimoles/liter tissue fluid (GPA fed). These means were significantly different ($p>>0.05$, Student's unpaired two tail t test) from the grouped means obtained by the flame photometry method (Table IV.6.3.b.).

Sodium Concentration (millimoles/litre tissue fluid)

Weeks	0	1	2	3	4	5	6
control	30.2±7.0	33.5±7.0	34.3±6.2	31.0±4.1	37.7±12.9	29.9±4.8	25.8±.2.3
GPA fed	29.5±1.1	30.4±3.7	33.2±7.2	31.4±4.3	27.1±2.4	33.0±6.3	26.7±4.4

Table IV.6.3.a. Total hind limb sodium concentrations (millimole/L tissue fluid) in control and GPA-fed rats at 0, 2, 4, and 6 weeks of age as measured by ^{23}Na NMRS. (n=6 in all cases)

Sodium Concentration (millimoles/litre tissue fluid)

	NMRS	flame photometry
control	31.57±6.9	39.6±5.9
GPA fed	30.48±5.8	42.4±5.9

Table IV.6.3.b. Mean total hind limb sodium concentrations (millimole/L tissue fluid) in control and GPA-fed rats averaged over 0,2,4, and six weeks of age as measured by ^{23}Na NMRS and flame photometry. (n=6 in all cases)

IV.6.4. Concentrations of phosphorus-containing metabolites

Please refer to figure IV.6.4.a. and IV.6.4.b. for sample phosphorus spectra of both control and analogue-fed animals. N.B. that aged matched comparisons between control and experimental animals produce similar and oftentimes identical results to comparisons of pooled control and week specific experimental animals.

In Table IV.6.4.a. the concentrations (millimole/L tissue fluid (t.f.)) and standard deviations of the PCMs at 0 through 6 weeks are shown for control and GPA-fed rats. These determinations of metabolite concentrations demonstrate the following:

Relative to pooled control values (17.9 millimole/L t.f. (6 week average)), creatine phosphate was depleted by 47% in three days, by 75% after two weeks and by 85% after four weeks of feeding the creatine analogue GPA to the experimental group (see Figure IV.6.4.b., Figure IV.6.4.c. and Table IV.6.4.a.). Similar age matched comparisons illustrate reductions of about 80% at both 2 and 4 weeks of feeding.

Refeeding normal chow to the experimental group caused an increase in the concentration of creatine phosphate to the level of 8.2 ±2.2 millimole/ L t.f. (45% of results of the pooled control) (see Figure IV.6.4.b., Figure IV.6.4.c. and Table IV.6.4.a.). A similar age matched comparison illustrates an increase to 50% of control.

ATP levels decreased to 3.8±.7 millimole/ L t.f. compared to the value of the pooled controls 5.6 millimole/ L t.f. after two weeks (68% of the pooled control) and to 2.6 ±0.7 millimole/ L t.f. (46% of the pooled control) after four weeks (see Figure IV.6.4.d. and Table IV.6.4.a.). Aged matched differences of the same time periods produce results of 79% and 46%.

Refeeding normal chow to the experimental group caused an increase in the concentration of ATP 4.2 ± 0.6 millimole/ L t.f. (75 percent of control) (see Figure IV.6.4.d. and Table IV.6.4.a.). Aged matched differences of the same time periods produce results of 77%.

Correcting these results to intracellular concentrations (using the correction factor obtained by determining the concentration of sodium per litre of tissue fluid) increased the concentrations of the PCM by an average of 20% (control mean CrP= 22.5 mM). The average increase in the standard deviations was approximately 2% (Figure IV.6.4.e., Figure IV.6.4.f. and Table IV.6.4.b.).

Differences between the concentrations of CrP and ATP in control and GPA-fed animals were significant ($p<<0.05$) at every week on the dietary regime (Student's one tail unpaired t test).

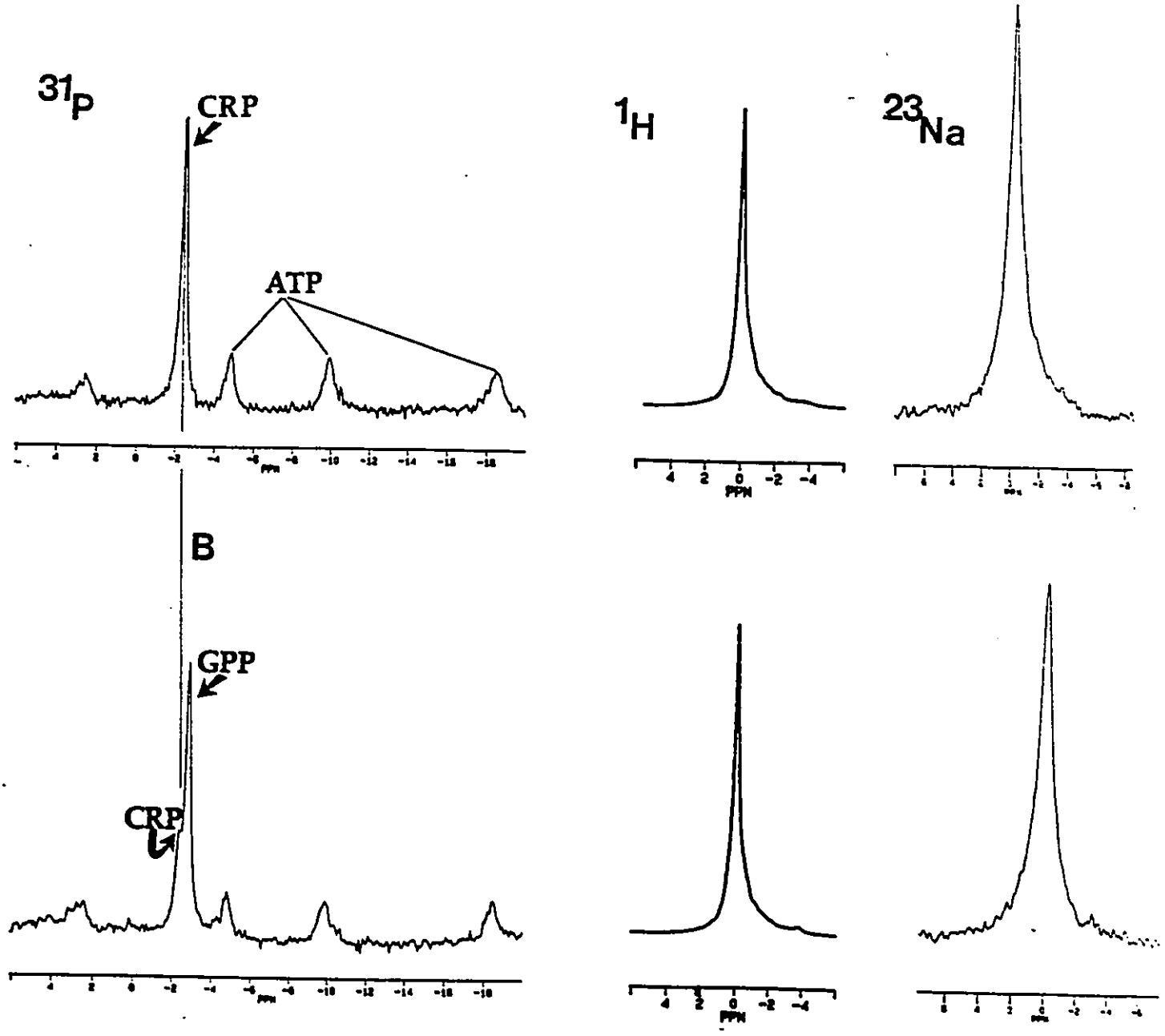

Figure IV.6.4.a. In vivo ^{31}P, ^{1}H, and ^{23}Na spectra of (A) control and (B) GPA-fed rat hind limb after 4 weeks on the dietary regime. Note the predominance of the GPP peak in the ^{31}P spectra of the Gp-fed animal and its absence in the control spectra.

PCM Concentration (millimoles/ L tissue fluid)

Weeks	[CrP] Control	[CrP] GPA fed	[ATP] Control	[ATP] GPA fed	[GPP] GPA fed
0	21.5±4.7	19.6±2.0	6.4±.4.0	5.4±6.0	0.0±0.0
3 days		9.6		5.1	7.0
1	17.2±3.0	8.0± 2.0	5.6±1.0	4.2±0.8	8.1±2.1
2	21.0±6.4	4.6±1.9	4.8±1.0	3.8±0.7	8.5±2.5
3	17.8±2.2	4.6±1.2	5.7±1.0	3.3±0.7	11.3±2.6
4	12.8±2.6	2.9±1.0	4.4±1.1	2.0±0.6	10.3±2.3
5	19.3±2.4	4.2±1.4	6.6±1.3	3.5±1.1	10.8±1.8
6	16.2±3.1	8.2± 2.4	5.4±0.7	4.2±0.6	9.2±2.8
mean	17.9		5.6		

Table IV.6.4.a. PCM concentrations, determined by NMRS, of animals fed ground rat chow (control) or ground rat chow supplemented with 1% GPA (experimental). n =6 for each group except the 3 day experiment (n=1) and the 6 week experiment (n=5). GPA-fed animals revert to the control diet at 4 weeks of age.

Intracellular PCM Concentration (millimoles/ L)

Weeks	[CrP] Control	[CrP] GPA fed	[ATP] Control	[ATP] GPA fed	[GPP] GPA fed
0	25.6±5.9	23.1±2.3	8.2±0.9	6.7±0.8	0.0±0.0
3 days		12.0		6.2	8.7
1	21.1±3.2	10.0±2.3	6.8±1.4	5.7±1.0	10.1±2.5
2	25.8±6.3	6.4±2.9	6.7±1.3	5.3±1.5	11.2±4.0
3	21.4±2.9	5.8±1.2	7.5±1.3	4.5±1.0	13.2±2.6
4	22.2±5.0	5.1±1.0	8.1±1.8	3.1±0.8	15.5±2.6
5	22.9±2.8	5.4±1.7	8.3±1.7	4.5±1.0	12.6±2.6
6	18.6±3.3	9.9±2.8	6.6±0.8	5.5±0.7	11.0±3.2
mean	22.5		7.5		

Table IV.6.4.b. PCM concentrations (determined by NMRS) corrected to intracellular concentration, of animals fed ground rat chow (control) or ground rat chow supplemented with 1% GPA (experimental). n=6 for each group except the 3 day experimental (n=1) and the 6 week experimental (n=5). GPA-fed animals revert to the control diet at 4 weeks of age.

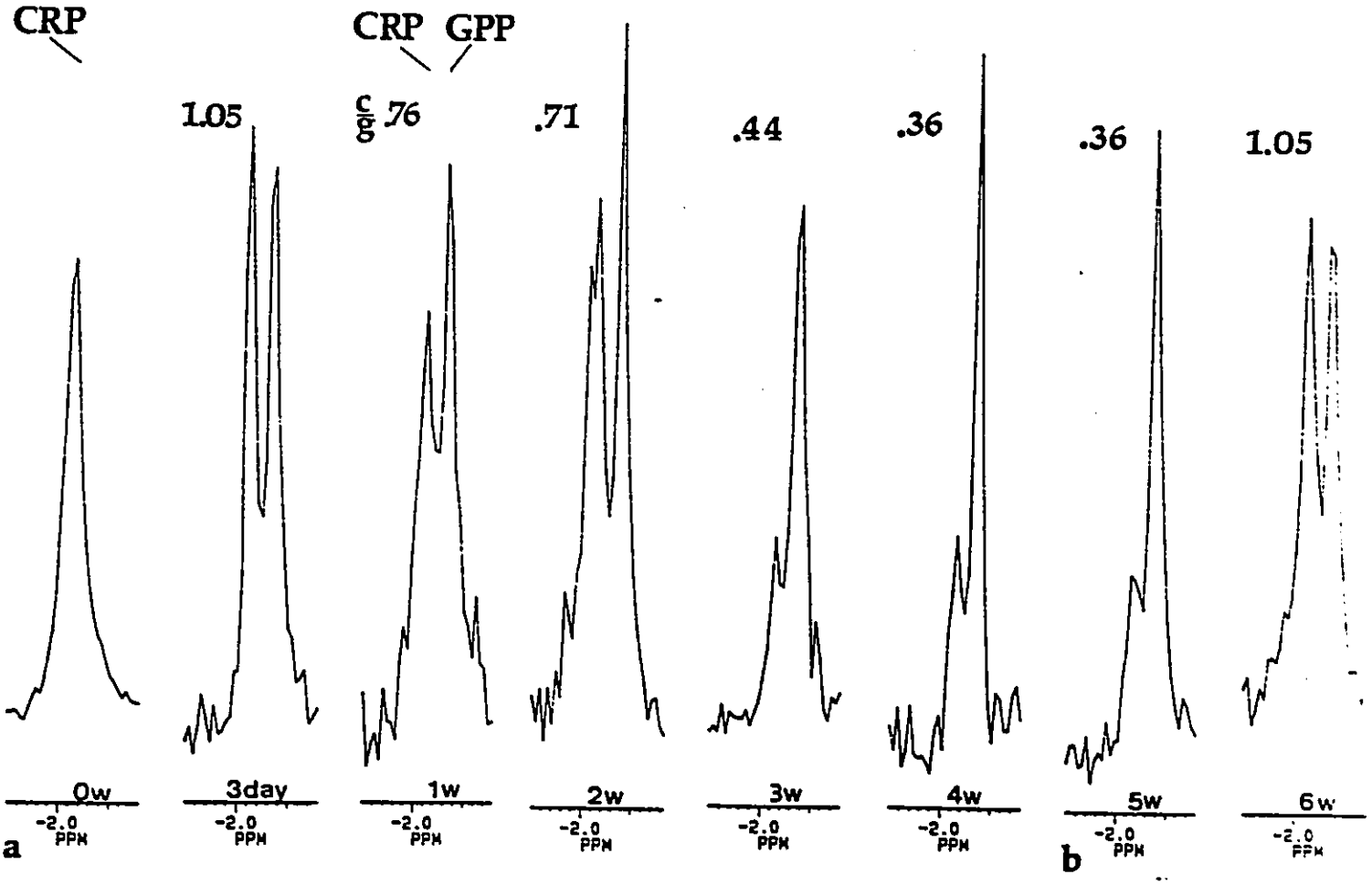

Figure IV.6.4.b. In vivo ^{31}P spectra in the region -3 to -1 ppm of the hind limb of an analogue-fed rat at weaning through 6 week of feeding the GPA-supplemented dietary regime. The ratios of CrP to GPP are indicated above each spectrum.

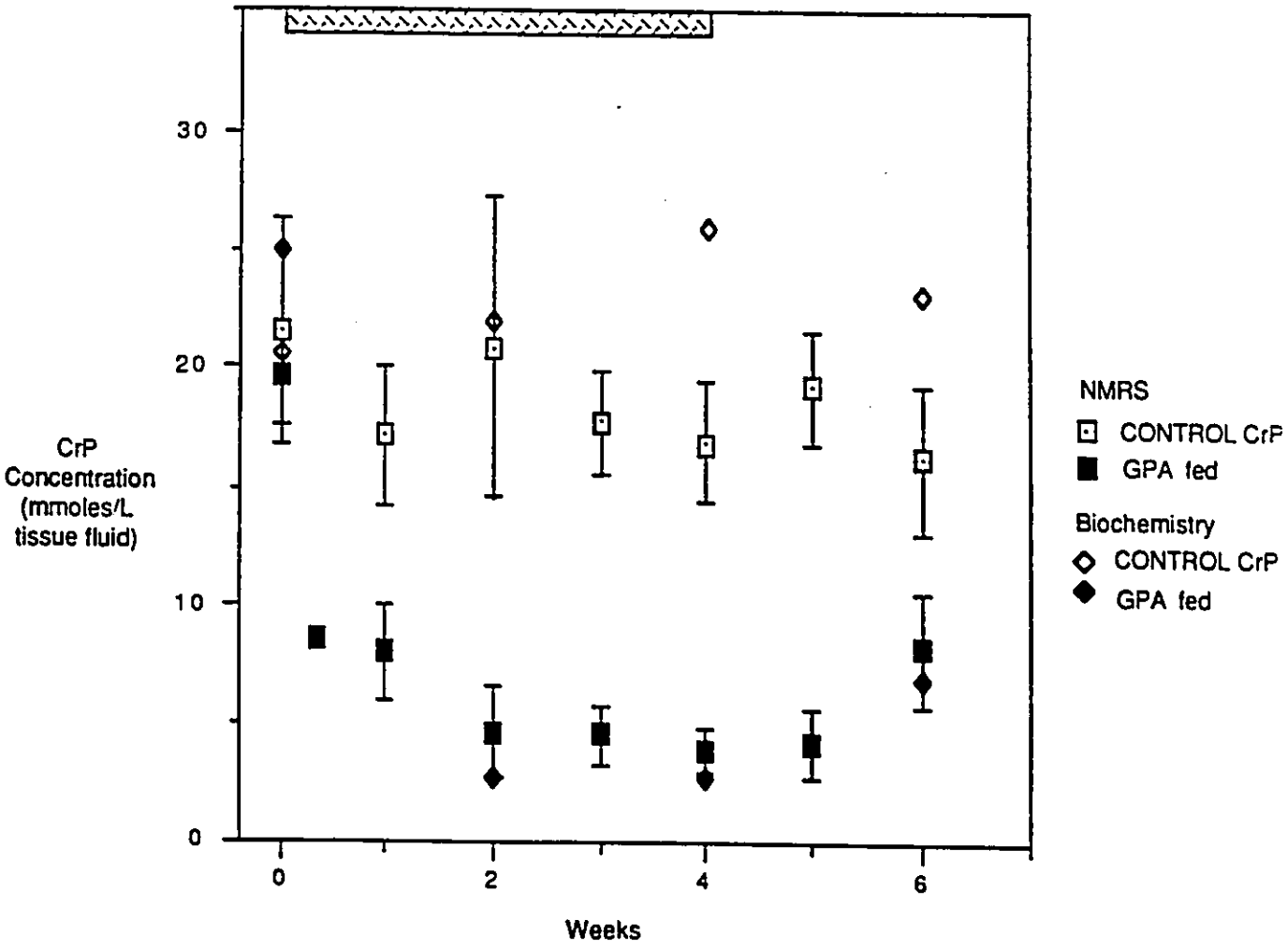

Figure IV.6.4.c. CrP concentrations, as determined by NMRS (squares) and biochemical assay (diamonds), of animals fed ground rat chow (control, open symbols) or ground rat chow supplemented with 1% GPA (experimental, closed symbols). n=6 for each group except the 3 day experimental (n=1) and the 6 week experimental (n=5). GPA is fed to the expermental group for four weeks (shaded area) after which the animals revert to the control diet.

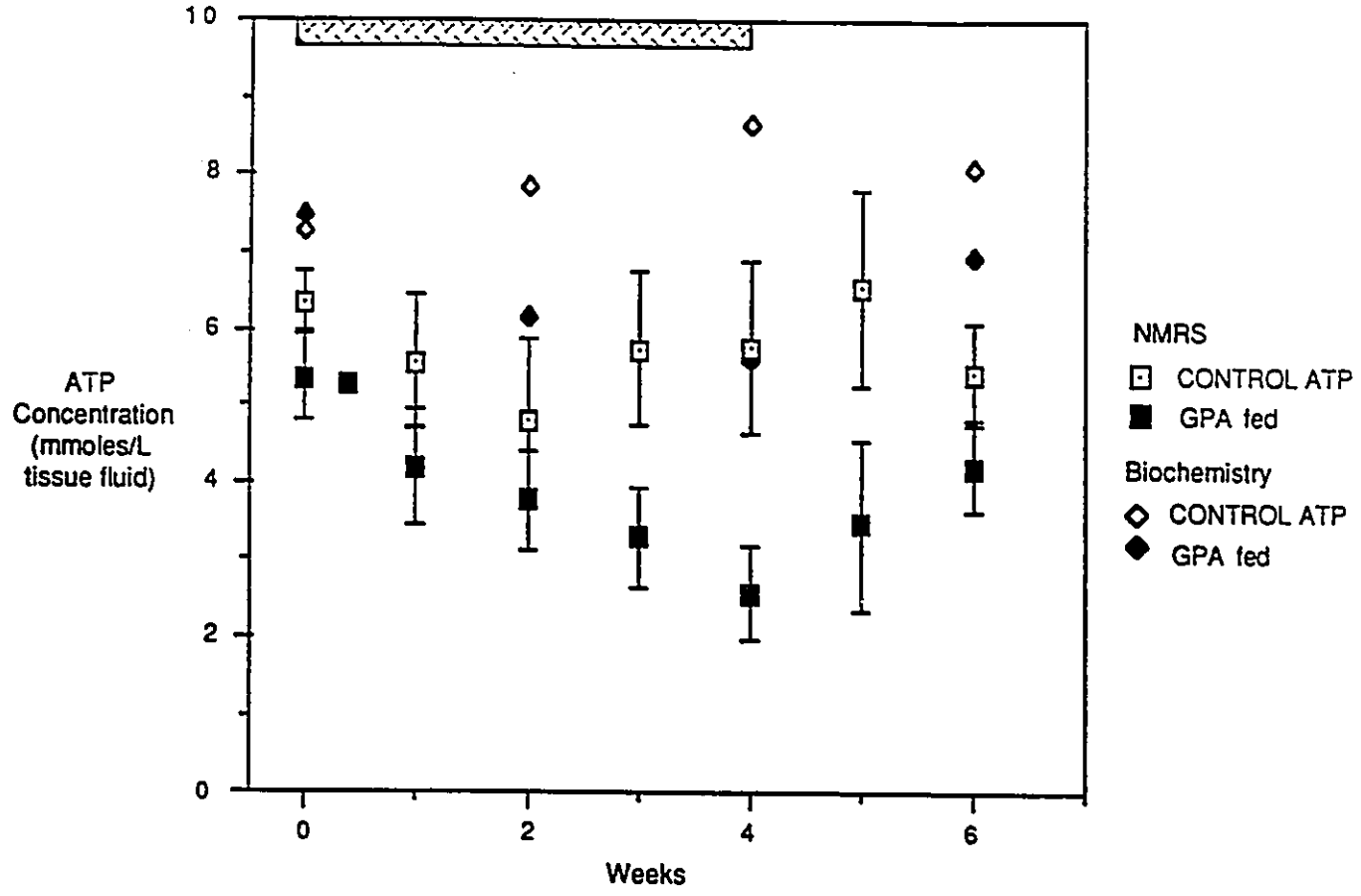

Figure IV.6.4.d. ATP concentrations, as determined by NMRS (squares) and biochemical assay (diamonds), of animals fed ground rat chow (control, open symbols) or ground rat chow supplemented with 1% GPA (experimental, closed symbols). n=6 for each group except the 3 day experimental (n=1) and the 6 week experimental (n=5). GPA is fed to the expermental group for four weeks (shaded area) after which the animals revert to the control diet.

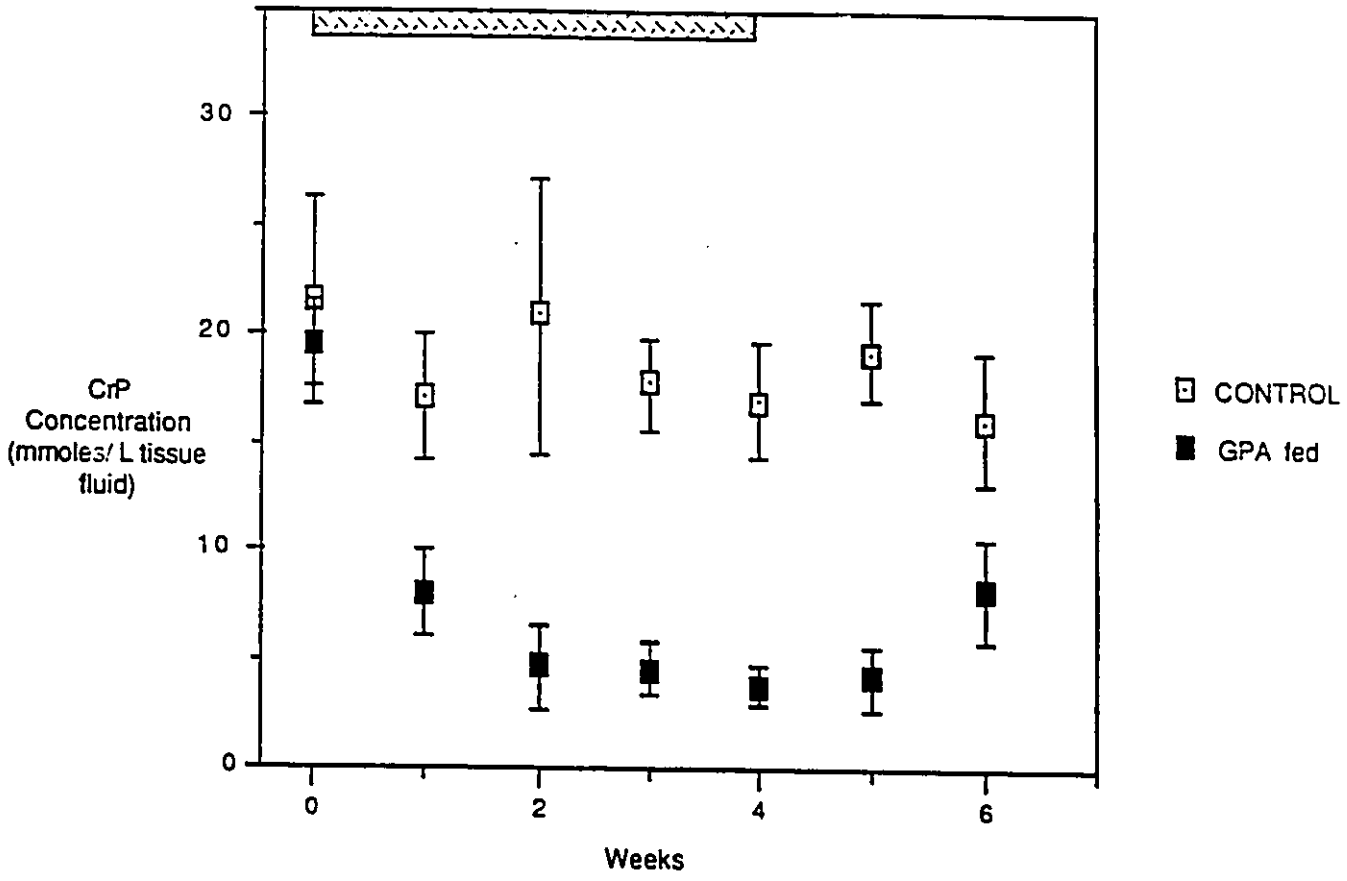

Figure IV.6.4.e. CrP concentrations, as determined by NMRS, of animals fed ground rat chow (control, open symbols) or ground rat chow supplemented with 1% GPA (experimental, closed symbols). n=6 for each group except the 3 day experimental (n=1) and the 6 week experimental (n=5). GPA is fed to the expermental group for four weeks (shaded area) after which the animals revert to the control diet.

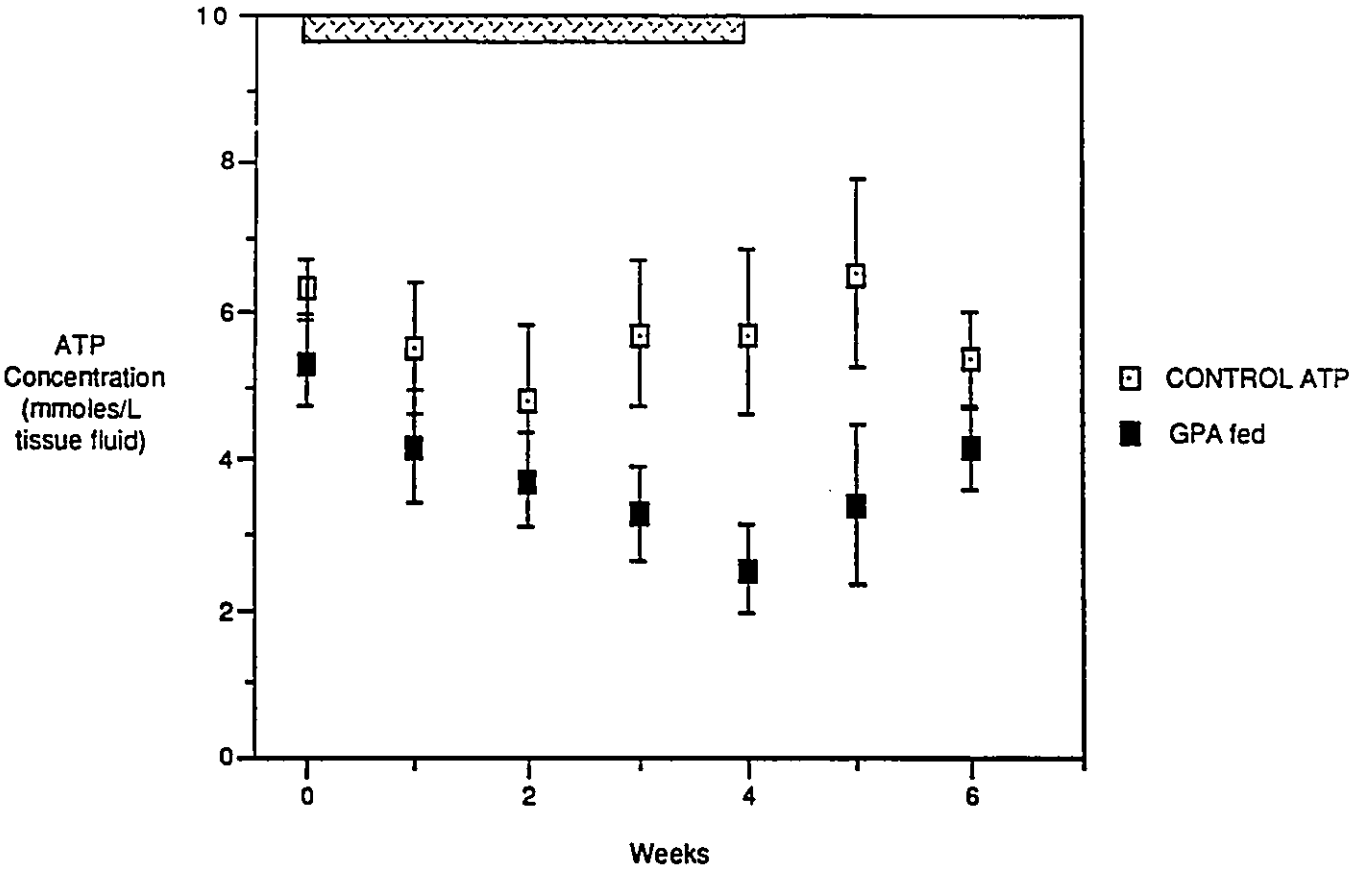

Figure IV.6.4.f. ATP concentrations, as determined by NMRS of animals fed ground rat chow (control, open symbols) or ground rat chow supplemented with 1% GPA (experimental, closed symbols). n=6 for each group except the 3 day experimental (n=1) and the 6 week experimental (n=5). GPA is fed to the expermental group for four weeks (shaded area) after which the animals revert to the control diet.

V. DISCUSSION

V.1. NMRS and biochemical analysis

V.1.1. The rates and extents of PCM depletion

The rates and extents of depletion and repletion of CrP and ATP found using the two techniques of NMRS and biochemical assay were similar. For example, NMRS indicates an 80% depletion in CrP at the conclusion of the four week feeding regime, while extraction and analysis indicates a 90% decrease from control values.

The NMRS monitoring of CrP depletion reveals three novel findings.

a) The time course of creatine/creatine phosphate depletion is rapid and efficient-- after merely three days of GPA feeding, muscle CrP is 50% depleted; a finding which would not have been observed using chemical assays without the sacrifice of many subjects. NMRS also highlights that during the early stages the loss of CrP is not matched by the gain of phosphorylated GPA.

b) The recovery of CrP concentrations to their normal levels upon return to the normal diet is slow. Only 50% recovery is reached after two weeks refeeding.

c) The data concerning the intratissue ATP concentrations are less definite. The 50% depletion recorded by both techniques is not as dramatic as that of the CrP as it occurs much more gradually. Our results agree with those reported by others (Shoubridge, 1984; Mainwood, 1985).

The difference in the time courses for the depletion of CrP and the accumulation of GP could stem from GPA having a relatively higher affinity and lower transport rate

for the transport protein than for creatine. The slow recovery rate for CrP is probably related to the slow removal/excretion of GP from the body.

The suggestion that the long term function of CrP is to "stabilize intracellular levels of ATP and total adenine derivatives by maintaining relatively high levels of the highly charge triphosphorylated form during surges of energy demand" (Veech,1979), is supported by the lengthy time required to deplete ATP from the muscle. If this is true, when depleted of CrP muscle concentrations of ADP and AMP would increase. This would result in a degradation of these PCMs to inosine and other purines. The result would be a net loss of the adenine nucleotide pool. The rate of this depletion would be proportional to the energy demands placed on the muscle. This is supported by the work of Veech (1979) and Meyer (1986).

Still uncertain is the reason why ATP levels increase towards normal values prior to those of CrP. Such anomalies require further investigation.

Although the results obtained by chemical analyses and NMRS experiments mirror those found by other authors, differences between our findings and those of others are apparent in the absolute concentrations of GPP obtained by both biochemical and NMRS techniques and the NMRS determination of CrP.

The protein concentrations of both the control and the GPA-fed animals are similar indicating that the growth of the GPA-fed animals is not impaired.

Our enzymatic analyses of the experimental group indicates that the total phosphorus-containing metabolite pool shows a 35% loss at the end of the GPA feeding regime. The results of our chemical analyses differ markedly from those of Meyer

(1986) who demonstrated a thirteen percent increase in the total PCM pool in his GPA-fed animals using similar techniques.

Similar determinations using NMRS would be tenuous as the noise surrounding the inorganic phosphate peak of our spectra is great and the peak is often indiscernible. However, assuming that the contribution due to Pi is similar in both the control and experimental groups, as supported by our results and those of Shoubridge (1984), then our NMRS results indicate that the total phosphate pool decreases approximately 15 percent. This result is similar to Meyer's who found a 10% percent decrease in the PCM pool using NMRS.

ADP is not directly quantifiable from NMRS spectra as the peaks of gamma and beta ATP are very similar in size. This may be explained to some degree by the binding effects of ADP with proteins or mitochondrial membranes, rendering it partially invisible to NMR (Gadian, 1982; Helzberg, 1987). For example the ADP bound to actin in myofilaments would be immobile and consequently undetectable by NMR (Helzberg, 1987).

For the above reason, free ADP (unbound) concentration is determined using the equation describing the equilibrium constant creatine kinase reaction. Our calculated free ADP level is 31 and 51 umoles/L tissue fluid for control and analogue-fed animals respectively (4 weeks on diet), assuming a creatine kinase equilibrium constant of 166 (Lawson et al, 1979). As highlighted by Meyer, these results are consistent with the model which attributes the diffusion of high energy phosphates between mitochondria and sites of ATP hydrolysis in normal muscle, to be due to creatine phosphate and creatine rather than ATP and ADP. Similarly AMP concentration could be derived from the myokinase equilibrium equation.

V.1.2. Comparison of the results of NMRS and biochemical analysis

As the text and tables of section IV.5. and IV.6. indicate, both biochemical assays and the Ackerman method of quantitative NMR spectroscopy provide insightful views into the metabolite changes which occur in muscle during creatine depletion. These methods have not previously been juxtaposed in dynamic, quantitative comparison. Cursory comparisons of the two techniques using the summary Table V.1.2.a. seems to indicate that they are not capable of producing similar results.

The major portion of these discrepancies can be very simply accounted for if one considers that there is very little ATP present in the skin, connective tissue, tendon and blood. Similarly there are negligible amounts of CrP in these tissues and fluids. For this reason NMR should and does give lower values than the biochemical muscle assay results. Averaging the differences between the two metabolites in the above table illustrates that NMRS determinations of ATP and CrP arrive at concentrations 33 and 20% lower than those obtained using conventional chemical methods. Recent experiments conducted by G.W. Mainwood have demonstrated that 20% of total leg water of the mature rat is associated with the skin, bone and blood. This evidence alone could nearly eliminate the differences in results seen between these two techniques.

Any remaining discrepancy between the two techniques may in part be attributable to the following reasons: tissue inhomogeneity, NMR visibility, extraction losses and inaccurate peak integration.

Tissue inhomogeneity. The rat hind limb is composed of a variety of tissue and muscle types. NMRS examination of the hind limb is not selective and looks at all tissues including skin and bone as well as underlying slow twitch muscles. Biochemical assays

are more tissue specific, however they are of limited size and can only be considered an approximate representation of the hind limb as a whole.

Extraction losses. NMRS avoids the complications and concomitant losses of creatine phosphate associated with muscle exposure, freezing and extraction during the course of the biochemical assays. Corrections applied to the biochemical techniques can only approximate these losses.

NMR visibility. The Ackerman method of quantitation assumes that the visibility of the protons of water and the phosphorus of the PCM is identical with their visibility in solution. Although this is a good approximation, this assumption is not entirely correct (Gadian, 1982).

Inaccurate peak integration. Fluctuations in a spectrum baseline or a poor signal to noise ratio may contribute to an inaccurate measurements of peak area. More accurate integrations are obtained by increasing the number of scans taken of of the sample, however this also increases the length of the experiment, and is not always possible.

The increasing discrepancy between NMRS and biochemical methods in the fourth and sixth week strongly suggests that leg size and body size may also be influencing the results as this is the period when both leg and body size are almost twice their starting values. Such evidence suggests that further investigation of the metabolic activities in rat hind limb should be performed on a more refined probe.

As previously mentioned, one of the major shortcomings of the NMRS technique is its low sensitivity. In this regard, as the beta peak of ATP may be partially distorted by its superimposition on the underlying phospholipid peak of subcutaneous fat and by its

susceptibility to peak aberrations by noise, the accuracy of its integrated value may suffer. This effect is compounded as its concentration decreases towards the fourth week of NMRS experimentation.

		mmoles/ l tissue fluid						
		NMRS Estimates			Conventional assay			
Week	PCM	n	mean	S.D.	n	mean	S.D.	% difference between techniques
0	ATP	6	6.4	4.0	5	7.3	0.8	-12.3
	CrP		21.5	4.7		20.7	1.8	+3.9
2	ATP	6	4.8	1.0	9	7.9	0.7	-39.2
	CrP		21.0	6.4		22.0	2.7	-4.6
4	ATP	6	4.4	1.1	11	8.7	0.8	-49.4
	CrP		12.8	2.6		26.0	2.1	-50.8
6	ATP	5	5.4	0.7	8	8.1	1.2	-33.3
	CrP		16.2	3.1		23.1	3.8	-29.9

Table V.1.2.a. Mean control values of ATP and CrP over a 6 week observation period comparing serial determinations made using NMR with cohort determinations made by biochemical techniques.

V.1.3. Comparison of the capabilities of NMRS and biochemical analysis

Despite the apparent similarities in the results provided by these two techniques they have markedly different capabilities. The relative capabilities of these two techniques are examined below in order to highlight our findings and the strengths and weaknesses of these quantitative methods. The points of comparison include; accuracy, substance under investigation, time necessary for an accurate determination, and the number of animals required to perform an accurate sampling.

Both techniques are capable of measuring substrate concentrations in millimoles per liter cellular fluid; however, neither yield information directly in this form. Biochemical assays yield millimoles per kilogram wet tissue weight and NMRS millimoles per liter tissue fluid (Ackerman method). Comparison of the accuracy of these techniques requires a common denominator of comparison and a standard by which to compare the results.

On fluid samples, both techniques, as documented by others (Dawson, 1982, Billadello, 1984) were found to provide similar if not identical results (Section IV 5) It should be noted however that NMRS analysis of rat hind limb in vivo cannot truly be considered a purely fluid sample. This is highlighted in the results (section IV 6) where the Q of the probe is contrasted for various samples and discussed in the previous section of the discussion. No method of "phantom" sample substitution permitted us to discount the presence of "rat" in an in vivo experiment. In contrast to this both Wilkie (1982) and Dawson (1982) have stated that skin, blood, and bone make no detectable contribution to their ^{31}P spectra.

Accurate assessment of metabolite concentration is the goal of both of the techniques under examination Biochemical assays are quite specific, and require very

little sample. Inherent in their nature, biochemical assays can normally be adapted to or developed for the quantitation of most metabolites. This adaptability hinges on the lability of the substance being quantitated; if it can be captured, it can be assayed, hence the necessity for quick frozen samples when working with tissue samples.

NMRS is nucleus rather than metabolite specific. If the metabolite under question does not contain a nucleus with a magnetic moment, or if the nucleus is not present in millimolar concentrations the technique is not suitable. In sharp contrast to biochemical determinations, NMRS requires a large homogeneous sample if results are to be relevant although tissue samples need not be altered in any way prior to observation/analysis.

Both techniques require repetition of measurements if their findings are to be considered significant. For example, to provide a completely reliable estimate of a given phosphate in a tissue sample, one might perform five samplings on five distinct animals. NMRS allows multiple readings without perturbating the sample. Mistakes resulting in animal fatality are rare. Biochemical assays destroy sample which can limit the number of times a sampling can be repeated. In addition, biochemical sampling is complicated by techniques which can in turn require a great deal of time to perfect. Five samplings of five animals using NMRS would require approximately 40 hours of NMR time. A similar experiment using biochemical techniques would require slightly less than ten hours.

NMRS becomes time efficient when more than one metabolite can be sampled during an experiment, as in the case of ^{31}P NMR. For example if three metabolites are examined simultaneously, the time saved is 66%. This economy is further accentuated if the nature of the study is to be longitudinal or if estimations are required at different times. One biochemical assay will destroy the sample, its source and any longitudinality.

Repeating measurements without influencing the outcome of subsequent readings is an advantage afforded to NMRS that cannot be over-emphasized. It permits subject animals to serve as their own control, eliminating the need for indicator tracers or specifically designed standards. As a result of this, the experimenter is able to ascertain how "non-perturbing" the procedure is by comparing starting and end point data. This feature is especially important in in vivo experiments as it permits the comparison of results obtained from the resting and active muscle/organ states in one subject. Quantitative NMRS techniques in turn enhance these results.

V.1.4. Technical considerations

In the Materials and Methods Section (Table II.5.2.a) a number of the technical aspects of the NMRS experiments are outlined. Their importance to the final outcome of the experiments should be briefly considered.

Our decision to use a probe which could be tuned to three frequencies provided more information and permitted a greater degree of flexibility compared to singly tuned coil. This includes tuning and matching samples of various sizes and conductivities. A multiple-tuned coil may have provided a better means of obtaining the same information (Ackerman, 1980; Blicharski, 1981; Styles, 1985)

Presaturation pulses were not applied before any NMRS experiments. Some authors (Meyer,1986) believe that these help to equalize the contribution of each FID to the final spectrum. This consideration is of little concern if spectra are acquired with recycle delays greater than $3T_1$ (Gadian, 1982), as in our experiments.

Pre-amplifier and probe tuning checks were performed prior to each experiment for each nucleus. These were assumed to be constant over the course of the experiment. If this assumption is not valid, some variability and insensitivity in the

results would arise. Performing experiments on standard solutions before and after the experiment would provide a check of inter-experiment reproducibility.

The changes in filling factor which are the result of different sized rats also influence probe Q and in turn, probe sensitivity. Only coil design can alleviate this problem (Bendall, 1986). A small surface coil might seem a suitable recourse, however this solution would certainly lower the signal to noise ratio and produce other problems associated with coil shape (Section I.3).

All the phosphorus spectra recorded include a standard peak of dimethylmethylphosphonate. Originally this internal standard was also to serve as a calibration signal for the ^{31}P experiment. The inter-experiment variability in the peak height and area expressed by this capillary forced the authors to abandon its use as anything other than a chemical shift reference.

Internal capillaries must be hermetically sealed, securely fastened, removable, verifiable, and positioned as close to the center of coil as possible. If all of these conditions are met then perhaps standards of this sort might be used as calibration signals. However, fluctuations in sample size and position radically influence shimming which will in turn influence the amount of signal obtained from the standard. This will markedly influence the usefulness of these capillaries as standards for any quantitative work.

Follow up experiments, similar to these, should be performed to evaluate the utility of surface coils of different dimensions in this type of work. Tailored pulse sequences should also be established in order to determine the contents of CrP, GPP, Pi and ATP with only one series of experiments.

The next phase of our experimentation should address the problem of quantitation of PCM after and/or during a muscle contraction. Such experiments will facilitate a more detailed understanding of the energy sources and costs involved in eliciting muscle contraction.

In this regard both chemical and NMRS determinations should be attempted. Technically both experiments would be difficult. The NMR work will require electrically isolating the muscle stimulation and tension transduction apparatus. Our muscle whole-calf-tension transducer (Appendix VI.5) has been designed for these investigations. The chemical approach will be limited by the speed at which the muscle tissue can be frozen and, as previously discussed, by the lack of suitable controls.

Caution should be exerted in chemical determinations of PCM in contracting muscle. Sabina's (1983) findings indicate that during tetanically-stimulated conditions normalization of PCM concentrations by wet weight yielded 25% lower results than the other methods. This variation is thought to be due to increased blood and water content of the muscle following exercise. Under resting conditions, coefficients of variation were similar when the metabolite data were normalized by any of: wet weight, total protein or total creatine values.

V.1.5. Comparison of the currently used methods of quantitating NMRS spectra

Oftentimes experimenters provide too little information on their data processing techniques to allow adequate assessment of their methodology. This is especially common when Sine-Bell or Gaussian lineshape enhancement is used without provision of specific and important details. The drastic effects on signal size and lineshape result in very impressive spectra but leave no point against which other investigators can compare their results. When quantitative data are being given this point needs attention

For this reason we attempted only to quantitate PCM which were well separated from other peaks and used no processing apart from line broadening on the data. Wray and Tofts (1986) used a similar approach. The measurement of the areas of the peaks of CrP and GPP necessitate the removal of the broad underlying peak of phospholipid.

Removal of broad peaks and separation of overlapping peaks are both problems in NMR studies. These two effects can be dramatically reduced by using FID processing. Examples of this type of processing include Gaussian and Lorentzian lineshape modification as used in recent investigations into the relaxation times of cancer cell proteins. Similar methods are described by Komoroski (1974). Such processing can affect some peak areas more than others since the effect is line shape dependent. For this reason a simple pulse sequence was used to eliminate the contribution of the fast relaxing phospholipids.

One intrinsic limitation to the accuracy of the Ackerman method is that the value of the concentration of NMR visible water protons must be known (Wray and Tofts, 1986). If any tissue water is bound it will not be seen in the ^{1}H water peak. We found a good agreement between our calculated ^{1}H concentration and values obtained from the literature. This suggests that the protons we observed are indeed from unbound water.

Future experiments will investigate the potential of combining NMR spectroscopy and magnetic resonance imaging to provide a more quantitative alternative to the Ackerman method of quantitating protons. This method will measure the true in vivo value and may be used for non-excisable tissues.

The technique adapted by Barany (1982) and Billadello (1984) uses the hydroxyl resonance at 69 ppm, uncontaminated by other muscle carbon resonances and

can be used to directly measure the lactic acid content of muscle. At the pH of muscle, this resonance appears ~1 ppm downfield from that of lactate (pH 3.8) placed in a capillary and inserted into the muscle sample. From the known quantity of lactate in the capillary and from the ratio of the lactate standard signal to that of the muscle lactate signal (assuming all lactate can be seen), the lactate content of the muscle can be calculated. This technique has the advantage of permitting quantitation directly within one spectrum.

A similar technique was attempted for our experiments. Experimentation using a great number of phosphorus-containing standards demonstrated that a capillary could not be suitably placed to assure its complete and/or regular inclusion within the spectra of the hind limb. Possible explanations include attenuation of the signal from the capillary by the sample surrounding it, or heavily weighted shimming which would make the capillary transparent to the NMR signal or diminish its relative intensity. If a suitable standard were found it would be better suited to in vivo quantitation if it were present in both the proton spectra and phosphorus spectra.

As previously discussed, the most commonly used quantitation technique equates a peak area within the spectra to the concentration of an independently measured freely mobile metabolite. Concentrations of the other metabolites are calculated as a mole fraction of the total pool of the NMR-sensitive metabolites. This method may have some usefulness in experiments where a measurement of the concentration of ß-ATP is easily obtained and when it can be assured that it is not changing. However, in humans in disease states, or dynamic muscle contraction situations, this is not the case.

A drawback common to all NMRS quantitation techniques stems from spectral integration. The integration of peaks with a low signal to noise ratio (less concentrated metabolites) results in comparatively less reliable results. For this reason, although

the peaks of ATP were less manipulated by NMR techniques prior to integration, their inherent variability may be higher. This trade-off may not be influencing our results as the variability in CrP results was indeed higher than that found for ATP (Results IV.6).

V.2. Animal Growth

V.2.1. Weight and Cross Sectional Area

Ad libitum GPA feeding has been shown to influence a number of physiological properties in rats and mice. Among those cited are decreased food intake and weight gain (Shields and Whitehair, 1973), decreased type II fibre size of gastrocnemius muscles (Shields et al, 1975), and decreased muscle size (Fitch et al, 1978).

It is clear from the results presented in Table IV.1.2.a that leg cross sectional area in GPA-fed animals was found to be significantly lower than control at four and six weeks of feeding from that of control animals (Table IV.1.2.a). The 6% difference, at age four and six weeks, in the mean body weight of the experimental group compared to the control group was found not to be significantly different (Table IV.1.1.a).

The difference in leg cross sectional area between control and analogue-fed animals indicates that GPA feeding may be interfering with muscle growth in some manner. The similar mean body weights between these two groups supports this hypothesis. These experiments do not provide us with information concerning the mechanism of inhibition of muscle growth.

Modifications to the present protocol which could be implemented to remove any remaining variability between control and experimental groups include: (a) feeding less chow to each group for the first three days of the experiment as GPA-fed animals eat less

than the controls at this time. This modification in feeding regime might serve to eliminate any possible disparity in mean body weights evidenced later in the experiment. (b) leg cross sectional area could possibly be measured by measuring the area in amputated hind limbs (Armstrong, 1984). This procedure would provide an accurate determination of the muscle area and the ratio of muscle to bone in these animals.

More accurate and quantitative measurements of muscle volume could be made using invasive techniques. In order to determine the means by which GPA feeding is exerting its negative effect on muscle growth, more experiments must be performed. Experiments with cultured muscle cells might help to provide information in this regard; elucidating substrate requirements for growth in muscle cells and determine whether the lack of creatine or the preponderance of GPA is hindering muscle growth.

V.2.2. NMRS Measurements of Volume

No differences between the leg volumes of the control and experimental groups, measured by ^{1}H NMRS were found at any age. The unexpected failure of ^{1}H NMR to monitor limb growth was perhaps attributable to the NMR hardware used in these experiments rather than to a failure of the technique itself. For example, if the calf muscle fills the coil's sensitive volume the proton area would not increase. This could be a result of shimming or occur as a corollary of the shape of the solenoid coil. Tests in which the volume of sample is calibrated by changing the size of the fluid/water containing cylinder as opposed to changing the volume by means of increasing or decreasing the size of the cylindrical Teflon insert could provide some insight into this hypothesis.

The disparity between the NMRS results and those obtained by more standard methods is clearly not a result of the proposed differences in water phase postulated by

Hazlewood and Pocsik[1] as spectra were obtained at five second intervals (ample time to permit full relaxation of the proton magnetic moment),

It is important to note that the 90° pulse width did not change over the course of the experiment, nor was it significantly different from one rat or one week to the next. All rats were placed in the probe in an identical manner; the axis of their body ran parallel to that of the probe, while the axis of their calf was held in a fixed position, perpendicular to the axis of the probe.

V.2.3. NMRS Measurements of Fat Content

As mentioned in Section III, the proton NMR spectral area attributable to subcutaneous fat was subtracted from the total proton NMR spectral area of the rat hind limb. Our results indicated that the average fat content of normal rat hind limb (8.6%) is on average 1.7% higher than that of the GPA-fed animals. These findings were statistically significant only after 4 weeks of feeding.

The research of Yoshikawa and Ohsaka on Wistar rats (150 g, approximately 9 weeks of age) has shown that the major component of the lipid peak is triglyceride. This peak represented 28 percent of the observable proton signal of skin, which is perhaps higher than expected given that their animals were fed rat chow ad libitum.

Similarities in measured fat content, or use, between the experimental groups also indicates that GPA may exert its effects primarily on muscle tissue. In Shields

[1] Hazlewood (1974) postulates two types of water free and bound. Bound water (4-5% of total) responds to relaxational sinks, it interacts strongly with protein (macromolecules) and has short relaxation times. The major phase, oriented multi-layer, has a longer relaxation time. This could be due to (a) paramagnetic impurities and or to diffusion of protons across local magnetic field gradients. or b) the water is free and in fast exchange with with a small fraction. The absorption line of the major fraction is10 times as broad as the line width of pure water. This suggests that water molecules are at least partly bound.

(1975), GPA-fed animals show a decreased food intake and body weight. This lends support to the hypothesis that these animals are being forced to meet some of their nutritional needs (if indeed they are the same as those of normal animals) by other means (ie. fat stores), later in the feeding regime. This, coupled with the accuracy of the technique and the changing nutritional requirements and ongoing maturation processes of these young animals may be masking any true significant difference in limb fat utilization.

The NMRS method for estimating the water content of muscle is, at best, accurate to within 10 %. More accurate determinations are possible if specific chemical assays are performed on the control and experimental animal tissues. Alternatively, estimates of water content made from NMR images of the tissue volume in conjunction with simultaneously obtained spectra from other nuclei would provide more accurate tissue and intracellular concentrations of these nuclei, as they would not be complicated by the proton signals of fat or influenced by possible edema. Experiments of this nature, although more complicated and more costly, have been performed by Hayes et al (1982). Similarly, more accurate estimations of fat content / true water content may be possible if more scans are taken during the proton experiments or if specific pulse sequences are designed to eliminate the contribution of the protons of fat from the spectra. This is not necessary for the purpose of these experiments.

V.3. Muscle Sodium and Potassium Determination

Our results indicate that although there is no significant difference in the sodium concentrations of the two experimental groups, there is a significant difference between the sodium concentrations obtained by NMRS and those obtained by flame photometry (Table IV.6.3.b). The flame photometric results yield concentrations which are 20 and 28% higher than NMRS for control and GPA-fed animals respectively.

This disparity may be due to the state of sodium ions in their cellular environment which is thought to be significantly different from their state in free solution (Ling,1962; Civan,1983). Although our results differ quantitatively from those of Chang and Woessner (1977) and Cope (1970) who conclude that approximately 65% of tissue sodium is invisible to NMRS, all of these experiments support the hypotheses of Ling and Civan. Cope explains that the sodium hidden from NMRS is in part a result of quadrupolar effects and in part because a significant proportion is bound to proteins.

Our NMRS results (approximately 30 mmoles/litre tissue fluid) are twice the value Cope obtained. They correspond well to the concentrations obtained by Cope after ashing. Performing flame photometric and NMRS analysis of ashed muscle samples would help to determine whether the comparatively high in vivo sodium concentration which we obtained by NMRS was spurious.

If sodium NMR is to be used as a method of determining intracellular metabolite concentrations then the standard deviation must be significantly decreased below the current value of 20%. Improvements should include a more easily tuned and matched probe, facilitating spectral aquisition. In addition, more accurate estimations of the ratio of intracellular and extracellular volume would also improve our results. Experiments which influence ion balance would be useful to determine the sensitivity of the technique.

V.4. Anaesthesia

Another series of very important observations were made concerning the use of different forms of anaesthetic. Two types of anaesthetic were used; Somnotol (sodium pentobarbital) and a combination of ketamine and xylazine. Although many advocate the administration of Somnotol in a dilute form, an injection of the concentrate produces more rapid anaesthesia. Unfortunately, overdosing animals with Somnotol is very easy. however accurate dosing produces anaesthesia for upward of one and one half hours. Tolerance appears to develop in animals given repeated doses of this drug (data not shown). It should be noted that Somnotol is extremely susceptible to contamination. This was evidenced by the rapid appearance of bacterial growth in the vial, and constant decline in potency of the anaesthetic. This occurred despite constant refrigeration and attempts to keep light from entering the vial when not in use.

The ketamine-xylazine combination was very effective at producing rapid anaesthesia. Animals given an intra-peritoneal injection of these drugs, using the method of Green et al. (1981), remained unconscious for approximately one hour. Overdose is possible but a rare occurrence. These animals always regained consciousness. Repeated administration did not seem to produce tolerance in our animal subjects. Concern of muscle rigidity and/or increased muscle tension with this combination does not seem to be valid. If our NMRS experiments could have been completed in three quarters, of the time use of the Ketamine-Xylazine combination is recommended.

Somnotol was used in all of our experiments. All contamination problems were overcome by cold storing the anaesthetic in the dark and discarding opened bottles after they had been used for three weeks.

V.5. Concluding Remarks

All of the investigations indicate that, if used wisely, NMRS can be an invaluable tool for the investigation of muscle metabolism in vivo. Our results lead us to conclude that the Ackerman method of quantitation by NMRS is an accurate and reliable method for measuring the concentrations of phosphorus-containing metabolites of muscle in vivo. In addition this technique has marked advantages over chemical determinations and the Ratio method (Table V.5.a.) that make it the only technique suitable for in vivo experimentation, longitudinal studies, or repeated measurements on muscle tissue.

	Method of Quantitation		
Problem or concern	Biochemical	Metabolite Ratios	Ackerman
Invasive to animal	YES	NO	NO
Deleterious to animal	YES	NO	NO
Based on a potentially fluctuating internal standard	NO	YES	NO
Valid for all coil shapes	NO	NO	YES
Accurate in systems where metabolites are short lived or changing (muscle contraction)	NO	NO	YES
Useful for the quantitation of many and different metabolites simultaneously	YES/ NO	NO	YES
Able to provide intracellular concentrations	YES	NO	YES

Table V.5.a. Comparison of the suitability of the metabolite quantitation techniques of Biochemical Analysis, the NMRS Metabolite Ratio Method and the Ackerman Method.

VI. APPENDICES

VI.1. Sodium ^{23}NMR Spectroscopy

A nucleus with nuclear spin I greater than 1/2 has asymmetric (non spherical, elliptical) charge distribution of the electrical charges. This property gives these nuclei (eg ^{23}Na spin 3/2, ^{39}K spin 3/2, ^{2}H spin 1, ^{15}N spin 1, ^{17}O spin 5/2) a quadrupole moment in addition to a nuclear magnetic moment (Foster, 1983). Molecular motion of these nuclei can cause field fluctuations, hence enhanced relaxation rates. The units depicting the magnitude of the moment are in charge times area however, they are usually related only by area where one unit is 10^{-24} cm^2. This is equivalent to 1 barn (Fukushima, 1981).

If a quadrupole nucleus is in close proximity to a positive charge of an electric field gradient that nucleus will position itself according to electrostatic forces in the orientation of highest stability. This orientation will serve to augment the interaction between the magnetic dipole moment and the magnetic field which is predicating the Larmor precession. This increased interaction increases the rate of precession of the nuclear moment, decreases the pulse length required for a 90° pulse, and often increases line width (Foster, 1983). As the total number of energy levels goes as 2I + 1, quadrupolar nuclei have more than two allowed energy levels. This provides these nuclei with a rapid means of relaxation. These energy levels are not evenly spaced and energy level transitions may occur between any and all levels (Beall, 1984).

VI.2. Components of an NMR spectrometer

VI.2.1. The magnet

Magnetic field homogeneity and consistency is extremely important in pulse NMR spectroscopy. Small variations in field strength will produce a range of values of ν at which a particular resonance occurs, and hence yield broad lines, which can obliviate fine spectrum structure. The homogeneity is assured by providing a relatively large gap between the pole faces of the magnet. The size of the heterogeneous region can be reduced, and the entire field corrected for much of its inhomogeneity by the use of current shims attached to the pole faces of the magnet or onto the probe (Fukushima, 1981).

For biological samples sensitivity is increased by using magnets of very high field strength. To obtain these high fields it is necessary to use a superconducting magnet which is in many ways similar to a standard permanent magnet. Such a device consists of a coil, usually composed of niobium-titanium wire, placed in an insulated flask of liquid helium. At this temperature NbTi has no resistance and a current , once set up, continues to flow indefinitely (Fukushima, 1981).

VI.2.2. The probe: coil and circuitry design

The NMR probe has three basic components the housing, the circuitry and the coil. All three components should be made of non-ferrous materials. Plastics and plexiglass and low grade solder should be avoided in probe construction. Protoboard (printed circuit (pc) board) and Teflon (except in experiments with ^{19}F) are both very good building materials. The housing (can) is most often made of a rigid aluminum cylinder (Fukushima, 1981).

The tank (tune and match) circuit in conjunction with the coil should tune easily to the desired frequencies and match the impedance of the rest of the spectrometer circuitry. This normally requires a variable capacitor for each of these functions in addition to a tank capacitor which brings the circuit within close range of the desired tuning frequency. Capacitors must be capable of handling a large wattage without power loss or "arcing". In addition the tank circuit should be physically and electrically isolated from the portions of the probe which contain the sample and, in the case of in vivo experiments, the equipment used for physiological maintenance. When constructing this tank circuit it is extremely important that all of the connections from the coil to the circuit capacitors be as short and as clean as possible (Fukushima, 1981, Brady, 1986).

Due to the inherent low sensitivity of the NMR experiment optimization of probe hardware is extremely important. In experiments with biological samples there can be significant power loss at the time of rf pulse application, through "eddy currents" established within the rf field (Fukushima, 1981). This loss is due to the conductive nature of biological fluids termed "lossiness" results in decreased probe sensitivity (Hoult, 1979; Gadian, 1979; Gadian, 1982). One can compensate for the degradation of sensitivity by reducing dielectric losses, induced by in vivo tissues on single tuned probe circuits and by using Faraday shields to further isolate the specimen from the coil and tank circuitry (Fukushima, 1981; Keller, 1985).

The signal to noise ratio obtained during an NMR experiment is largely determined by the probe and its coil. Factors to consider when designing a coil to optimize this ratio include the coils filling factor (how much of the area in the coil is being sampled), the nuclear magnetization, the Quality factor of the coil, the Larmor angular frequency and the size of the sensitive volume of the coil (Fukushima, 1981).

The Quality or Q factor is one of the most important parameters to optimize when designing a coil and a probe. Q is directly related to inductance and frequency and inversely related to resistance:

$$Q = \frac{2pV_0 L}{R}. \qquad \text{VI.2.2.i.}$$

Maximizing Q serves to increase the sensitivity of the coil and maximize the effect of the application of the rf pulse. High Q's are normally obtained by increasing coil inductance and decreasing power loss however, the inductance is only obtained at the expense of resistance. Normally not a problem in in vivo experiments, excessively large Q's bring about long ring down times which are counterproductive to effective experimentation and should be kept below 10 ms (Fukushima, 1981; Shaka, 1985).

Coil conduction media is a large determinant of coil Q. It is often advantageous to use flat (sheet) stock (metal) rather than cylindrical (wire) stock to make the coil. The material should be highly conductive, free of corrosion, and pliable. We have found that the coil should be smooth and free of kinks, this minimizes the possibility any arcing and subsequent power loss at kink points on the surface of the coil (Brady, 1986).

When considering a coil design for in vivo experimentation the main consideration is accessibility of the coil to the area of study, however attention must be given to assure that the sensitive volume of the coil corresponds to the volume under investigation (Fukushima, 1981). Two basic coil shapes are used in physiological experimentation; the surface coil and the solenoid coil. These are illustrated in Figure VI.2.2.a.

The solenoid coil normally performs both the transmission and the reception of the rf signal on the same coil. The single surface coil set up functions similarly. The second surface coil configuration, the cross coil, has two coils arranged in either a perpendicular or (in most cases) a concentric fashion (the larger diameter coil encircling the smaller). During experimentation one of the coils transmits, normally the larger, while the other, smaller coil, receives (Bendall, 1984).

There exist several advantages to the use of a single surface coil versus a cross coil configuration (Ackerman, 1980; Shaka, 1985). The two most important are the limited space requirements of the single coil design and its comparatively lower susceptibility to microphonics and movement during experimentation (Bendall, 1984) However, it is impossible to obtain a uniform, isolated sensitive volume using just inhomogeneous B1 methods and a single inhomogeneous rf coil. Due to this, rf absorption is not the same throughout the sample. The result of this is that pulse angles will differ throughout the sample (Ackerman, 1980; Shaka, 1985). Thus a minimum of two inhomogeneous rf coils is needed or at least one pulsed field gradient to reduce or eliminate signals from regions where the sensitive volume curves back into the sample surface making results unreliable. A further limitation is that only the depth and the thickness of the sensitive volume can be controlled by varying the rf pulse method (Bendall, 1986).

Alternatively, multi- pulse techniques, also known as depth pulses, can be used to eliminate such signals. These gains are not free from inconvenience, there is approximately a 20 percent loss in measured signal intensity when these pulse sequences are used (Bendall, 1986). Recent modifications of this configuration were made by Bendall (1984) wherein both coils are used to transmit while only the smaller coil is used to receive purports to alleviate most of the problem of the curvature of the sensitive transaxial volume.

In contrast to the types of problems which exist with the surface coil, the solenoid coil has problems of positioning. The solenoid, as a result of its shape, has a sensitive volume, in direct contrast to that of the surface coil (Figure VI.2.2.a.),which is confined to its interior (Gadian, 1982). As a result of this any specimen to be examined using a solenoid must have a somewhat cylindrical shape for example a limb or a test tube. This difference alone makes the solenoid coil considerably easier to use than the surface coil as no elaborate pulse sequences or NMR techniques are needed to obtain accurate and reproducible results.

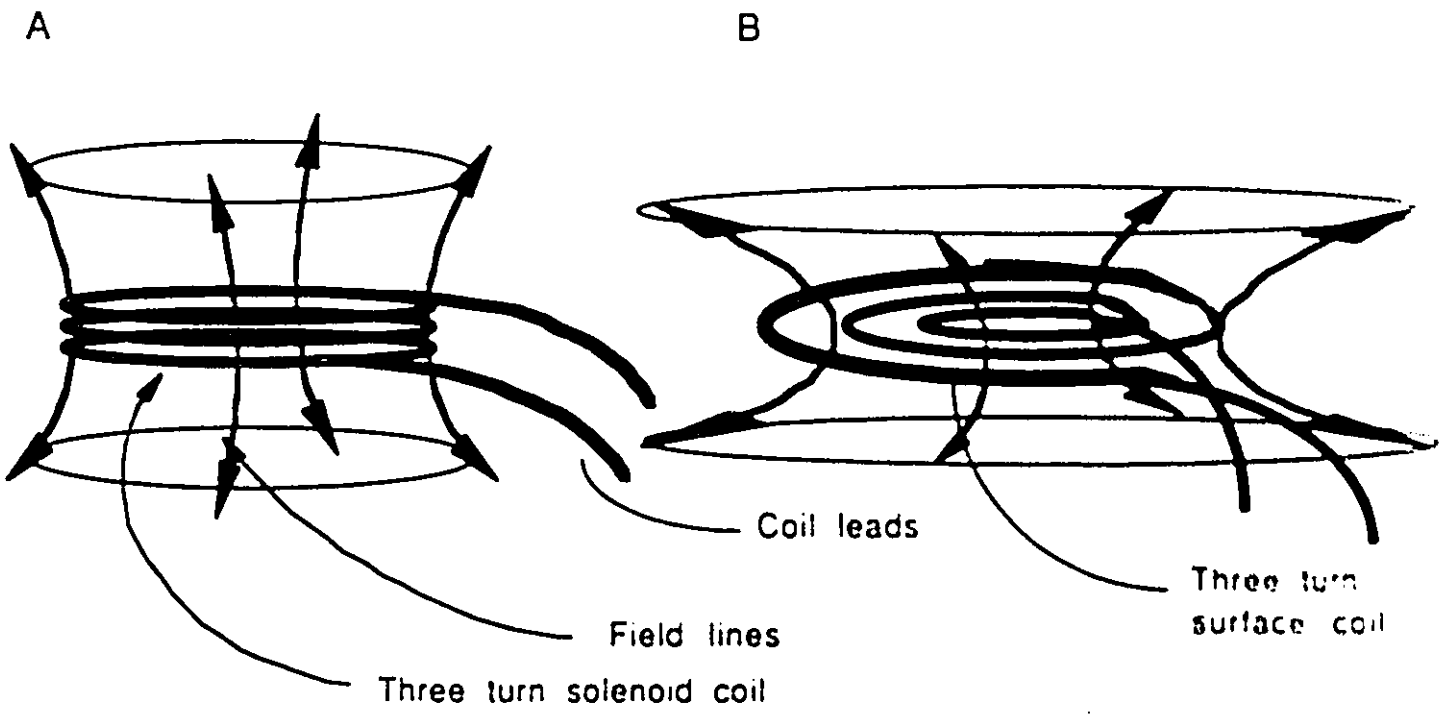

Figure VI.2.2.a. Three turn solenoid (A) and surface (B) coils and their field shapes

When constructing a coil several factors must be considered (Fukushima, 1981). First, the length of coil and number of turns is one of the predominant effects of the Q of the probe and the probes resonance circuit frequency. Generally the number of turns needed in a coil will make the length equal to 70% of the diameter (Q increases very slowly after length exceeds diameter). Factors determining length of the coil in in vivo experiments include the size of the sample, its concentration, and its accessibility to position of the coil. In addition the wire diameter should be equal to the spacing between the turns (Fukushima, 1981). Alternatively the number of turns can be approximated using the following equation where a is the diameter and b the length of the coil (inches) and L is the inductance in microhenries:

$$L = \frac{n^2 a^2}{(9a+10b)} . \qquad \text{VI.2.2.ii.}$$

In considering a coil shape for our experiments we also had to consider future experiments which would be performed with our probe, and the apparatus which would be used in these investigations. We chose to use a solenoid coil because of a) the homogeneous nature of that type of coil b) the shape of the limb and the relative homogeneity of its muscle types. c) our desire to facilitate the acquisition of spectra in a short period of time and d) because our animals would be growing fairly rapidly and a the coil chosen would have to be suitable for all ages and sizes of rats. This orientation would force the surface coil into a folded/bent configuration which has certain disadvantages.

VI.3. Pulse sequences

For NMR pulse experiments H1 and † are usually chosen in such a way that a precession angle of π /2 results, thus maximizing Mxy (Becker, 1979). This is accomplished by applying a pulse in a direction perpendicular to the magnetization vector. For example if the nuclear magnetization is parallel to the static magnetic field H at thermal equilibrium, when a pulse is applied along the X direction it re-orients the magnetization into the Y plane. When the pulse is switched off it will cause a nuclear induction signal in the pick up coil (Meyer, 1982). As time elapses the magnetization continues to precess in the XY plane while it continues gradually to gain magnetization along the Z axis with a rate constant R1 as described below.

The total magnetization vector at any time is the sum of smaller magnetization vectors. The contribution to the magnetization which arises from one such small segment is called a spin isochromat. An isochromat arises from a small volume experiencing a homogeneous fields (Foster, 1983). After a 90° pulse, each of those components of the magnetization will precess at its own characteristic Larmor frequency. Therefore, the magnetization from those portions of the sample with slightly larger magnetic fields will precess faster than those which are in a smaller field. The result of this is that the different contributions of the magnetization will dephase from each other (Figure VI.3.a.) (Meyer, 1982).

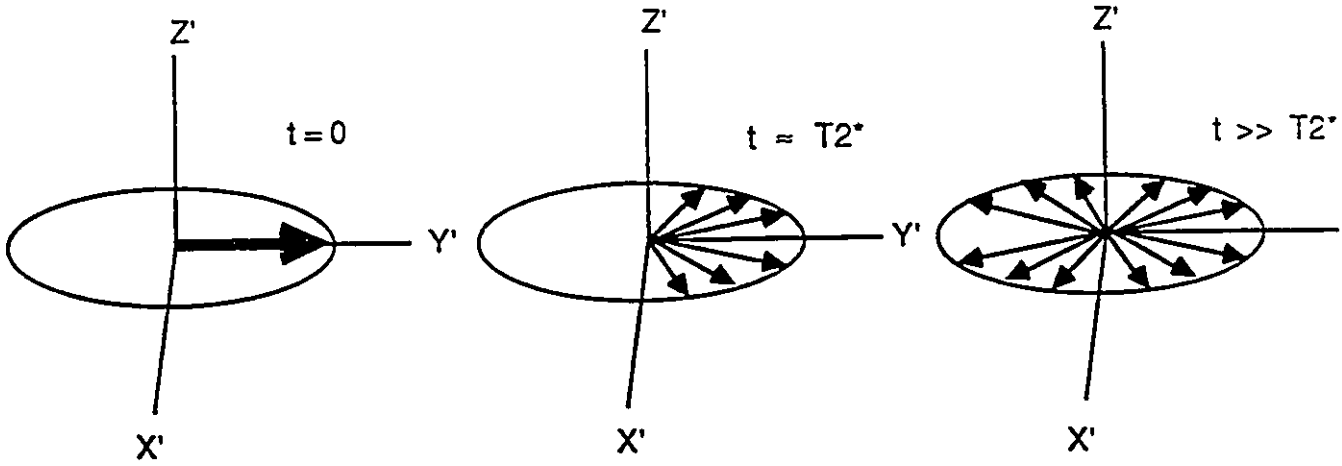

Figure VI.3.a. The results of a pulse applied along x' (rotating reference frame) to a magnetization vector along Z' in an inhomogeneous field (Fukushima, 1981).

Application of a second or a series of pulses to the recovering nuclear magnetization will deflect the magnetization vectors in a manner similar to that described above. As the relaxation process is occurring, the number of directions in which the magnetization will be deflected as a result of these new pulses will increase until the magnetization is fully relaxed and no longer susceptible to anything but a pulse applied in a perpendicular direction (Gadian, 1982). This technique has some very important applications, one of which will be discussed below.

In instances where nuclei of a sample exists within markedly different magnetic environments with consequently greatly different T_2^* s it is possible to remove the effect of the inhomogeneity by the use of a composite pulse sequence (Bendall, 1984; Wray and Tofts, 1986). Similar techniques are used to remove the contribution of one nuclei to a spectra if it has a markedly different T_2 from the other molecules containing

the nuclei of interest. One such method is the Hahn echo pulse sequence (Fukushima, 1981) which is schematically drawn and explained below (Figures VI.3.b. and VI.3.c.)

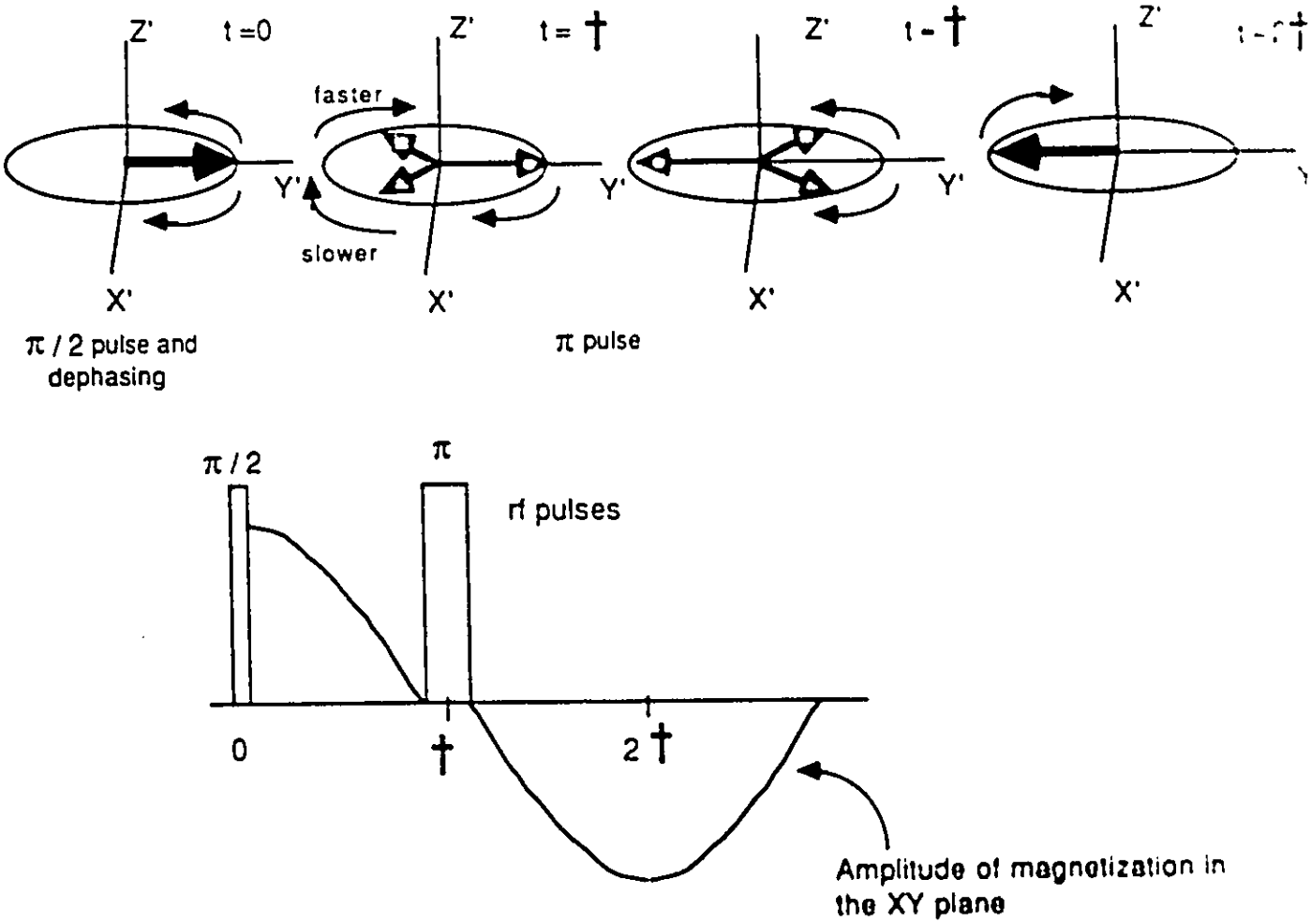

Figure VI.3.b. Magnetization in the rotating frame as a consequence of the application of the Hahn spin echo pulse sequence.

Shortly after the application of a 90° pulse along X', a 180° pulse is applied from a similar direction. The pulse separation, † seconds, allows for a dephasing of the magnetization in the X'Y' plane. Any magnetization in the Z' direction at the time of the second pulse goes into the -Z' direction. Similarly, any magnetization in the X'Y' plane

is rotated 180°, with no consequence to the overall net magnetization. As a consequence of this 180° inversion any of the faster isochromats are now follow the slower isochromats instead of preceding them. As a result the isochromats head back towards the -Y axis. This refocussing agglomerates all of the isochromats. Consequently it enhances the signal from the normally rapidly dephased sample. The reunion of the magnetization takes place 2τ after the original time of application of the 90° pulse.

In the case of in vivo phosphorus spectra taken from tissues either in vivo or in vitro, the Hahn echo pulse sequence will, if τ is properly chosen, remove the broad resonance contribution of phospholipid and bone from the spectra of the other phosphorus-containing metabolites (PCM) such as ATP and creatine phosphate (Thulborn and Ackerman, 1983; Helzberg, 1987). This removal is desirable if quantitative measurements of any sort are to be made from the phosphorus spectra (Meyer, 1982; Wray and Tofts, 1986).

Improperly choosing the tau value between rf excitation pulses effects the peak height of the beta peak of ATP (Figure VI.3.d.). This highlights the remarkably short T_2 of ATP (Beall, 1984). Its brief life span made accurate T_2 measurements impossible. This fact necessitated the use of a second pulse sequence to reliably integrate the area of the beta peak of ATP.

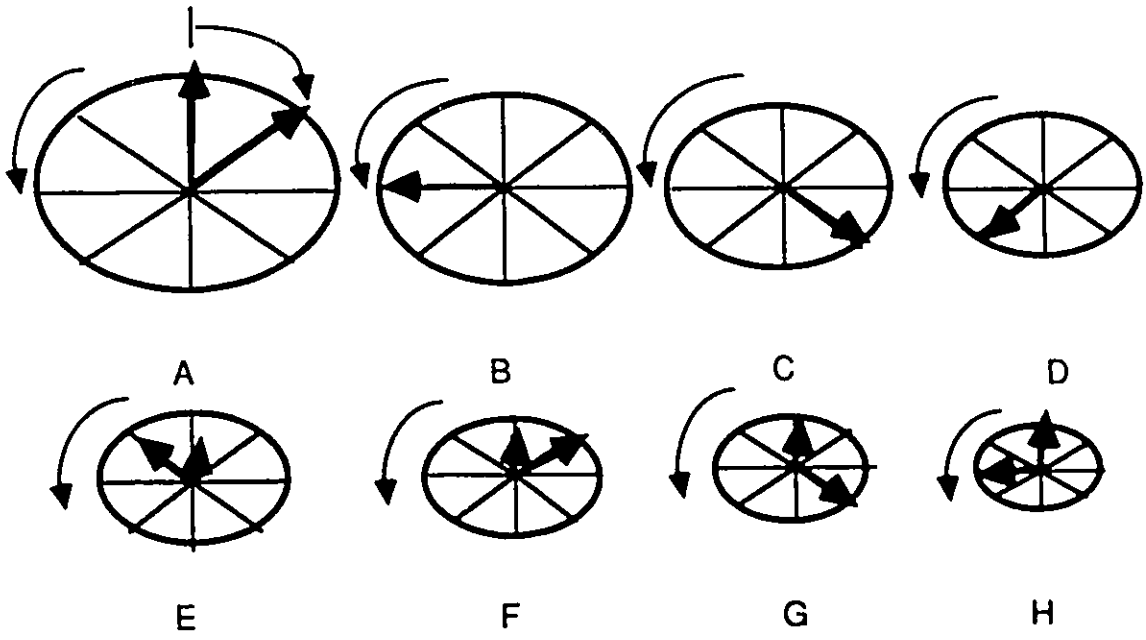

Figure VI.3.c. The relaxation process of a spin isochromat oriented along the Z' axis after the application of a 90° pulse along a perpendicular axis. The diagrams A-H depict, in chronological order, the loss of magnetization along the Z' axis (hub) and the simultaneous increase of magnetization along the X'Y' plane (spokes and rim), which occurs with the application of this pulse. As time elapses the Z' component is regained and the X'Y' component is lost.

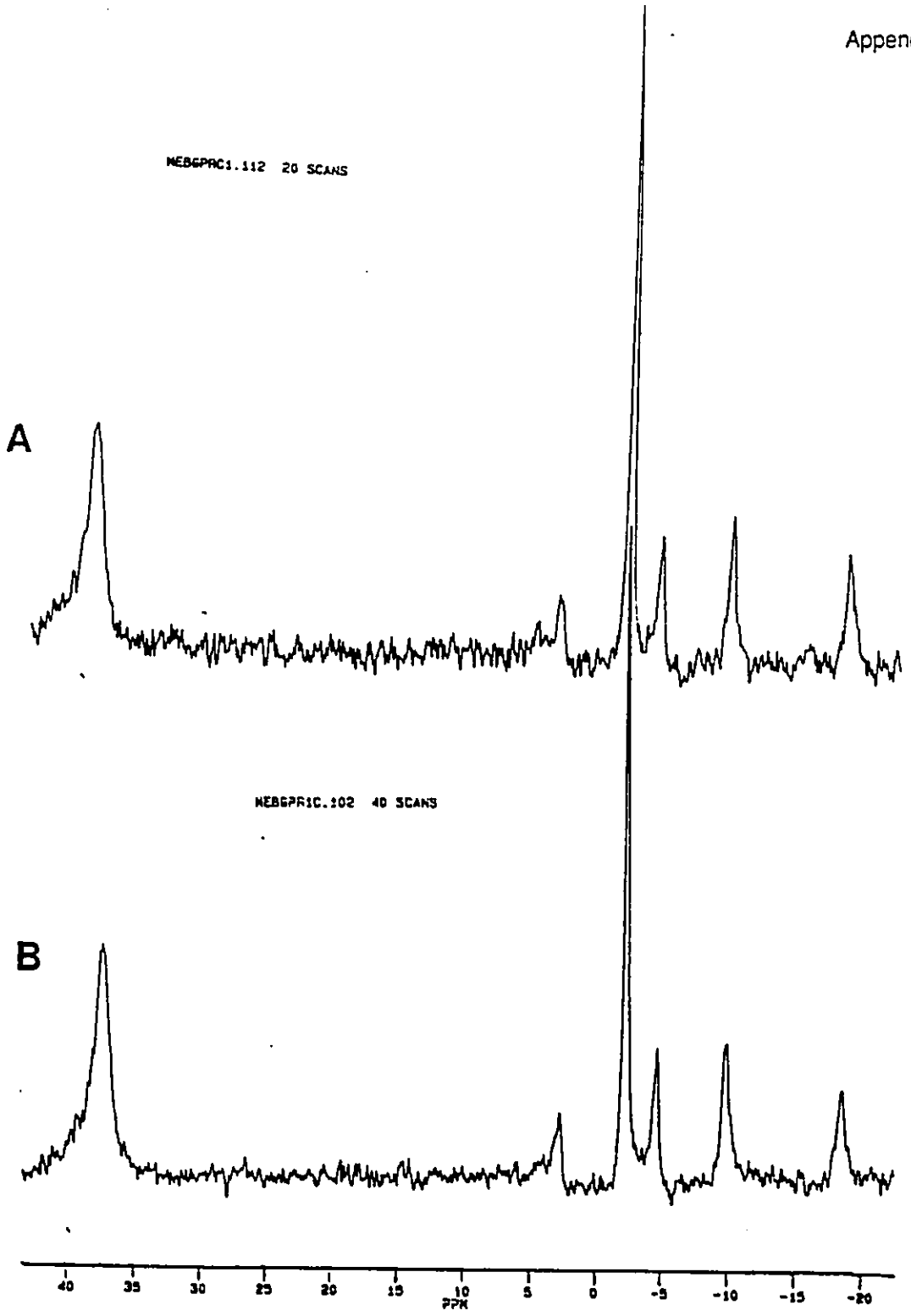

Figure VI.3.d. 31P in vivo spectra of the hind limb of a rat taken (A) with an inter-pulse tau of 2 ms and (B) with an inter-pulse tau of 1 ms. Note the difference in the peak heights of the beta peak of ATP.

VI.4. Schematic diagrams of early probes

The following diagrams illustrate the rat hind limb probe (functional end) at the first stages of experimentation. Our zealous efforts to attempt to follow the strength of muscle contraction during tetanus while monitoring the changes in PCM concentrations were not well rewarded. These investigations yielded a very functional transducer (see appendix VI.5.) and method of immobilizing the hind limb for stimulation. The surgical methods necessary for nerve stimulation were also perfected.

Briefly, Figure VI.4.a.i. diagrams the probe head (top view), specifically the positioning of all of the holes through which the level of the leg was adjusted to suit rats of different sizes. Figure VI.4.a.ii illustrates the provides a lateral view of the probe, illustrating the transducer on the underside of the probe. The transducers tension monitoring leads ar also shown. In addition the plexiglass horseshoe used to stabilize the foot is drawn. Above the plane of the probe, the threaded nylon rod which holds the leg stabilizing apparatus firmly to the probe (depicted in Figure VI.4.b.) is clearly visible. Similarly Figure VI.4.a.iii illustrates the probe head from the rear. In this view the coil and its accompanying protective Teflon cover, the nylon stabilizing rod, the nerve stimulation leads and the transducer are clearly visible. In addition the plexiglass inserts, used to adjust the level of the horseshoe and transducer are also shown.

It should be noted that investigation into the energy costs of muscle contraction are possible with this "set up". Lacking is a simple method to assure the electrical isolation of the stimulation apparatus from the coil. This should guarantee "glitch" free spectra. Subsequent probe head designs have partially solved this problem as they are were constructed entirely of PC board, and Teflon as opposed to plexiglass.

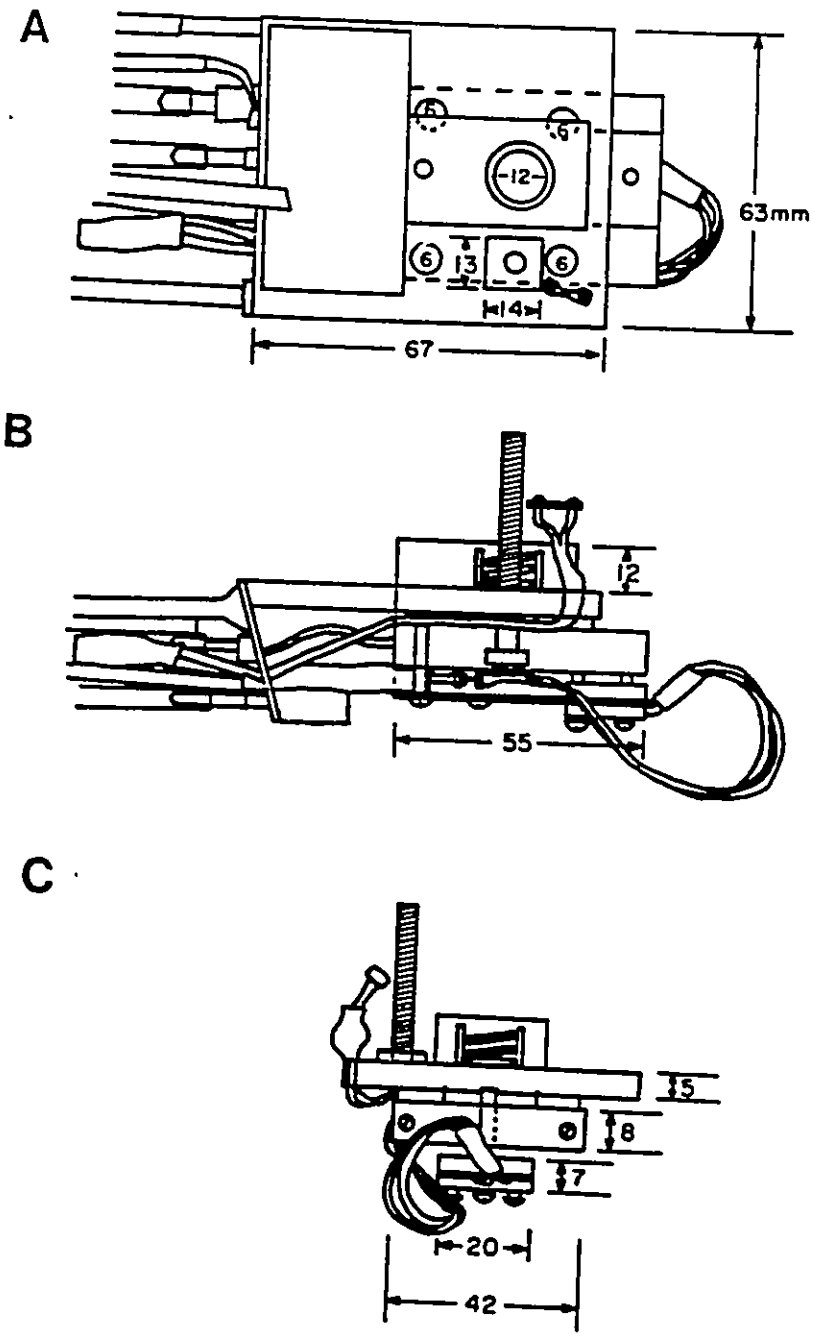

Figure VI.4.a. Schematic diagram of the first probe head used in our NMRS investigations. All measurements are in millimetres. (A) Top view of the plexiglass probe head. (B) Lateral view of same. (C) Hind view of same. Components are labeled in figure VI.5.e.

VI.5. Schematic diagrams of the tension transducer

The following figures depict the tension transducer and all of its component parts. The transducer was constructed entirely of aluminum and plexiglass. It was sensitive below a gram and was very easily calibrated. Please see the legends accompanying each figure for a complete description of the transducers components.

The key descriptors of the strain gauge are determined by the anatomy of the rats which will be used during experimentation. These include the length of the transducer and the estimated force the rat will be able to generate. Once these have been determined the transducer beams materials and their dimensions can be selected. The active length of the gauges is entirely dependent on their nature and size. Their positioning on the beam is also critical to their ability to operate accurately.

The length of the beam must be approximately one inch. The width of the beam must be approximately one half inch. These measurements are a function of the rats anatomy and available space. The beam was made of aluminum as it is light, easy to work with and non-magnetic.

A stock aluminum strip measuring 3/4 of an inch wide was chosen and cut down leaving an active length of 7/8 of an inch. Experimentation determined that at tetanus the rat hind limb generates approximately one pound of force. The application of this force should produce a measurable deflection of the beam at both the point of pressure application and the location of the strain gauges. A 2mm deflection at the former point seemed possible.

Equation VI.5.i. expresses the thickness of the beam as a function of the other beam descriptors.

$$H^3 = \frac{WL^3 12}{3EBD}. \qquad \text{VI.5.i.}$$

Where L is the length of the beam from fixed end to the point of pressure application. W is the magnitude of the applied force. E is Youngs modulus for aluminum (E is 10×10^6). B is the width of the beam. D is the deflection at the point of pressure application (2 mm or 7.87 thousands of an inch). (figure VI.5.a., VI.5.c. and depicts these measurements)

Substituting known values H is found to be 35.67 thousands of an inch. Adjusting the equation for available stock thickness (only 40 one thousands was available in that range) the width of the beam required adjusting. It was cut back to 0.532 inches.

The ability of the strain gauges to measure deflection determines the sensitivity of the transducer. At their point of attachment the strain on the gauges is determined by equation VI.5.ii.

$$\text{ø} = \frac{MY}{I}. \qquad \text{VI.5.ii.}$$

where ø is the strain in pounds per square inch, M is movement at the location of interest, Y is the vertical displacement distance from neutral to the point of interest (maximum at H/2 or 0.020" in this case), and I is the section movement in inches^4 or $BH^3/12$. (see figures VI.5.a., VI.5.b. and VI.5.c.)

Substituting into equation VI.5.ii. σ is found to be 5294 psi at the point of maximum deflection. E or the amount of strain at that location is described by equation VI.5.iii. or in this instance 529.4 μstrains at the point of pressure application.

$$E = \frac{\sigma}{E}. \qquad \text{VI.5.ii.}$$

If the signal from the four arm bridge is 500 Ω at 10V excitation (input) then the voltage read (output) is 10.6 mV.

At the centre of the point of attachment of the strain gauges the force will be proportionately less. The mitigating factor will be the length of the moment arm. The location of the gauges is 0.882 inches behind the point of force application. Stress at gauge will be 4667 psi.

Based on this information, using the aforementioned equations and a 6V excitation voltage and a gauge factor of 2.07 (four active arms) the outgoing voltage will be approximately 9.19 mvolts.

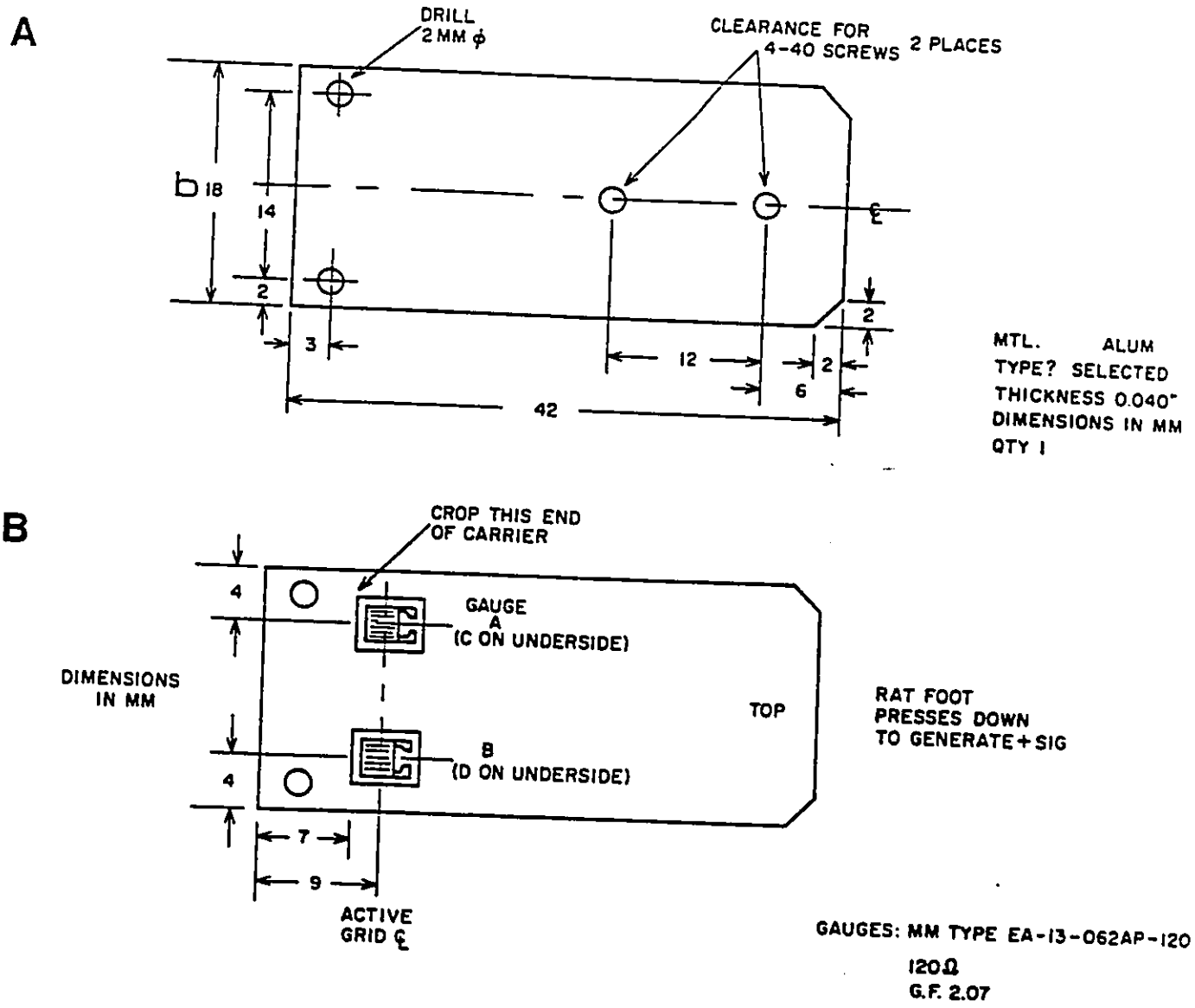

Figure VI.5.a. (A) Top view of the aluminum cantilever which serves as the base for strain gauge and plexiglass pedal attachments. (B) Top view of same depicting the position of the strain gauges. All measurements in millimetres.

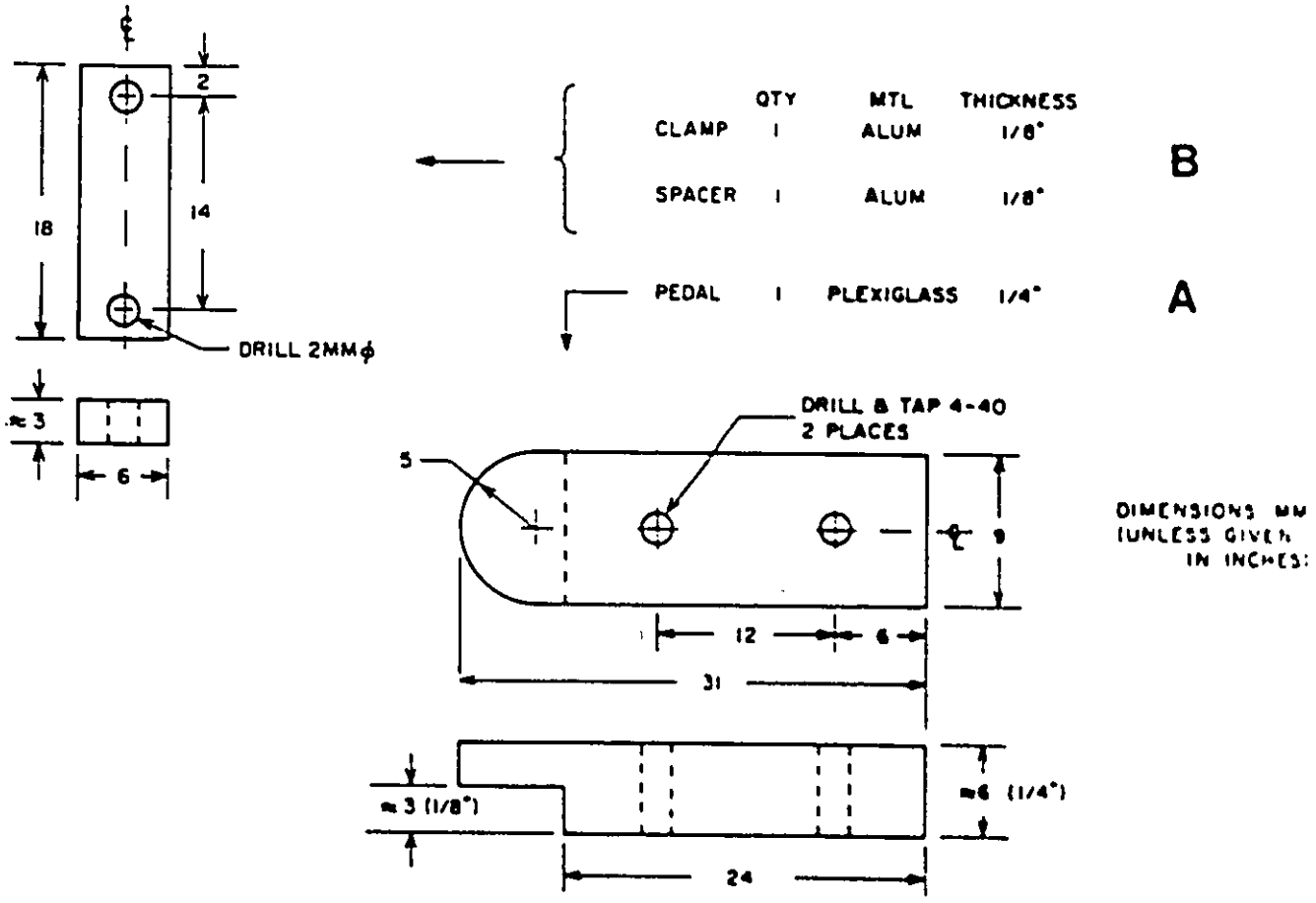

Figure VI.5.b. (A) Top and lateral view of plexiglass pedal. The pedal fits into the horseshoe used to stabilize the foot. (B) The clamp and spacer used to secure the aluminum cantilever and accompanying apparatus to the horseshoe shaped foot support. All measurements in millimetres.

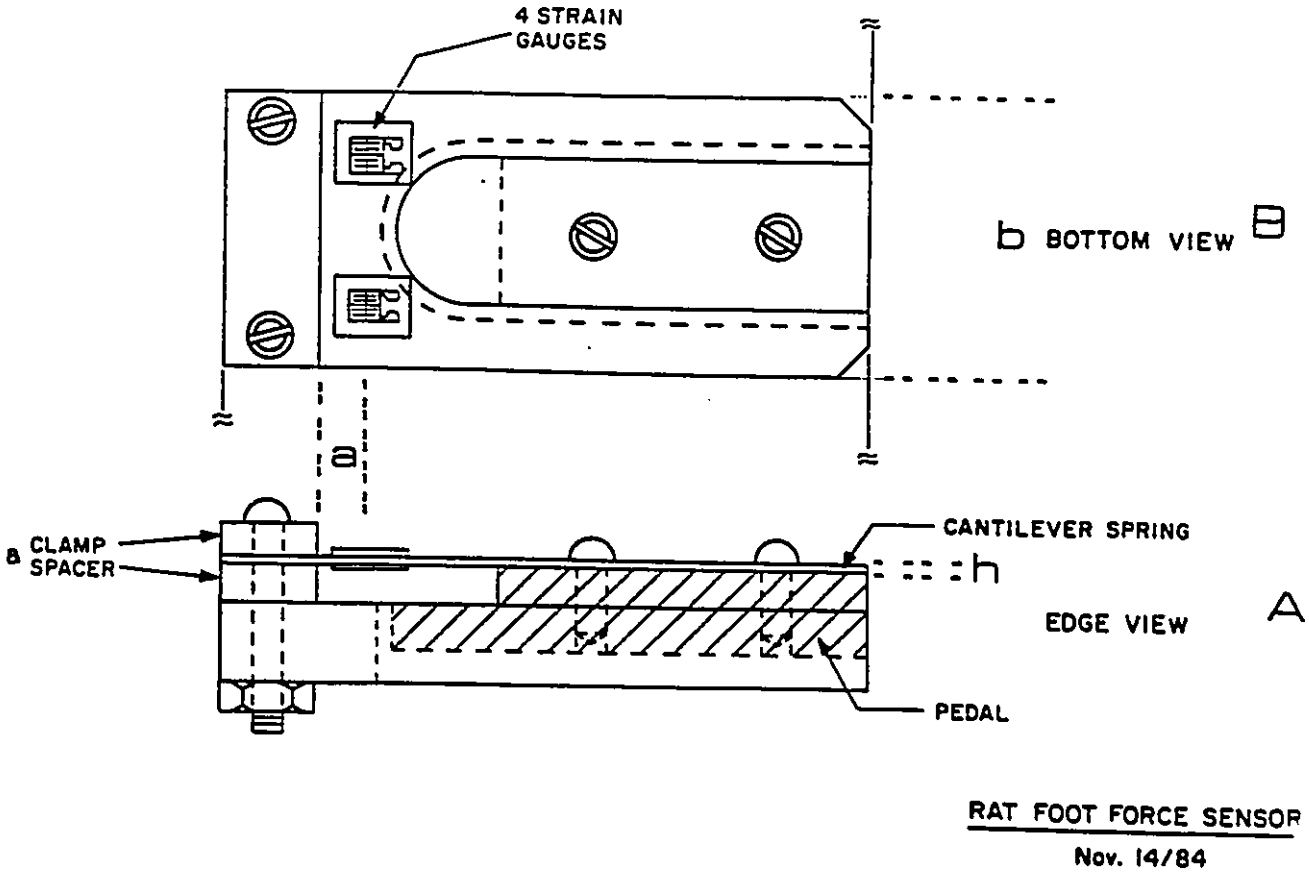

Figure VI.5.c. (A) Top view of aluminum cantilever depicting the position of transducers, plexiglass foot pedal and spacing clamp. (B) Lateral view of same.

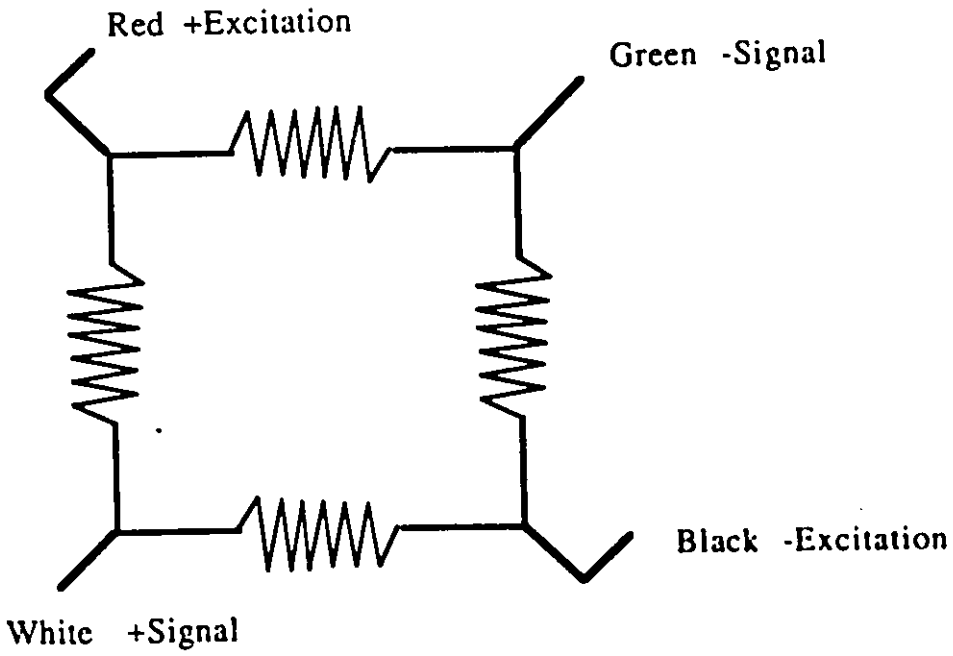

Figure VI.5.e. Wheatstone bridge depicting the circuitry of the 4 arm transducer. Each gauge is depicted as a resister. Note that the gauges are MM type EA-13-062AP-120, 120 Ω, G.F. 2.07. Their sensitivity is 9.2 mV for 1 lb. force applied one inch from clamped edge and 6V excitation.

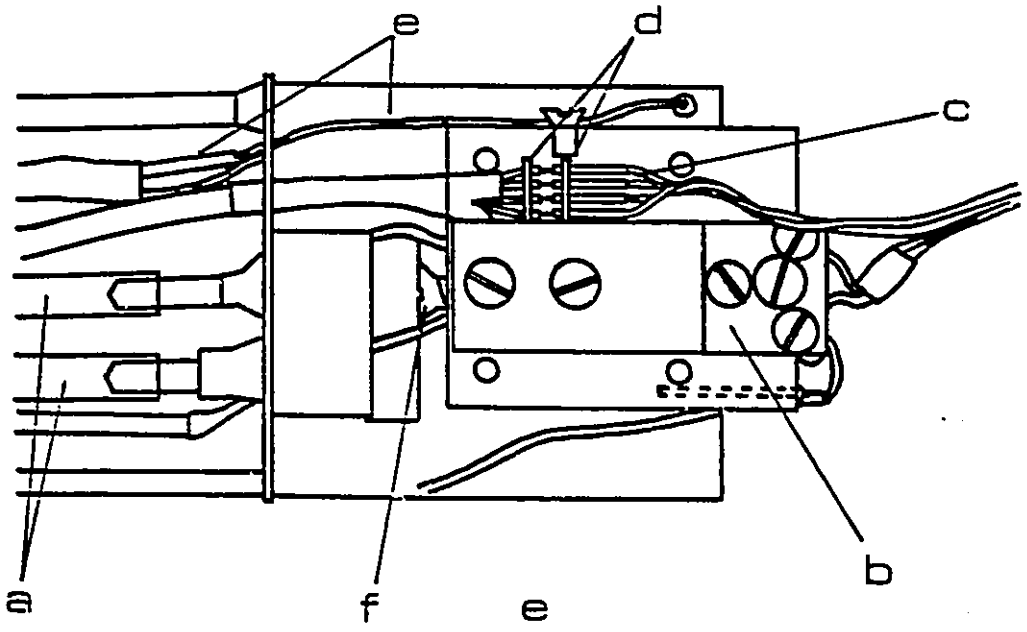

Figure VI.5.d. Bottom view of the completed force sensor. Depicted are a) tuning rods, b) sensor, c) electrical leads and (d) connector from sensor, e) electrical lead for nerve stimulation, f) screw to which weights are attached for gauge calibration

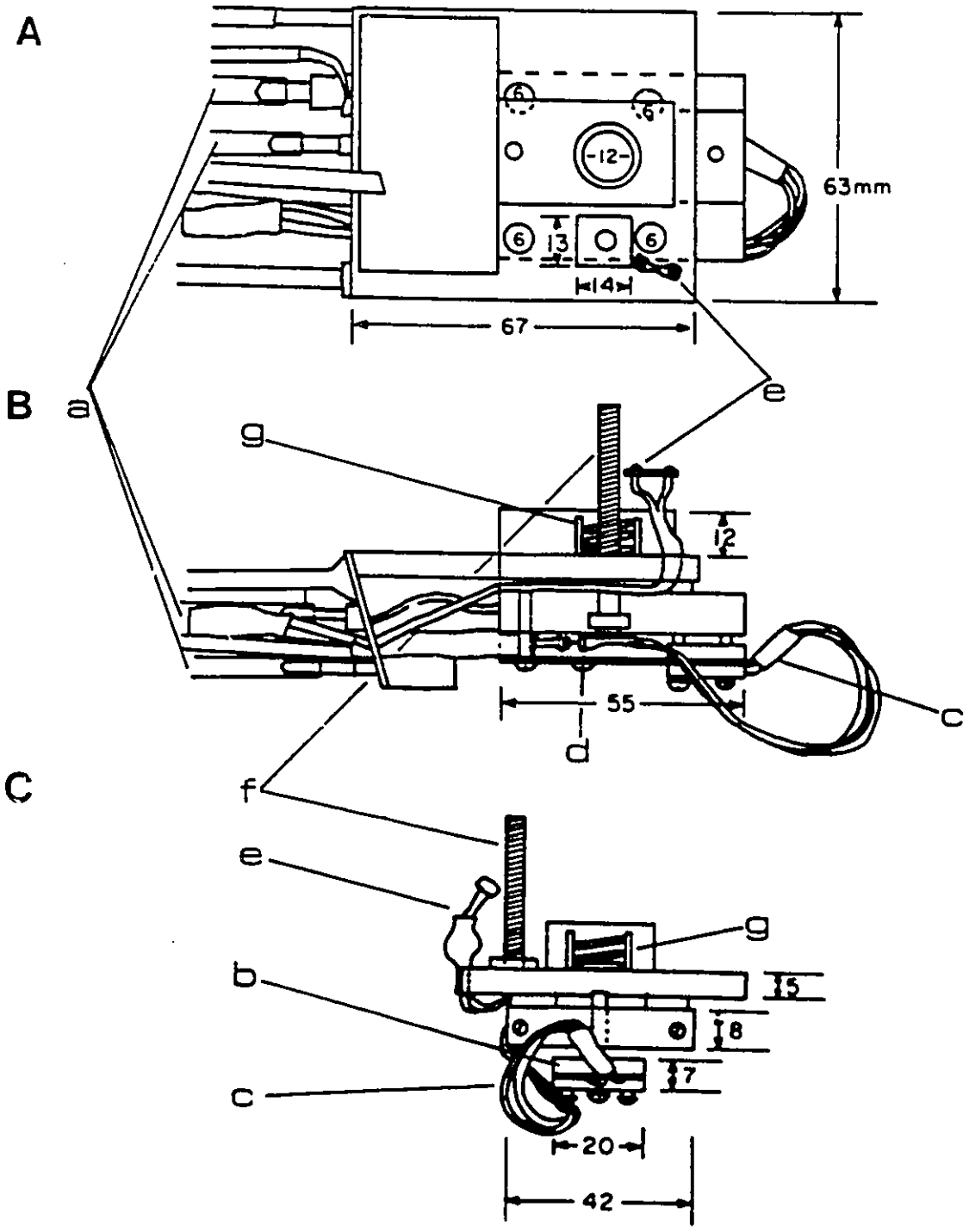

VI.5.e. (A) Lateral view of the completed force sensor.in position within the stabilizing horse shoe. (B) Rear view of same. (C) Top view of same. Depicted are a) tuning rods, b) sensor, c) electrical leads and (d) connector from sensor, e) electrical lead for nerve stimulation, f) nylon post to which a stabilizing piece of plexiglass is attached to stabilize the knee and limb. g) coil. All measurements in millimetres.

VI.6. Estimation of the metabolite concentrations of rat hind limb muscles

Each of the muscles of the hind limb has its own specific fibre type composition (see Table VI.6.a.) and concommitantly its own distinct concentrations of CrP, Cr and ATP (as determined by Mainwood, 1987). The EDL and soleus have predominently one fibre type hence, if equations were developed to express their metabolite concentrations in relation to their fibre type compostion they would be similar to those provided below.

In the equations describing EDL and soleus F and S represent Fast and Slow twitch fibres respectively. The number preceding these letters represents the percentage contribution of this type of fibre to each of these muscles. For example EDL is thought to be 100% Fast twitch while Soleus is 13% fast and 87% slow.

In the equations describing the gastrocnemius and hind limb X, Y, and Z represent the unknown molarities of each of CrP, Cr and ATP.

EDL
100 F = 21.7 mmoles CrP/kg wet weight
100 F = 26.7 mmoles Cr/kg wet weight
100 F = 6.0 mmoles ATP/kg wet weight

Soleus
13 F + 87 S = 11.7 mmoles CrP/kg wet wgt
13 F + 87 S = 21.2 mmoles Cr/kg wet wgt
13 F + 87 S = 3.9 mmoles ATP/kg wet wgt

Gastrocnemius (mixed)
93 F + 7 S = X mmoles CrP/ kg wet wgt
93 F + 7 S = Y mmoles Cr/ kg wet wgt
93 F + 7 S = Z mmoles ATP/ kg wet wgt

Hind limb
92.3 F + 7.7 S = X mmoles CrP/ kg wet wgt
92.3 F + 7.7 S = Y mmoles Cr/ kg wet wgt
92.3 F + 7.7 S = Z mmoles ATP/ kg wet wgt

After solving the EDL equation for F, F can be substituted into each of the soleus equations to give a value for S in the equation for each metabolite. Subsequently these values for F and S are substituted into the corresponding gastrocnemius and hind limb equations in order to determine their concentration

of CrP, Cr and ATP.

Using CrP as an example, the substitutions result in the following equation.

$$93\left(\frac{21.7}{100}\right) + 7\left(\frac{(11.7 - [\,13\,(\,\frac{21.7}{100}\,)\,])}{87}\right) = 20.9 \text{ mmoles CrP/kg wet weight}$$

	Estimated mass (mg) of the following fibre types in each hind limb muscle		
	FOG	FG	SO
Plantaris	155	206	25
Soleus	19	0	149
Gastrocnemius (R)	76	12	47
Gastrocnemius (W)	10	106	0
Gastrocnemius (M)	310	1372	82
Tibialis anterior (R)	63	86	5
Tibialis anterior (W)	85	519	2
Extensor digitorum longus	40	157	2
Tibialis posterior	24	59	2
Flexor digitorum longus	14	34	2
Flexor hallicus longus	104	449	10
Peroneals	127	229	30
Sum	1027	3229	356
Percentage	22.3	70.0	7.7

Table VI.6.a. Fibre type composition by mass of each of the muscle of rat hind limb (Armstrong and Phelps, 1985).

VII. REFERENCES

1. Ackerman, J.J.H., D.G. Gadian, G.K. Radda and G.G. Wong (1981). J. Magn. Reson., 42:498-500

2. Ackerman, J.J.H., T.H. Grove, G.G. Wong, D.G. Gadian, G.K. Radda. (1980).Nature, London, 283:167-170

3. Alger, J.R., L.O. Sillerud, K.L. Behar, R.J. Gillies, R.G. Shulman, R.E. Gordon, D.Shaw (1981). Science, 214: 660

4. Armstrong, R.B., R.O. Phelps (1984). The American Journal of Anatomy, 171:259-272

5. Arnold, D.L., P.J Bore, G.K. Radda, P. Styles, D.J. Taylor (1984). Lancet (i):1367-1369.

6. Arnold, D.L., P.M. Matthews and G.K. Radda (1984). Magnetic resonance in medicine 1:307-315

7. Barany, M., K. Barany, C.T. Burt, T. Glonek and T.C. Myers (1975). **

8. Beall, P.T., S.R. Amtey and S.R. Kasturi (1984). NMR Data Handbook for Biomedical Applications Permagon Press.

9. Becker, E.D., J.A. Ferretti, P.N. Gambhir (1979). Analytical Biochemistry, 51:9: 1413-1420

10. Beis, I. and E.A. Newsholme (1975). Biochem. J. 152:23-32

11. Bendall, M.R. , D. Foxall, B.G. Nichols, J.R. Schmidt. (1986). Journal of Magnetic Resonance, 70:181-186

12. Berne, R.M. and M.N. Levy (1983). Physiology, Mosby

13. Bessman, S.P. and P.J. Geiger (1981). Science Wash. DC, 211: 448-452,

14. Bessman, S.P., C.L. Carpenter (1985). Ann. Rev. Biochem., 54:831-862

15. Bevington, A., K.I. Mundy, A.J.P. Yates, J.A. Kanis, R.G.G. Russell, D.J. Taylor, B. Rajagopalan and G.K. Radda (1986). Clinical science, 71:729-735

16. Billadello, J.J., J.K. Gard, J.J.H. Ackerman, R. Gross (1985). Analytical Biochemistry, 144:269-274

17. Blicharski, J.S. (1981). Journal of Magnetic resonance, 43:449-455

18. Bonas, J.E., B.D. Cohen and S. Natelson (1963). Microchem. J., 7:63-77

19. Brady, M.E., P. Morris (1986). Unpublished observations.

20. Cain, D.F. and R.E. Davies (1962). Biochem. Biophys. Res. Commun. 8: 361-366

21. Chance, B., S. Eleff, W. Bank, J.S. Leigh, R. Warnell (1982). Proc. Natl Acad Sci 79:7714-7718.

22. Chang, D.C. and D.E. Woessner. (1978). Journal of Magnetic Resonance, 30:185-191

23. Chang, L.H., B.M. Pereira, M.A. Weinstein,M.A. Keniry, J. Murphy-Boesch, L. Litt and T.L. James (1987). Magn. Reson. Med. 4 (in press)

24. Chang, L.H., W.M. Chew, P.R. Winstein and T.L. James, (1987) J. Mag. Res. 72:168-172

25. Chasiotis, D. (1983). Acta Physiol. Scand. suppl. 518:1-68

26. Chevli, R. and C.D. Fitch (1979). Biochem. Med. 21:162-167,

27. Civan, M.M., H. Degani, Y. Margalit and M. Shporer. (1983). Am. J. Physiol. 245:C213-C219

28. Cope, F.W. (1965) Biochemistry 54:225-227

29. Cope, F.W. (1970). Biophysical Journal, 10:843-858

30. Cowan, BE, D.Y. Sze, S.T. Mai and O. Jardetzky (1985). FEBS. Lett. 184, 130

31. Crow, M.T. and M.J. Kushmerick (1983). Fed. Proc. 42:14-20

32. Dawson, M.J. (1982). Bioscience Reports 2:727-733

33. Dawson, M.J. (1982). Bioscience reports, 2:727-733,

34. Dawson, M.J., D.G. Gadian and D.R. Wilkie (1978). Nature, 274:861-866

35. Dawson, M.J., D.G. Gadian, D.R. Wilkie (1977). J.Physiol. 267:703-735

36. Dawson, M.J., D.G. Gadian, D.R. Wilkie (1980). Phil. Trans. R. Soc. Lond B289:445-455

37. Deutz, N.E.P, W.M.M.P.J. Bovee and R.A.F.M. Chamuleau (1986). Journal of Neuroscience methods, 16:157-161,

38. Doyle, D.D., M. Barany (1982). Febs. Letters., 140:2:237-240

39. Drahota, Z. (1961). Physiologia Bohemoslovenica 10:160-165

40. Edwards, R.H.T., M.J. Dawson, D.R. Wilkie, R.E. Gordon, D. Shaw (1982(i)) Lancet 725-731.

41. Eggleton, P., G.P. Eggleton (1927). Biochemical Journal 21:190-195

42. Ennor, A. H. and H. Rosenberg (1952). Biochem. J. 51: 606-610

43. Evelhoch, J.L., C.S. Ewy, B.A Siegfried, J.J.H. Ackerman (1985). Magnetice Resonance in Medicine, 2:1-8, 31P

44. Fiske, C. H. and Y. Subbarow (1929). J. Biol. Chem. 81: 629

45. Fitch, C.D. and R.P. Shields, W.F. Payne and J.M. Dacus (1968). J. Biol. Chem. 243:2024-2027

46. Fitch, C.D., M. Jellinek and E.J. Mueller (1974). J.Biol.Chem. 249:1060-1063

47. Fitch, C.D., M. Jellinek, R.H. Fitts, K.M. Baldwin and O. Holloszy (1975). Am. J. Physiol. 228:1123-1125,

48. Fitch, C.D., R. Chevli (1975). Analytica Biochemistry 68:196- 201

49. Fitch, C.D., R. Chevli, J.S. Petrofsky and S.J. Kopp (1978). Life Sciences 23:1285-1292

50. Foster, M.A. (1983). Mag Res in Med and Biology Permagon Press

51. Fukushima, E., S.B.W. Roeder (1981). Experimental Pulse NMR. A nuts and bolts approach. Addison-Wesley Publishing Company, Inc. Reading, Massachusetts

52. Gadian, D.G. (1981). Bioscience Reports, 1:449-460

53. Gadian, D.G. (1982). "NMR and its application to living systems", Oxford University Press. Oxford

54. Gadian, D.G. (1982). Nuclear Magnetic Resonance and its Applications to Living Systems NY; Oxford University Press

55. Gadian, D.G. and F.N.H. Robinson (1979). J.Magn. Reson. 34:449-**

56. Gadian, D.G. and G.K. Radda (1981). Ann. Rev. Biochem. 50:69-**

57. Ganong, W.F. (1977). Review of Medical Physiology, 8th edition, Lange Medical Publications, Los Altos, C.A.

58. Green, C.J. (1979). Animal anaesthesia, Laboratory Animals Handbooks 8, Laboratory Animals

59. Green, C.J., J. Knight, S. Precious and S. Simpkin. (1981). Laboratory animals 15:163-170

60. Gupta, R.K. , P. Gupta (1982). Journal of Magnetic resonance. 47:344-350

61. Hartree, E.F. (1972). Analytical Biochemistry 48:422-427

62. Hayes, C.E, T.A. Case. D.C. Ailion. (1982). Science, 216:1313-1315

63. Hazlewood, C.F., B.L. Nichols (1969). Hopkins Med. J. 125:119-133

64. Hazlewood, C.F., B.L. Nichols, D.C. Chang, B. Brown (1971). Hopkins Med. J. 128:117-131

65. Hazlewood, C.F., D.C. Chang, B.L. Nichols, D.E. Woessner (1974). Biophysical Journal. 14:583-606

66. Helzberg J.H., M.S. Brown, D.J. Smith , J.C. Gore, E.R. Gordon (1987). Hepatology 7:1:83-88

67. Hintz, C.S., M.M-Y. Chi, R.D. Fell, J.L. Ivy, K.K. Kaiser, C.V. Lowry and O.H. Lowry (1982). Am.J. Physiol. 242:C218-C228,

68. Hood, D.A., Gorski, Jan and R.L. Terjung, Am. J.Physiol. 250:E449-E456

69. Hoult, D.I. (1978). Progress in Nuclear Magnetic Resonance Spectroscopy 12:41

70. Hoult, D.I. and R.E. Richards (1976). J.Magn. Reson. 24:71-85

71. Hoult, D.I., P.C. Lauterbur (1979). J. Magn.Reson. 34:425

72. Hoult, D.I., S.J.W. Busby, D.G. Gadian, G.K. Radda, R.E. Richards and Seely, F.J. (1974). Nature (London) 252:285 ****

73. Idstrom, J.P., V.H. Subramanian, B. Chance, T. Schersten and A.C. Bylund-Fellenius (1985). Am. J. Physiol. 248:H40-H48

74. Iles, R.A., A.N. Stevens, J.R. Griffiths (1985). Biochem.J. 229:141-151

75. Jacobus, W.E. (1985). Ann. Rev. Physiol. 47:707-725

76. Jones, G.J. (1984). Journal of Microscopy, 136:3:349-360

77. Keller, U.R. Oberhansli, P. Huber, L.K. Widmer, W.P. Aue, R.I. Hassink, S. Muller, J. Seelig (1985). European journal of Clinical Investigation, 15:382-388.

78. Kirk, K., J.E. Raftos, P.W. Kuchel (1986). J. Mag.Res. 70:484-487

79. Kiyohara, T., N. Kobayashi (1968). Kumamoto Medical J., 21:4

80. Kobayashi, N., K. Yonemura (1967). Japanese Journal of Physiology, 17:698-707.

81. Komoroski, R.A., G.C. Levy, (1974). Magnetic Resonance Review, 3:3:289-324.

82. Kushmerick, M.J., R.A. Meyer (1985). Am. J. Physiol. 248: C542-C549

83. Lamprecht, W. and P. Stein (1965). Creatine phosphate. Methods of Enzymatic Analysis, pp 610-616 Academic Press, NY, NY

84. Lawson, J.W.R. and R.L. Veech. (1979). J.Biol Chem. 254:6528-6537

85. Lederman, Sally Ann (1983). American Journal of Clinical Nutrition 37:663-668

86. Ling, G.N. (1962). A physical theory of the living state. New York, Blaisdell

87. Lipmann, F., O. Meyerhof, 1930, Biochem. Z. 227:84-109

88. Lohmann, K. (1929). Naturwissenschaft 17:624-625

89. Lundsgaard, E. (1930). Biochem. Z. 217:162

90. Mahanna, D.A. (1980). Exp. Neurology 68:114-121

91. Mainwood, G.W. (1987). Unpublished results

92. Mainwood, G.W. and K. Rakusan (1982). Can. J.Physiol. Pharmacol. 60:98-102,

93. Mainwood, G.W. J.Totosy de Zepetnek (1985). Muscle and Nerve 8:774-782

94. Mainwood, G.W., J. Totosy de Zepetnek (1986). Myocardial and Skeletal Muscle 519-525

95. Mainwood, G.W., M. Alward, B. Eiselt (1982). Can J. Physiol. Pharmacol. 60:120-127

96. Mainwood, G.W., M. St. Jean (1987). Unpublished results.

97. McGilvery, R.W. and T.W. Murray (1974). J. Biol. Chem. 249:5845-5850

98. Meyer R.A. and R.L. Terjung (1980). Am. J. Physiol. 239:C32-C39,

99. Meyer, R.A., H.L. Sweeney and M.J. Kushmerick (1984). Am.J.Physiol. 246:(C15):C365-C377,

100. Meyer, R.A., M.J. Kushmerick and T.R. Brown (1982). Am. J. Physiol. 242:C1-C11

101. Meyer, R.A., M.J. Kushmerick, T.R. Brown (1982). Am. J. Physiol. 242:C1-C11,

102. Meyer, R.A., T.R. Brown and M.J. Kushmerick (1985). Journal of Physiology, 248:C279-C287

103. Meyer, R.A., T.R. Brown, B.L. Krilowicz and M.J. Kushmerick (1986). Am. J. Physiol. 250:C264-C274

104. Moon, R.B. and J.D. Richards (1973). J. Biol. Chem. 248:7276-7278

105. Murphy-Boesch, M. J. and Koretsky (1983). J Magn.Reson. 54:526

106. Odeblad, E., B.N. Bahr and G. Lindstrom (1956). Arch. Biochem. Biophys. 63:221-225,

107. Olgin, J., R. Connett and B. Chance (1985). Biophysical Journal 47:2:370

108. Peck, J.W. (1978). Physiol Behav. 21:4:599-607 -

109. Petrofsky, J.S., C.D. Fitch (1980). Pluegers Arch. 384:123-129,

110. Pocsik, I. Furo, I. Tompa, K. Neumark, T. Takacs J. (1986). Biochimica et Biophysica Acta 880:1-9

111. Pople, J.A., W.G. Schneider, H.J. Bernstein (1959). High Resolution Nuclear Magnetic Resonance Spectroscopy, McGraw-Hill Book Company Inc. N.Y., N.Y.

112. Roberts, J.D. NMR (1959). Applications to Organic Chemistry. McGraw-Hill Book Company Inc. N.Y., N.Y.

113. Rowley, G.L., A.L. Greenleaf and G.L. Kenyon (1971). J. Am. Chem. Soc. 93:5542-5551

114. Sabina, R.L., J.L. Swain, J.J. Hines, E.W. Holmes (1983). J. Applied Physiol. 55:2:624-627

115. Sakaguchi, S. (1925). J.Biochem. 5:25-31

116. Schnall, M.D., H. Subramanian, J.S. Leigh and B. Chance (1985). J. Magn. Reson. 65:122

117. Shaka, A.J., J. Keeler, M.B. Smith, R. Freeman (1985). Journal of Magnetic Resonance 61:175-180

118. Shields, R.P., C.K. Whitehair, R.E. Carrow, W.W. Huesner and W.D. Van Huss (1975). Lab. Invest. 33:151-158,

119. Shinar, H., G. Navon (1984). Biophysical Chemistry 20:275-283

120. Shoubridge, E.A., A.J. Challiss, D.J. Hayes and G.K. Radda (1985). Biochem. J. 232:125-131

121. Shoubridge, E.A., G.K. Radda (1984). Biochemica et Biophysica Acta 805:79-88

122. Shoubridge, E.A., G.K. Radda (1987). Am J. Physiol. 252:C532-C542

123. Siefkin, A.D., B.G. Nichols (1986). Am. Rev. Respir. Dis. 134:509-512

124. Styles, P. M.B. Smith, R.W. Briggs, G.K. Radda. (1985). Journal of magnetic resonance 62:397-405

125. Thulborn, K.R. and J.J.H. Ackerman (1983). J. Mag. Reson. 55:357-371

126. Thunberg, T. (1911). Zent. Physilog. 25:915-916

127. Tofts, P.S. and S. Wray (1985). J.Physiol., 359:417-429

128. Totosy-de Zepetnek (1984). M.Sc. Theses Dept. of Physiology University of Ottawa

129. Veech, R.L., W.R. Lawson, N.W. Cornell and H.A. Krebs. (1979). J.Biol. Chem. 254:8994-6547

130. Walker, J.B. (1979). Creatine: Biosynthesis, regulation and function. In: Advances in enzymology. Alton Meister ed. John Wiley and sons. New York. 50:177-242

131. Wray, S. , P.S. Tofts (1986). Biochimica et Biophysica Acta 886:399-405

132. Yoshikawa, K., A. Ohsaka (1979). Physiol Chem. and Physics. 11:185-188

133. Yoshikawa, K., A. Ohsaka (1979). Physiol. Chem. and Physics 11:185-188